Optimization Design and Performance Analysis of Circulating Fluidized Bed Combustion System Focusing on Reduced Emissions

Ph. D Mechanical Engineering Thesis

SUBMITTED BY:

SHAFIQ UR REHMAN

2009-Ph.D-MECH-07

SUPERVISED BY:

PROF. DR. ASAD NAEEM SHAH

Department of Mechanical Engineering

University of Engineering & Technology Lahore, Pakistan

DEDICATIONS

I dedicate my PhD work to my parents, wife, children and numerous companions. An extraordinary sentiment appreciation to my loving guardians, whose uplifting statements and push for determination ring in my ears. My brothers and sisters have never left me alone and are extremely outstanding. I additionally dedicate this thesis to my many family members and friends who have endorsed me all through the procedure. I will dependably value all they have done.

ACKNOWLEDGEMENT

Thanks and praises to Allah Almighty, the Lord of heaven and Earth, who enabled me to complete this research work. After that, I am indebted to all those who helped me in any form at any stage of my work.

Special thanks to Prof Dr Asad Naeem Shah whose supervision and guidance played a key role in the completion of this project in a timely manner while maintaining a high standard. He has been very kind and helpful in every regard.

I am thankful to the members of my advisory committee, Prof Dr Fiaz Hussain Shah and Prof Dr Ijaz Ahmad Chaudhry for their help and guidance. I am also indebted to the Chairman Mechanical Engineering Department and the Dean Faculty of Mechanical Engineering for providing research environment in the department which helped me to complete this job. I also want to pay thanks to the faculty, administrative and lab staff, and all those who extended help at any stage of my work.

This research work wouldn't have been completed without the funding provided by Higher Education Commission (HEC) of Pakistan (under the "International Research Support Initiative Program (IRSIP); INSPIRE / KEP (HEC and British Council Islamabad funded project titled "Research cooperation for innovation in coal combustion and promotion of modern mining practices in Pakistan"); and the Coal Fired Power Project (CFPP), Government of Pakistan.

Last but not least, the moral support of my all family members has been an asset during this busy routine.

ABSTRACT

In context with abundant availability of low rank coals in some developing counties including Pakistan, a comprehensive investigation program was carried out. In the first phase of this program, lab scale study had been conducted at SGS Pakistan and Changsha University of Science and Technology (CUST) China to investigate the coal quality characteristics, combustion characteristics and performance indices of the samples taken from the Salt Range and Trans–Indus Range located at latitude 32–34° and longitude 71–74° in Punjab, Pakistan. In the second phase, emission characteristics of the said coals were investigated with different proportions of lime stone and biomass during combustion in FBC pilot facility. Experimental optimization of key process parameters such as Ca/S molar ratios (MR), limestone particle size and bed temperature etc. was also made to minimize the gaseous emissions particularly Sulfur Dioxide (SO_2).

It was found from the results of quality characteristics that the coal samples have high ash (14–50%), ultra-high sulfur (3.3–11.1%), low moisture (3–10%), high volatile matter (VM) 24–41% and low carbon (23–57%) with low to medium gross calorific value (GCV) of 10.2–25.7 MJ/kg. The average ash fusion temperature (AFT) of the samples is greater than 1350 °C which reveals that the coal is non-slagging. On average the coal has low slagging Index, medium fouling Index, good combustion parameters and better performance indices.

Referring to the combustion characteristics, the ignition temperatures (T_i) of all the coals are in the range of 355–392 °C i.e. less than 400 °C indicating that the coal is easy for ignition. Value of ignition characteristics index (F_z) is greater than 2.0 showing that these coals have very good ignition characteristics. Value of flammability index (C) for all the coals is in the range of 2.6–3.1 indicating that these coals have very good flammability characteristics. The value of stable firing index (M) is from 3.5 to 4.1, leading to the fact that these coals have better characteristics for stable firing.

With reference to the emission characteristics, different values of MR (i.e. 2, 3, 3.5 & 4) were used to investigate the SO_2 reduction which remained 40–72% for coal A (Trans–Indus Range) and 41–78% for coal B (Salt Range), respectively. The MR of 3.5 was the critical value revealing the predominant decrease in SO_2 reaching upto 72% and 78% for coal A and coal B, respectively. Further, bed temperature in the

range of 750–800 °C was found to be critical for the maximum alleviation of SO_2 at the same MR. It was observed that desulfurization of coal was maximum with the fine particle size range of 2.0–2.8 mm. In addition to this, co–firing of 30–60% biomass exhibited a decrease in SO_2 emissions of 47.5–68.3% and 36.3–67.8% for coal A and coal B, respectively. Also, NO_x emissions were reduced up to 16% and CO emissions were abated up to 78%.

Thus the study contributes to the research community working on utilization of low quality (high sulfur) coal reserves to meet the projected energy need in Pakistan as well as in other developing countries.

CONTENTS

LIST OF TABLES

LIST OF FIGURES

NOMENCLATURE

AFT	:	Ash Fusion Temperature
Al_2O_3	:	Aluminum Oxide
ASTM	:	American Standard of Testing and Material
BFBC	:	Bubbling Fluidized Bed Combustion
C	:	Carbon
Ca/S	:	Calcium Sulfur Ratio
$CaCO_3$	:	Calcium Carbonate
CaO	:	Calcium Oxide
CaO	:	Calcium Oxide
$CaSO_4$	:	Calcium Sulfate
CFBC	:	Circulating Fluidized Bed Combustion
CFC	:	Chloro Fluoro Carbon
CH_4	:	Methane
CHNS	:	Carbon, Hydrogen, Nitrogen and Sulfur
CO	:	Carbon Monoxide
CO_2	:	Carbon Dioxide
CO_x	:	Carbon Oxide
CUST	:	Changsha University of Science and Technology
DTG	:	Differential Thermo Gravimetric
FBC	:	Fluidized Bed Combustion
FC	:	Fixed Carbon
Fe_2O_3	:	Iron Oxide
FGD	:	Flue Gas Desulfurization
F_z	:	Ignition Characteristics Index
GCV	:	Gross Calorific Value
H	:	Hydrogen
H_2S	:	Hydrogen Sulfide
H_2SO_4	:	Sulfuric Acid
HC	:	Hydro Carbon
HCN	:	Hydrogen Cyanide
HFO	:	Heavy Fuel Oils
IM	:	Inherent Moisture

K_2O	:	Potassium Oxide
M	:	Stable Firing Index
MBT	:	Main Boundary Thrust
MFT	:	Main Frontal Thrust
$MgCO_3$	:	Magnesium Carbonate
MgO	:	Magnesium Oxide
MJ	:	Mega Joule
MR	:	Ca/S Molar Ratio
MSW	:	Municipal Solid Waste
MW_e	:	Megawatt Electric
MW_{th}	:	Megawatt Thermal
N	:	Nitrogen
N_2O	:	Nitrous Oxide
Na_2O	:	Sodium Oxide
NCV	:	Net Calorific Value
NH_3	:	Ammonia
NO_2	:	Nitric Oxide
NO_x	:	Nitrogen Oxide
PCC	:	Pulverized Coal Combustion
PFBC	:	Pressurized Fluidized Bed Combustion
PM	:	Particulate Matter
S	:	Sulfur
SiO_2	:	Silicon Dioxide
SO_2	:	Sulfur Dioxide
SO_x	:	Sulfur Oxide
STA	:	Simultaneous Thermal Analyzer
T_c	:	Cyclone Temperature
TDH	:	Transport Disengaging Height
TG	:	Thermo Gravimetric
T_i	:	Ignition Temperature
TM	:	Total Moisture
U_{mb}	:	Minimum Bubbling Velocity
U_{mf}	:	Minimum Fluidizing Velocity
VM	:	Volatile Matter

CHAPTER NO.1

INTRODUCTION

1.1 Overview

The increasing demands of energy resources, the continuous and rapid depletion of the petroleum oil reservoirs and the resulting rise in the prices of liquid & gaseous fuels have caused the global shift back to utilization of solid fuels in thermal power plants. Amongst the solids, coal is the most abundant economical primary source of sustainable energy that can meet the present energy demands. These factors have diverted the attention of engineers and technologists to develop an efficient and environment friendly coal firing system for power generation. Hence in the recent years various coal power technologies have been developed world wide [1].

In the past, coal had been utilized as a source of energy in the locomotive steam engines used for the transportation on rail-roads since 1814. It was also used in the steam power plants for propulsion of marine ships (steamers) utilizing steam turbine since 1884 and later on for electric generation. These plants utilized the static bed for coal burning with the coal particle of sizes (6 to 30 mm) and lower air velocity (1.0 m/s). These plants had low combustion efficiency and high emissions level of pollutants that was neglected at that time. In 1938, pulverized coal combustion (PCC) was introduced with pneumatic transport of very fine coal particles (<0.1 mm diameter) and higher velocities (15–30 m/s). This system has the advantage of the highest combustion efficiency of about 99 percent but it produces high NO_x emissions because of higher combustion temperatures (>1100^{o}C) and to control SO_2 emissions, it needs flue gas desulfurization (FGD) unit which is an expensive technique [2].

The coal firing systems were gradually replaced by the liquid and gaseous fuel combustion systems because of their compactness, convenience and clean operations. Moreover, the awareness of environmental protection from the harmful emissions particularly sulfur dioxide produced during the combustion of coal discarded the use of coal in most of the applications. Petrol (gasoline) and diesel oil (1884 and 1893 respectively) are well known refined petroleum products being used in automobile engines of light & heavy vehicles. While heavy fuel oils (HFO) are used in thermal

power plants for electric power generation. Table 1.2 shows the global fossil fuel reserves in year 2012 [3].

During the last 50 years, the rapid growth in the number of passenger cars and other automobiles has caused declination in the petroleum reservoirs all over the world [4]. The search for the alternative fuels for the automobiles and other power plants started in late 1970s and the scientists proposed the use of natural gas and methanol in the road vehicles and solid fuels for the stationary power plants [5].

Table 1.1 History of energy utilization [6, 7]

Year	Annual Energy Consumption (MJ/person)	Country/ Area
1400	109	Northwestern Europe
1875	322	England
1970	962	United States
2011	9025	Pakistan
2012	408,574	Norway
2012	275,878	Australia
2012	167,572	Switzerland
2012	254,779	Netherland
2012	318,572	United States
2012	176,524	Germany
2012	202,824	New Zealand
2012	131,441	Ireland
2012	404,038	Canada
2012	139,116	Denmark
Increase in energy consumption is not linear, the improvement in quality of life begins to level of when per capita energy consumption rises to about 200,000 MJ/person.		

Keeping in view the increasing demands of energy resources (Table 1.1) and the present situation of petroleum, natural gas and coal reserves (Table 1.2) one can

conclude that coal is undoubtedly the only fossil fuel that may be the source of sustainable energy on our planet. Coal is the world's most abundant and widely distributed fossil fuel, with global proven reserves of nearly 1000 billion tones and has been a key component of electricity generation mix worldwide [1, 3]. Coal provides more than 40% of the world's electricity [8] and this share is predominant for some countries such as South Africa (93%), Poland (92%), China (79%), India (69%) and the United States (49%). Moreover, the growing energy needs of the developing world are leading to the fact that coal will remain a key component of the power regardless of climate change policy [9].

Table 1.2 Global fossil fuel reserves [9]

Fossil Fuel	2012
Petroleum	35.5 Years
Natural Gas	56 Years
Coal (high rank)	109 Years
Coal (low rank)	490 Years

In Pakistan, power generation from coal is currently gaining more interest as compared to oil and gas [10]. Coal in Pakistan is of low grade such as lignite in Sindh (Thar and Lakhra) and sub-bituminous in Baluchistan and Punjab (Salt Range and Trans Indus Range) [11]. The coal reserves of Salt Range and Trans Indus Range are approximately 500 million tons [12]. In general Pakistani coal contains high sulphur (ranging from 3 to 11%) except Thar coal. Coal based power generation could represent an economic solution by using low grade Pakistani coals and their blends with better quality imported coals, which would ensure high performance and compliance with environmental regulations [13]. The Fluidized bed combustion (FBC) technology could prove better option to utilize such low grade high sulfur coals in coal fired steam as well as power generation systems with controlled emissions of nitrogen oxides (NO_x) and sulfur oxides (SO_x) [14 -16].

1.1.1 Evolution of Fluidized Bed Combustion (FBC) Technology

In early 1960s, the idea of burning coal in a fluidized bed was innovated for higher thermal efficiency and lower emissions level of NO_x and SO_x. The idea was advocated

by the scientists (1968) and the first fluidized bed boiler was developed known as bubbling fluidized bed combustor (BFBC) [17]. Continued efforts in this field concluded a number of designs of BFBC in UK, USA, and China. In 1980, circulating fluidized bed boiler (CFB) (the next generation in this field) was developed in China [18]. A CFB boiler has the facility to burn a variety of solid fuels efficiently and to recycle the unburnt and partially burnt coal particles through the combustion zone. In fluidized bed combustors, coal particles of the size (0.1–0.5 mm) are transformed into a fluid like state by their contact with an upwardly flowing air or gas stream. These particles remain in a semi suspended condition during combustion.

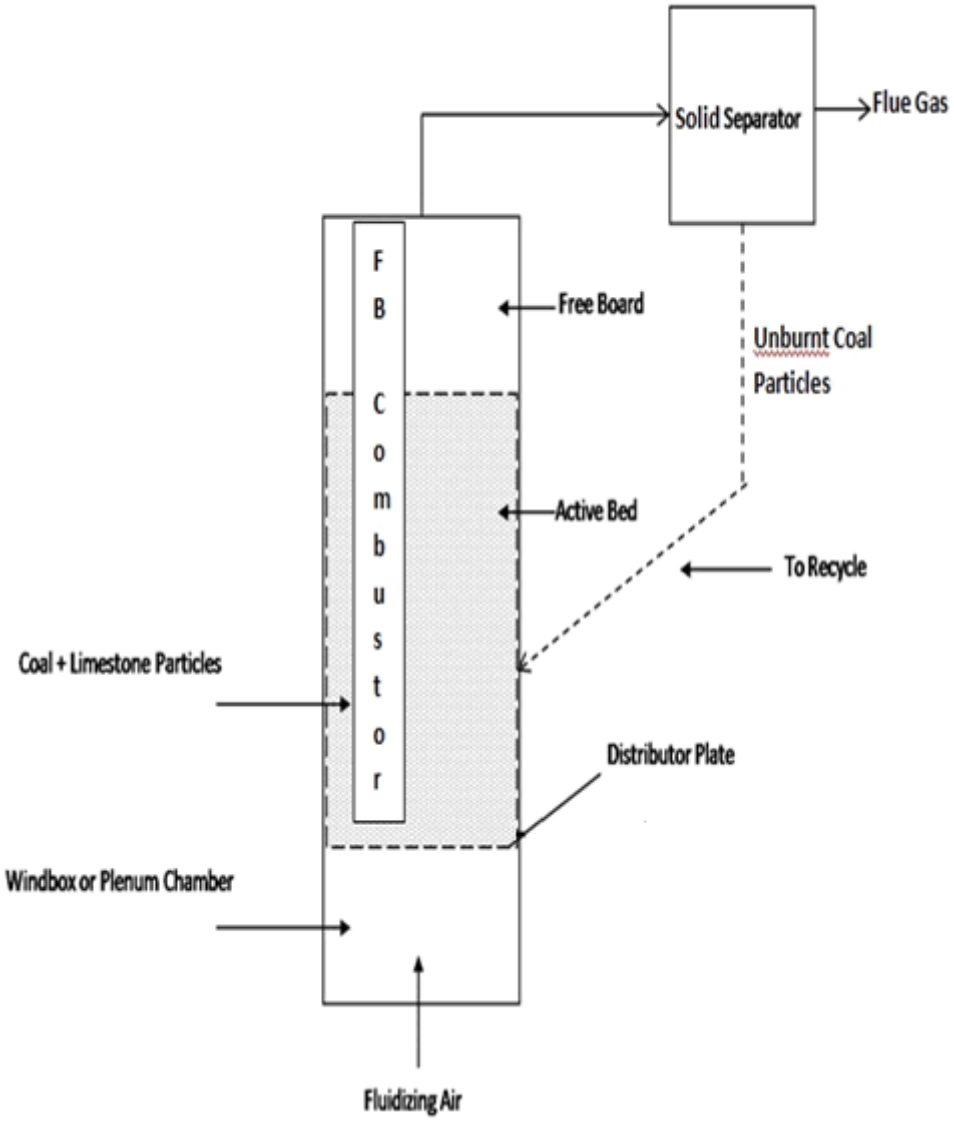

Fig. 1.1 Schematic of a fluidized bed combustor (FBC) [19]

In FBC the coal and limestone are fed through a number of feed points evenly distributed normally above the distributor plate. A distributor plate may be a

perforated steel disc used for uniform supply of air required for good fluidization. In larger plants the distributor plate may consist of nozzles and caps. The schematic of FBC is shown in Fig. 1.1 [19].

The fluidizing velocity of air referred as superficial velocity and the coal particle size affects the hydrodynamics and the operation of a fluidized bed combustor. Smaller particles of less than 0.03 mm diameter, have larger inter particle forces (Vander Waals forces) that cause the particles to stick together to form bubbles. These bubbles are helpful to some extent in the better solid–air mixing but on the other hand they increase elutriation i.e. entrainment of unburnt coal particles with the gas stream thus reducing the combustion efficiency. Formation of large size bubbles, known as slugging, makes the fluidization poor and causes pressure unbalances and vibrations in the bed. In BFBC the superficial velocities are kept higher than that of fixed bed (1.5 to 2.5 m/s), so that the shear forces are larger than the cohesive forces of the particles [20].

The total residence time of coal particles in the combustion zone is an important factor for their complete combustion so as to raise the combustion efficiency. This time can be increased by increasing the height of active bed and free board. This can also be achieved by installing a solid separator to collect solid–gas mixture leaving the combustor and by re–injecting the partially burnt particles in the fly ash back to combustor. This arrangement is known as circulating fluidized bed combustion system. In a circulating fluidized bed, the range of the superficial velocities are from 3 to 8m/s and coal particle size from 0.1 to 0.5mm. A cyclone separator is installed just after the freeboard and it separates partially burnt denser and heavier particles from the lighter ash particles flying through the cyclone. The higher superficial velocities are necessary in CFBC so that the particles may have sufficient K.E to complete their recycling in the combustor [2].

1.1.2 Advantages of FBC

The primary advantages of fluidized bed combustion are high level coal combustion efficiency, low bed temperature that corresponds to low NO_x and economical elimination of SO_2 using a cheaper sorbent–limestone. In PCC about 40 to 60% of the investment is required for SO_2 control by flue gas desulfurization (FGD). Limestone or dolomite particles of size 0.1 to 0.2 are added as sorbent for capturing SO_2 formed by the combustion of sulfur, as given by equation 1.1 to 1.3.

$$CaCO_3 \text{ (Limestone)} \xrightarrow{\text{Heat}} CaO + CO_2 \text{ (Calcination Reaction)} \quad (1.1)$$

$$S \text{ (Sulfur in the coal)} + O_2 \xrightarrow{\text{Combustion}} SO_2 \quad (1.2)$$

$$CaO + SO_2 + 1/2\ O_2 \xrightarrow[\text{(Bed ash)}]{} CaSO_4 \text{ (Sulfation Reaction)} \quad (1.3)$$

The second major advantage of FBC is the thermodynamic stability because of lower operating temperature of furnace between 800 ^oC and 900 ^oC as compared to 1100 ^oC and above in PCC. It is well known fact that NO_x emissions are much reduced when the combustion temperature is lowered. Moreover, at lower temperatures the sintering i.e. sticking of ash and its depositions on boiler tubes is also negligible. FBCs have much larger heat transfer coefficient (20 times or above) than the conventional boilers and high rate of power about 4.5 MW/m^2 of cross–sectional area of combustor. So FBC systems require smaller equipment and space for its installation [2].

1.1.3 Other Solid Fuels

Fluidized bed combustion was primarily meant for the efficient combustion of coal with low harmful emissions but it is found equally useful for obtaining thermal energy from the waste materials. Municipal solid waste (MSW) and used rubber tyres have been tested by their co–combustion with coal producing cheap energy output with minimum air pollution [21].

FBC has been proven an attractive option for converting agro residues e.g. white wood, wheat straw, rice and coffee husk, olive residues into economical energy with environmental benefits. It is found that co–combustion of coal & biomass has been effective in reducing N_2O emissions. This technology reduces the ash related problem particularly the combustion of biomass such as sintering, agglomeration and deposition etc. [22–24].

The circulating fluidized bed boilers are now extensively used in the steam power plants using coal because of high combustion efficiency and relatively low emissions of sulfur & nitric oxides. This technology is still being developed and further significant improvements can be expected [25].

The combustion of different fossil fuels i.e. heavy fuel oils and coal in the thermal power plants is one of the major sources of environmental pollution (Table 1.3). The scientists are continuously working to improve the design and operational conditions in the combustion systems so as to meet the standard of emissions imposed by

corresponding environmental protection agencies of different industrialized countries. Table 1.3 indicates the combustion generated emissions of harmful gases in USA (only) [24].

Table 1.3 Combustion generated emissions of harmful gases in USA [24]

Source	Emissions (millions ton /year)		
	SO_x	NO_x	HC
Stationary Thermal Plants (Boilers etc.)	18.2	9.1	1.1
Transportation Vehicles	0.8	8.5	8.0
Industrial Processes	4.3	0.7	11.1

1.1.4 Emissions from FBC of Coal

Coal has variety of metamorphic composition. Volatile matter is the portion of coal that is liberated as gases and vapors when coal is heated. It may consist of CO, CO_2, CH_4, H_2S, NH_3, HCN etc. mostly combustibles. The remainder portion after emission of volatiles is known as char, it consists of pure carbon (fixed carbon) and non–combustible matter such as SiO_2, Al_2O_3, Fe_2O_3, CaO, Na_2O, K_2O, MgO etc. Some of these compounds are reactive during the combustion process while some others act as catalysts [26].

Sulfur dioxide and oxides of nitrogen are well known gaseous compounds first noticed in terms of their toxic effects on the surrounding vegetation, animals and health of human beings. With the advancement in the instrumentation used for measurements, the number of combustion products that may cause environmental pollution are constantly increasing. At the same time the technologies to reduce and eliminate these harmful compounds are being advanced. At present more than 40 gaseous compounds and solid particles have been detected in the combustion of coal which cause environmental pollution [27, 28].

Because of the large number of reactants in the volatiles as well as in the char as mentioned above and number of known and unknown catalysts present in the combustion zone, it is not realistic to simulate the combustion and emission processes by using equilibrium kinetics only. This is the major reason for the uncertainties and the disagreements in the conclusions drawn from these studies. Nevertheless the

experimental results are more realistic and reliable source to optimize the CFBC system for minimum combustion generated pollutants [29].

1.1.5 Emissions Control

There are considerable challenges in meeting the rapidly growing energy demands as well as in achieving an environment friendly coal firing system. In the literature, number of investigations and research findings are available in connection with the emissions control from FBC of coal, but most of these findings cover a very limited range of combustion generated pollutants. The researchers have considered normally one or two of the parameters that influence some of gaseous or solid emissions [30].

1.2 Objectives

This research is intended to study the geology and investigate the quality characteristics, combustion characteristics & combustion performance indices of Salt Range and Trans–Indus Range coal through lab scale testing. Experimental investigation of gaseous emission characteristics of the coal with addition of limestone and biomass during combustion in fluidized bed and optimization of process parameters to reduce these emissions especially SO_2 through pilot scale testing.

This will be accomplished through the following objectives:

i) Extensive literature review on coal quality characteristics, combustion characteristics and emission characteristics through available books, research journal articles and world–wide web.
ii) Investigation of coal quality characteristics through lab scale testing from SGS Pakistan and Changsha University of Science and Technology (CUST) Changsha, Hunan, China.
iii) Study of coal combustion characteristics and performance indices through lab scale testing from CUST China (GB Standards).
iv) Investigation of the effect of limestone addition on major gaseous emissions (such as SO_2, NO_x, CO_x etc.) of high sulfur coal during combustion at FBC pilot facility.
v) Investigation of the effect of biomass on major gaseous emission characteristics (SO_2, NO_x, CO_x etc.) of high sulfur coal during co–firing at FBC pilot facility.

vi) Optimization of multi variant process parameters to reduce major gaseous emissions of high sulfur coal during coal combustion and co–firing in FBC pilot facility.

vii) Comparison of experimental results with the theory and previous studies of noble Researchers in this field.

1.3 Scope

i) Collection of thirty coal samples for lab scale testing from different coal mines of Salt Range and Trans Indus Range situated in the northern part of Punjab province of Pakistan.

ii) Lab scale testing of 30 coal samples for quality characteristics and combustion characteristics from two different labs i.e. SGS Pakistan and CUST China.

iii) Selection of coal mines for pilot scale testing on the basis of lab scale testing results.

iv) Collection of two tons of representative coal samples: Coal A, from multiple mines of Trans–Indus Range and coal B from different mines of Salt Range.

v) Collection of 500 kg limestone from Salt Range for desulfurization study at FBC pilot facility.

vi) Investigation of emission characteristics of collected coal samples during combustion at FBC pilot facility with and without limestone addition.

vii) Study of emission characteristics during co–firing of coal and biomass.

viii) Optimization of process parameters to reduce major gaseous emissions especially SO_2.

1.4 Organization of Report

In order to investigate emission characteristics, it is not only important to study combustion characteristics, parameters and performance indices, but also to understand coal geology and quality characteristics which provides basis for design of coal fired boilers and furnaces. Experimental optimization of different process parameters is necessary to reduce gaseous emissions. Keeping in view all above mentioned issues, this dissertation report has been organized, as below:

i) A comprehensive literature review on reserves, history and importance of coal as a sustainable energy resource, its utilization for electricity generation, different

technologies employed worldwide for effective utilization of different qualities of coals and its co–firing with other solid fuels such as biomass, opportunity fuels etc. is presented in Chapter 2.

ii) Theory of fluidized bed combustion (FBC) system, major parts, general arrangement its various types, their applications and preference of circulating fluidized bed combustion (CFBC) over other systems, are explained in Chapter 3.

iii) Combustion in CFBC, parameters affecting combustion and emissions from CFBC are given in Chapter 4.

iv) Material and Methodology has been discussed in Chapter 5.

v) Experimental results and discussion has been made in detail in Chapter 6.

vi) Chapter 7 is dedicated to Conclusions and Recommendations.

CHAPTER NO. 2

LITERATURE REVIEW

Literature review was made using e–library of University of Engineering & Technology Lahore, Pakistan. Before finalizing the title of the research, the keywords 1. Fluidized; 2. Combustion; 3. Coal, were entered to know the number of references in this field in the form of research papers and books etc. The number of references found was 4873 since the innovation of concept of FBC.

To reduce the list, refinement was made by the full text online availability and the number reduced to 1050. Further refinement was made by the document type i.e. the papers published in a journal or presented in a conference, particularly those published in the years from 2007 to 2012, the number of research papers available were 247.

The abstract of these 247 research papers were downloaded and gone through to understand the developments in the science and technology of FBC. Further segregation was made for the gaseous emissions from FBC of coal; the number of research papers precisely related to the title of interest was just 10 amongst this collection, published during 2007–2012. However, the number of publications increased with time up to 2015 and most of them were studied in detail to know the status of the problem of emissions control from fluidized bed combustion of coal and other solid fuels.

Following is the summary of the latest research findings based on experimental and mathematical studies made by the scientists and engineers published during the last ten years. It is quite apparent that most of the researchers have covered very limited aspects related to emissions control specially reduction of SO_2 from fluidized bed combustion of high sulfur coal.

2.1 Coal geology, Resources and its Power Potential

The world has huge reserves of coal and prices are lower, in comparison to oil and gas. Depletion time of coal reserves is much more than 100 years, which is approximately three times bigger than oil and gas. Thus, coal being sustainable energy source will become energy substitute for oil and gas in future [1, 3]. Coal–fired plants continue to be the largest source of electricity generation all over the world and share

of coal in the world power generation mix is more than 40% [9, 13, 31]. However, the share is declining due to exploitation of the renewable resources. In Pakistan, power generation policy has recently shifted the interest from oil and gas to coal based power generation [10]. At present, the share of coal in power generation of Pakistan is less than 1% [12]. The share of coal in the Pakistan energy mix could be increased considerably using low grade coals such as sub–bituminous ones in Salt Range, Trans Indus Range in Punjab and Baluchistan, and ignites in Thar and Lakhra (Sindh). These low grade local coals are of high potential for economic power generation for Pakistan. Furthermore, the coals can be blended with better quality imported coals for higher performance and compliance with environmental regulations.

One feasible method for small to medium scale power production is fluidized bed combustion (FBC). This technology is flexible enough to utilize low grade and noncompliant quality coal whilst maintaining low emissions of sulfur oxides (SO_x) and nitrogen oxides (NO_x) [15, 32].

In the literature, geological aspects and combustion perspectives of Pakistani coals have not been fully investigated. The regional geologic studies of the coal–bearing areas in Northern Pakistan were conducted under Potwar Regional Framework Assessment Project (PRFAP) and the assessment of coal resources for Pakistan was done under Coal Resources Exploration and Assessment Program (COALREAP), a joint study by US Geological Survey (USGS) and Geological Survey of Pakistan (GSP) [33]. Latest work on regional geology, local geology, coalfield stratigraphy and coal resources of Salt Range and Trans Indus Range has been done by “Snowden” for Mines and Minerals Department of Punjab in Pakistan [34]. The study has confirmed that there are 500 million tons of coal reserves in Salt Range and Trans Indus Range [35].

Daood et al. [36] performed the combustion test of Thar lignites in pilot scale facility and examined the emissions of the coal like NO_x, CO, CO_2 and SO_2 with slagging and fouling analysis of ash samples at different combustion conditions. Zaidi et al. [37] studied the coal reactivity and char formation for the five coals collected from Lakhra, Sindh, Sore–Range & Sharigh, Baluchistan, Makarwal, Punjab in Pakistan and Sin Kiang in China. Iqbal et al. [38] investigated four coal samples from Islamkot, Thar parker and studied the effect of particle size on peak and burn out temperatures and increase in VM on removal of inherent mineral. Naveed et al. [39] investigated the

coal of Eastern Salt Range (Chakwal) and recommended the coal for gasification. However, the work on Salt Range and Trans Indus Range coal is very limited.

This study focuses on the geology, coal field stratigraphy and combustion perspectives of the coals from the Salt Range and Trans Indus Range. It will help engineering community, government and private sector to make decisions for the investment in design, engineering and installation/setup of coal mines and small to medium size coal–fired power plants. It will help to exploit indigenous coal resources of Punjab in particular and of Pakistan in general to produce cheap electricity as compared to oil–fired power plants and to bridge the gap between demand and supply of electricity for better economic growth.

2.2 Effect of Process Parameters on Emissions

Above results are in accordance with the investigation of Braganca and Castellan [40] which reveals that SO_2 retention efficiencies are 48%, 60%, 68% and 77% at MR values of 1, 2, 3 and 4 respectively during coal combustion in FBC. Their results also show that the amount of limestone utilization lies in the MR range from 1 to 4 to meet the environmental norms and further rise in MR value will not be economically feasible. According to the study of Tarelho et al. [41], the range of MR is from 1 to 5 for various developed/ developing countries to meet the SO_2 emission norms and high SO_2 removal efficiencies can be attained at MR = 3.5.

Limestone reacts with SO_2 in presence of O_2 to form calcium sulfate ($CaSO_4$).

A number of reactions are possible including the following:

$$CaCO_3 + SO_2 + \frac{1}{2}O_2 \rightarrow CaSO_4 + CO_2 \qquad \Delta H = -303 \frac{kJ}{mole} \qquad (2.1)$$

$$CaO + SO_2 + \frac{1}{2}O_2 \rightarrow CaSO_4 \qquad \Delta H = -481 \frac{kJ}{mole} \qquad (2.2)$$

Stoichiometric calculations show that one mole of limestone feed can reduce one mole of sulphur [42]. Molar volume of $CaSO_4$ is greater than that of either CaO or $CaCO_3$ which leads to the plugging of pores and therefore, complete conversion of the adsorbent particle is impossible. Also sulfation only proceeds at the outer surface of the CaO particle. The sulfation process continues until external pores are blocked significantly and an impenetrable $CaSO_4$ shell is formed leaving a considerable amount of unreacted CaO core. The increase in SO_2 emissions for both coals beyond

MR of 3.5 value may be due to equilibrium of sulfation and reduction of $CaSO_4$ [43]. According to Cheng et al. [44] operational parameters including MRs, furnace temperature, residence time and SO_2 partial pressure affect the sulfation reaction.

Anthony et al. [43] are of the view that there is still dispute over the explanation of maximum temperature for optimum sulfur retention in FBC boiler and its value depends on the types of coal, adsorbent used for desulfurization and other operational parameters. The seize in SO_2 reduction beyond 800 $^{\circ}C$ in current study may be attributed either to one or more possible reasons including physical properties of limestone such as solid sintering and choking of porous structure, reductive decomposition of $CaSO_4$, or a net balance between limestone sulphation and $CaSO_4$ decomposition at high bed temperatures.

2.3 Experimental Research

Experimental study on a lab scale FBC to find the effect of operating conditions on nitrogen oxides emissions was made by Svoboda et al. [45].

They declared that bed ash e.g. CaO, $CaSO_4$, Fe_2O_3 and fly ash freeboard concentration play an important role in the formation of NO and N_2O emissions. They also found that influence of O_2 concentration on NO_x and N_2O emissions is more pronounced at lower operating pressures

Lyngfelt et al. [46] made experiments on a 12 MW CFB boiler to optimize the system. They suggested the advanced air staging to minimize NO and N_2O emissions. They found that increase in excess air causes gradual reduction in SO_2 and CO but it increases NO & N_2O emissions. They suggested more feed points for high VM fuel i.e. biomass for even distribution of fuel and oxygen.

Abe et al. [22] made observations on a 71 MW_e PFBC for the level of emissions of gaseous pollutants. They attempted to estimate the concentration of these gases using ASH equations. They concluded that temperature is the major factor governing the reaction kinetics and hence related the concentration of NO_x and CO with T_c–the cyclone temperature and the concentration of N_2O & SO_2 with the inverse of bed temperature T_b.

Liu and Gibbs [47] carried out tests on a bench scale bubbling fluidized bed combustion to study the effects of limestone addition on NO_x and N_2O emissions. These tests revealed that in addition to reducing N_2O emissions from char

combustion, the calcined limestone enhances the conversion of char N to NO/NO_x similar to the case of volatile N. They proposed the possible reaction mechanism to explain the experimental results.

2.4 Mathematical Modeling

Altindag et al. [48] investigated the SO_2 capture in FBC of high sulfur coal mathematically as well as online concentration measurements of gaseous species along the combustor. They concluded that free board sulfur capture is enhanced significantly with recycling of elutriated sorbent particle particularly for the fuels rich in combustible sulfur.

A simplified mathematical expression to estimate SO_2 emissions from PFBC was proposed by Shimizu et al. [49]. They concluded that solid attrition of limestone particle is one of the important parameters in determining the reaction rate of SO_2 capture. They declared that experimental results agreed well with the model result.

Gungor et al. [50] developed a 2–D model of coal combustion in a CFB boiler, to predict emission species using equilibrium kinetics. They concluded that these emissions depend more on operational gas velocity than the bed temperature. CO and N_2O emissions increase with increase in fluidizing velocity. While SO_2 decrease by the increase in excess air.

The performance of PFBC was determined by Huang et at. [51] using ECLIPSE process simulator. They solved the mathematical equation using least square algorithm to predict the overall efficiency of a pressurized FBC. The predictions indicated that ash, moisture, sulfur content is found the most significant factor influencing the performance of a coal power plant.

The study of Khan et al. [52] showed that co–firing of coal with biomass is the most feasible method to increase the share of renewable energy in world energy mix. Co–firing is the most efficient with lowest risk in comparison with other available options to utilize renewable energy sources. However, there are still some obstacles that need to be removed to make co–firing more successful.

Among the available technologies, fluidized beds are proving to be one of the best because of their flexibility, stability, and efficiency. They provide the necessary window of variability needed to handle this diverse renewable fuel.

Larry Baxter [53] investigated the issues of biomass–coal co–firing and summarized the state–of–the–art in each area. He demonstrated that co–combustion of biomass–

coal offers low–risk, and is of low–cost, sustainable and renewable option which promises reduction in SO_x, NO_x and net CO_2 emissions. Technical issues associated with co–firing include fuel supply, handling and storage challenges, potential increases in corrosion, decreases in overall efficiency, ash deposition, pollutant emissions, carbon burnout, ash marketing, negative impacts on SCR performance and overall economics of the system. Moreover, co–firing may also reduce soil and water pollution depending upon the chemical composition of the biomass used, may cause slagging and fouling and affect flame location. Sami et al.[54], also explained that the different programs carried out in the United States and Europe have demonstrated that co–firing biomass with coal in large utility boilers can be beneficial to the utilities as well as to the environment. Most biomass fuels have very little or no sulfur and therefore net SO_2 emissions can also be reduced. However, co–firing of coal and biomass has gained popularity with the electric utilities producers.

Hupa [55] explained the experimental results from 12MW CFBC for SO_2 emission as function of fuel mixture during combustion of wood and bituminous coal. Their results showed that SO_2 emission is decreasing with increase in proportion of biomass in fuel mixture and vice versa for increase of coal proportion. There is almost 50% decrease in SO_2 emission with 50% biomass proportion.

Demirbas [56] studied the results of extensive application and concluded that co–firing of biomass with coal has the capability to reduce both NO_x and SO_x emission. Co–firing may also reduce fuel costs, minimize waste and reduce soil and water pollution, depending upon the chemical composition of the biomass used.

2.5 Co–Firing of Coal with Biomass

Renewable energy sources such as biomass can partly replace the fossil fuels with the consequent reduction in gaseous emissions such as SO_2, CO, CO_2 and NO_x etc. The other merits of biomass include the low risk with economic benefits. Over the past few years, co–firing of biomass with coal is gaining interest of researchers and community working in energy sector for the best utilization of renewable resources, conservation of coal reserves and reduction in gaseous pollutants [54, 57, 58].

Biomass has a comparatively higher volatile content and therefore needs more residence time in the freeboard to completely burn the volatiles. Another reason is also related to fuel composition. As biomass can have a higher ash content and such biomasses do not follow shrinking core model but rather a shrinking sphere model,

which results in an ash layer surrounding the fuel particle and makes the oxygen diffusion difficult. Also, heat exchangers located in the freeboard of common fluidized bed boilers decrease the temperature and therefore inhibit conversion of CO to CO_2. Irregular or improper feeding could result in higher CO emissions as well [59]. Larger fuel particle size and high ash content have been reported to contribute to high CO levels. Small scale units can produce high CO emissions due to shorter freeboards characterized by smaller residence times. Significant methane formation has also been observed during de–volatilization which subsequently converts into CO and CO_2 later in the freeboard [54]. In this regard, as the NO_x emissions are dependent on unburned carbon content in the fly ash, the lower the NO_x emissions, the higher the unburned carbon [60].

In the previous literature it is found that there is an increase in CO_2 emission with increase of biomass proportion which is due to insufficient combustion. But some studies reveal that CO_2 emission is less for higher biomass proportions which is not in line with the other studies. These observations signify the role of heterogeneous reactions (on the char surface), of char–carbon with CO_2 and water vapor, at typical FB temperatures [59].

Narayanan et al. [61] investigated that the co–firing of biomass with coal reduced the SO_2 emission up to 50% for maximum biomass to coal ratio of 60:40. During their study it was also found that the decrease in SO_2 remained up to 16% and 36% with co–firing of 20% and 40% biomass, respectively. Hein et al. [62] explained the results of 2–years research project launched by the European Commission in which the co–combustion, in laboratory, pilot and full–scale units was studied with the objective to investigate the effect of biomass addition on the gaseous emissions. They confirmed that co–combustion of biomass with coal has a significant effect on SO_2 reductions reaching up to 75%.

Calcium carbonate is a common sorbent used for SO_2 capture. But it is also useful for reducing CO_2 emissions. Sun et al. [63] made experiments to study CO_2 removal by carbonation of CaO in FBC. They formulated a sintering model to describe the behavior of calcination and carbonation of calcium carbonate in CO_2 absorption.

Liu and Gibbs [47] studied the effect of CaO on NO_x and N_2O emissions from char combustion using a BFB combustor. These tests revealed that in addition to reducing N_2O emission, calcined limestone also enhances the conversion of Char–N into NO_x similar to conversion of Volatile–N e.g. NH_3 and HCN into NO_x and N_2O.

Smolik et al. [30] experimentally determined the influence of calcareous sorbent on particulate emissions from AFBC. They concluded that applications of $CaCO_3$ as sorbent increased the emissions of coarse particles and reduced the fine particle emissions.

CFB Adsorption is an effective method for emissions control i.e. to utilize different sorbents to reduce or eliminate gaseous and particulates e.g. to scrub SO_2 emissions through adsorption onto calcined lime and to eliminate mercury vapors through adsorption by activated carbon etc. To analyze CFBA, Mao et al. [64] introduced a mathematical model based on 3–D Navier Stokes equations for particle flow. The numerical solution of mathematical model agreed well with a bench scale operation of a prototype CFBA reactor.

It has also been reported that the major part of Fuel–N in biomass may convert into ammonia (NH_3) during combustion, therefore, co–firing may result in lower NO_x emission. In addition to that a part of SO_2 produced during co–firing of coal and biomass is captured/absorbed by alkaline ash, thus causes the reduction in net SO_2 emission as well [65-68]. The previous studies of Narayanan et al. [61] and XIE et al. [69] have revealed a significant decrease in NO_x emissions with the increase of biomass proportion on account of the volatile products present in the biomass.

XIE et al. [69] studied the emissions in CFBC during co–firing of coal and biomass, and their results revealed a general increase in CO emissions with increase of biomass proportion owing to high volatile contents of the biomass as compared to coal. However, CO emission exhibited some haphazard results during co–firing relative to coal combustion. The higher CO emissions with greater fluctuations were eliminated with the excessive air. It has also been reported in literature that CO emission is dependent on temperature, residence time of gaseous products, mixing of fuel particles with air and oxygen concentration, Permchart and Kouprianov [70], Gutierrez et al. [71] and Armesto et al. [72].

Comparing with coal, wood used as a biomass has small amount of Fuel–N. Therefore, co–firing with the biomass is deemed to decrease NO_x emissions. The Fuel–N in biomass most probably is responsible to produce more ammonia (NH_3) content relative to HCN, with the consequent decrease in NO_x. NH_3 involves in NO_x formation, and also serves as a reducing agent to form N_2. Actually, major part of Fuel–N in coal is left in the char and forms NO_x which is reduced by the NH_3 released

by biomass. The operating conditions play a pivotal role in the release of HCN (form of fuel–N) of coal–volatiles, which further oxidize to NO_x and N_2O [73, 74].

In FBC systems, the temperature is usually below 900 °C, however thermal NO_x are normally produced at the temperature above 1500 °C [75]. So the probability of thermal NO_x formation is eliminated, thus only fuel NO_x are involved [76].

2.6 Oxy–fuel Combustion

Oxy–fuel combustion of coal is gaining attention for capturing CO_2 and to protect the atmosphere from higher CO_2 concentrations. Tan et al. [77] studied the effect of SO_2/CO_2 recycling on NO_x and SO_2 emissions. In this scheme CO_2 concentration is initially increased by eliminating nitrogen from air before combustion and by recycling a part of the flue gas. This option is under active research to reduce CO_2 concentration in the atmosphere.

Jia et al. [78, 79] conducted a series of tests on oxy–fuel firing of coal in CFBC. Test results showed that stable combustion conditions could be obtained with a CO_2 concentration in the flue gas above 90%. And the co–firing of coal with biomass and wood pallets did not affect the combustion conditions.

Liu et al. [80] studied the mechanism of direct sulfation of $CaCO_3$ using O_2/CO_2 coal combustion for low NO_x & high sulfation efficiency. The sulfation efficiency in conventional coal combustion is usually low because of sintering of the sorbent. In contrast in O_2/CO_2 the calcination is inhibited and the limestone is subjected to direct sulfation. The diffusivity of product layer is not affected by sulfation because of its porous structure owing to CO_2 formation [81].

Jia et al. [82] examined a 800 kW pilot plant for the emissions of SO_2 & NO_x during oxy–fuel CFB combustion test. They found that emission of CO and NO_x are comparable but there is increase in SO_2 emission due to poor sulfation. They suggested further exploration to reduce SO_2 emission by using the petroleum coke.

Roy et al. [83] studied NO_x formation in Oxy–fuel coal combustion. They found a lower concentration of NO emission under CO_2–CO conditions as compared to air conditions but concentration of N_2O was higher and it further increased by recirculation.

2.7 Trace Elements

Naturally trace amounts of mercury is present in coal and during combustion it is emitted in the form of vapors and particulates. Yoo et al. and Pudasainee et al. [84, 85] studied the mercury emissions from the coal power plants. They observed that air pollution control devices i.e. selective catalytic reducer (SCR), electrostatic precipitator and flue gas desulfurizer in series can achieve the co–benefit for mercury removal up to 75%.

Furimsky [86] studied the trace element emissions such as As, Pb, Cd, Se and Hg from FBC of coal. He observed that limestone had a diluting effect on trace element content of ash and concluded that these emissions can be minimized by raising the air to coal ratio. The calculation procedure was based on chemical equilibrium involving minimization of total free Gibbs energy.

There are considerable challenges in achieving an optimized and environment friendly coal firing system. In the literature, number of investigations and research findings are available in connection with the emissions control in FBC of coal but most of these efforts cover limited aspects of combustion generated pollutants.

It was concluded after going through the research efforts made by the scientists in this field that for the simultaneous reduction of major harmful emissions from CFBC, a comprehensive experimental work to be performed to know the effects of all possible factors that may influence the emissions of known gaseous environmental pollutants. In this regard FBC experimental facility located at low carbon combustion center, University of Leeds, was used with all the required equipment and the facilities to perform a detailed series of experiments. Detail of FBC experimental facility could be provided here.

This dissertation based on experimental work is intended to determine the effect of all possible factors that can influence the emissions of all major gaseous environmental pollutants. The experimental work was performed on a pilot scale FBC combustor at the University of Leeds, Leeds UK.

In the experimental work the effect of number of operating variables on the emissions of CO, CO_2, NO_x, and SO_2 etc. have been studied. The influencing parameters taken into account are the bed combustion temperature, excess air, gas velocity through combustion, calcium to sulfur molar ratio, limestone particle size, co–firing with

biomass, Effect of different percentages of biomass on the emissions in FBC Pilot scale facility.

The experimental results were discussed in detail with the most probable reasons and the concluding remarks of the author are expected to be very useful in updating to CFBC designs for the minimum possible emissions.

CHAPTER NO. 3

FLUIDIZED BED COMBUSTION

Fluidization is defined as a process in which the fine solid particles are transformed into a fluid like state through contact with an upwardly moving gas. Bed is the name given to the body of gas/air carrying solid particles with it. A fluidized bed displays the characteristics similar to those of a liquid i.e. an object denser than the bulk of the bed will sink, while one lighter than the bed will float. In FB combustor the particles are well mixed with air and remain in the semi–suspended state during combustion.

Fluidization vessel or combustors are commonly vertical cylinders but they may have rectangular or any other cross–section. The height of the combustor is determined by the residence time required by the coal particles to complete their combustion reaction. This time depends mainly on the average size of the particles and the velocity of air through the bed, called superficial velocity of the combustor is made divergent i.e. the minimum cross–section at the bottom and gradually increasing with height as shown in Fig. 3.1.

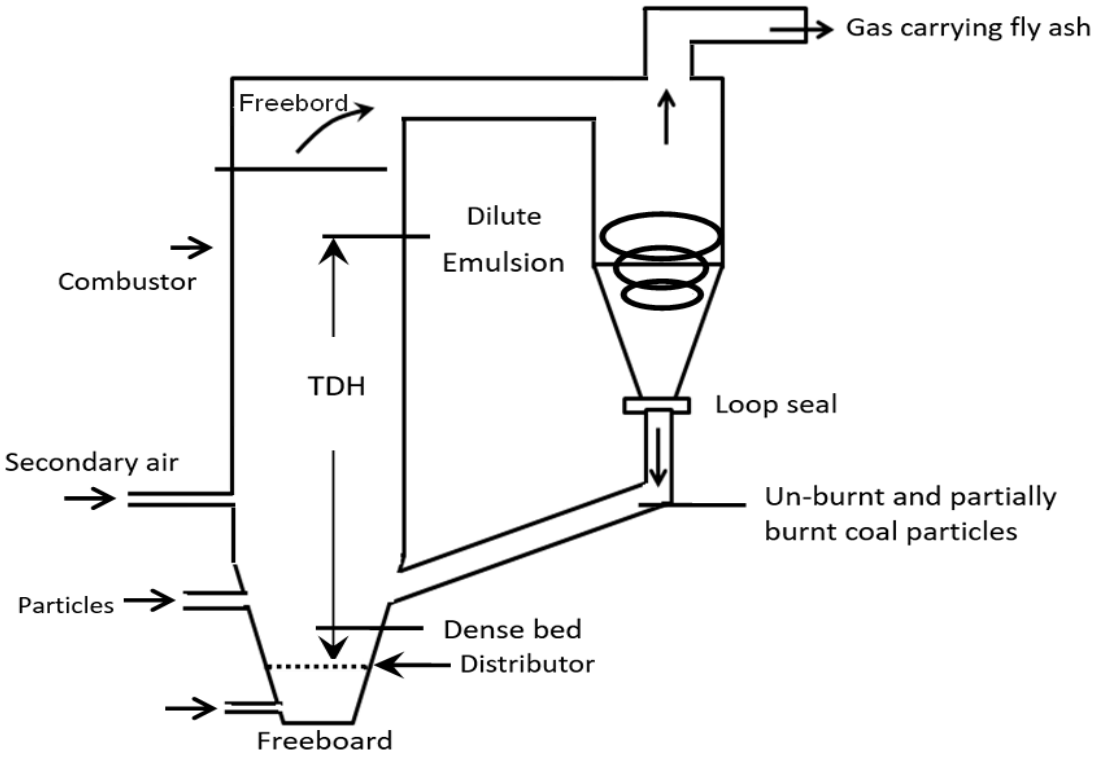

Fig. 3.1 Schematic of circulating fluidized bed combustion (CFBC) system [25]

This configuration enables the bed to expand uniformly when superficial velocity of air is increased, thus increasing the size of voids i.e. the empty spaces between particles. This divergence in cross–section is also helpful for uniform fluidization. The bed density is maximum in the lower part close to distributor and it reduces gradually with the height so the upper part carries a dilute emulsion of particles and the gas.

The distributor is used for uniform supply of fluidizing air. In small sized plants e.g. lab scale FB combustor it is a simple perforated steel disc; while in larger plants there are number of designs of distributors in use as shown in Fig. 3.2. A fluidized bed has an open space above its bed.

The lower part surface known as free board. In bubbling regime, the bubbles erupt at the surface of the bed and leave their particles carried with them into the freeboard. Amongst these the lighter particles are entrained with the gas due to its drag while the larger particles disengage from the gas in the freeboard and return to the dense bed due to gravitational force. This process of disengagement of particles reduces along the height of the freeboard and beyond certain height the number of particles disengaging from the gas is negligible. This height is called transport disengaging height (TDH). The cyclone separators are located above TDH.

A cyclone separator is a simple device used for separating the solid particles from the flue gas for a minimum pressure loss as shown in Fig. 3.3. The upper part of the cyclone is cylindrical in shape and the lower part is conical. The gas–solid suspension enters the cyclone tangentially through the rectangular duct. The solids being denser than the flue gas move in the outer vortex along the walls of cyclone under the action of centrifugal force while the flue gas moves upward through the inner vortex. The solid particles slide down the walls and are collected at the bottom for recycling. Some fine particles which escape through cyclone entrained with the gas are captured in the bag house or electrostatic precipitator before passing to the stack.

The coal and sorbent (limestone) particles are continuously injected through the ports located in the lower section of the combustor. The number of feed ports depends on the size & power of the plant. In larger plants, feed ports are equally spaced for uniform supply of particles. The spreaders are also used for uniform distribution of particles in some plants. Over bed feeding is used frequently while under–bed feeding is better for uniform heating. The coal particles are a minor fraction in the bed material about 3–5%, other matter being bottom ash, spent sorbent particles, silica

sand and synthetic materials used to avoid agglomeration in the bed. The bed temperature is controlled primarily by adjusting the coal feed rate. The fluidizing air is distributed into primary and secondary air for lower emissions level of NO_x. The primary air enters the combustor below the distributor while secondary air is injected at some height above the dense bed.

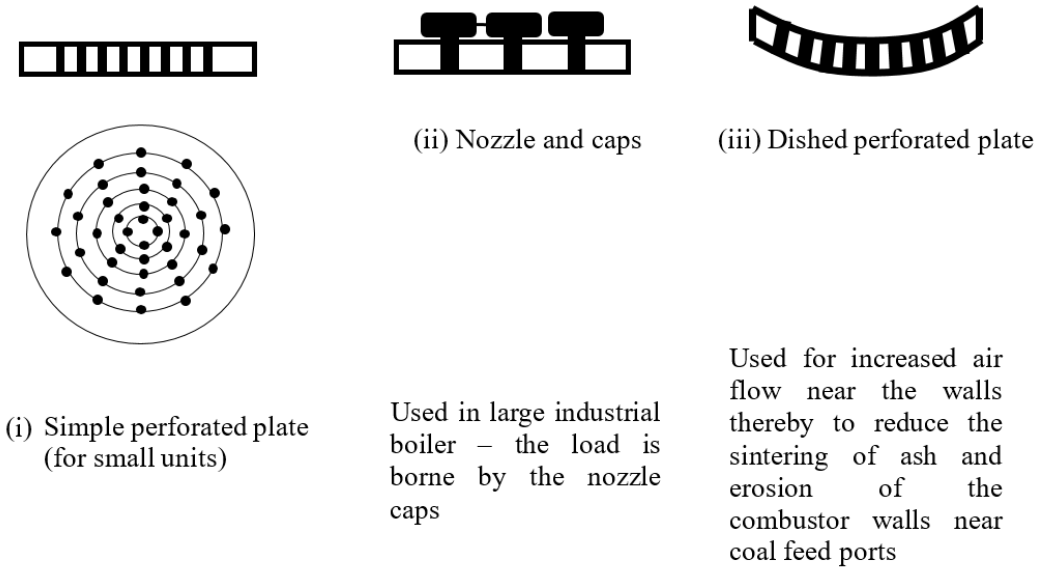

Fig. 3.2 Types of air distributor for FBC [25]

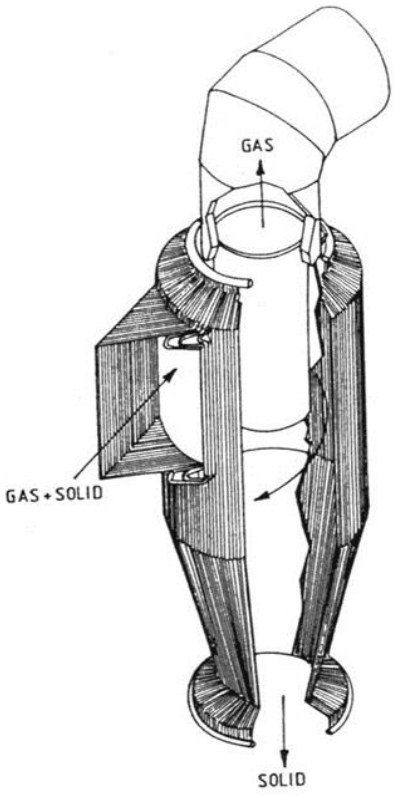

Fig. 3.3 A pictorial view of cyclone separator [25]

In a fluidized bed combustor, the fluidizing air has to lift a large mass of solids against gravity and overcome the resistance of distributor. It consumes a considerable amount of energy up to 7% of the total power generated. This is the major issue or the drawback of FBC plants that reduces the overall efficiency.

3.1 Hydrodynamics of Coal Combustion Systems

The hydrodynamic state of a fluidized bed depends on the velocity of flow through the bed and the size & density of particles. In a static or fixed bed the coal pieces in the size range of 5 mm to 30 mm are sitting on a stationary perforated grid through which the combustion air passes to oxidize the carbon in the coal particles. The velocity of oxidizing air is low and the particles do not move relative to each other. This system has low combustion efficiency and high NO_x and SO_2 emissions that was neglected in the past. Effect of fluidizing velocity on hydrodynamic regimes is given in Fig. 3.5.

3.1.1 Minimum Fluidization Velocity

When the velocity of air through a bed of coal particles in the size range of 0.1 mm to 0.5 mm is increased, the pressure–drop across the bed increases. The bed expands and the void fraction increases. When the pressure drop equals the weight of bed material divided by the cross–sectional area of the column i.e. the drag force exerted by the moving air on the particles just balances the weight of the bed, the bed is called just fluidized and the velocity of the air is called minimum fluidization velocity U_{mf} [87]. This velocity can be calculated by equating the above mentioned forces:

$$\begin{aligned}&(\text{pressure drop through the bed})(\text{area of the bed})\\&= (\text{vol of the bed})(\text{fraction of vol occupied by the solids})(\text{density of particles}\\&- \text{density of gas}) \times \text{gravity}\end{aligned}$$

$$\Delta p \times A_{cs} = (A_{cs} \times L)(1-\epsilon)(\rho_p - \rho_g)g \qquad (3.1)$$

$$\frac{\Delta p}{L} = (1-\epsilon)(\rho_p - \rho_g)g \qquad (3.2)$$

where ϵ is the void fraction.

The pressure drop across the bed has been determined experimentally for different Reynold numbers i.e. combustor dimensions and particle sizes. Substituting for Δp and expressing it in terms of R_e & A_r, the following empirical relationship has been agreed upon to calculate minimum fluidizing velocity as given in Fig. 3.4 [25].

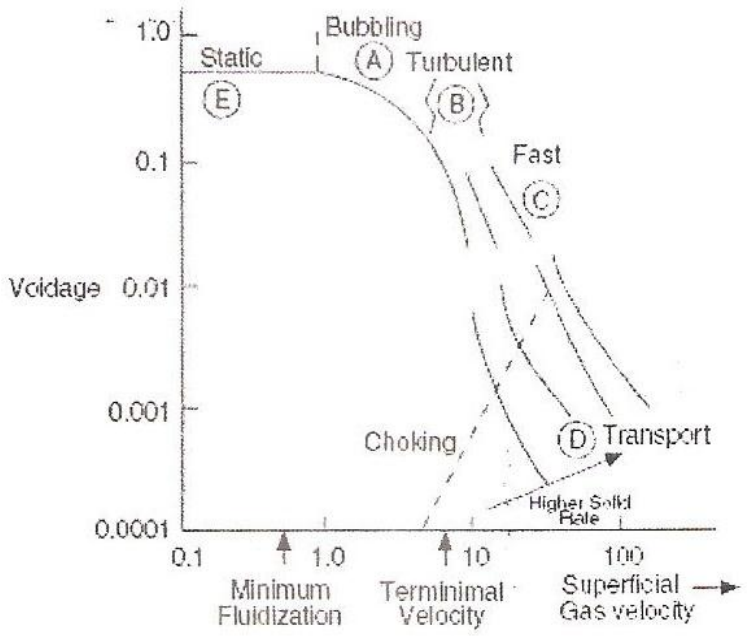

Fig. 3.4 Different gas–solid flow regimes [25]

$$Re_{mf} = \frac{U_{mf}.dp.\rho_g}{\mu_g} = [(27.2)^2 + 0.408\ Ar]^{0.5} - 27.2 \qquad (3.3)$$

Where Ar = Archimedes number = $\frac{dp^3(\rho_p - \rho_g)\rho_g.g}{\mu g^2}$

dp = mean particle diameter

ρ_p = density of particle and μ_g and ρ_g are the viscosity and density of the gas

For a particle of dp = 0.1 mm, U_{mf} = 2.04 cm/s and for dp = 2 mm, U_{mf} = 1.67 m/s

3.1.2 Bubbling Fluidized Bed (BFB)

When the velocity of air is increased slightly above U_{mf}, the gas bubbles are observed moving up in the bed. The velocity at which this occurs is called the minimum bubbling velocity U_{mb}. These bubbles are gas voids with very little or no solids in them. The gas solid suspension around the bubbles and elsewhere is called emulsion phase. These bubbles are helpful in better solid–air mixing as well as in raising the coefficient of heat transfer but at the same time they increase the entrainment of partially burnt coal particles with the outgoing gas thus reducing the combustion efficiency. The bubble size increases with the gas velocity, particle diameter and its distance above the distributor. They grow to a maximum size depending on U & dp and beyond that they collapse.

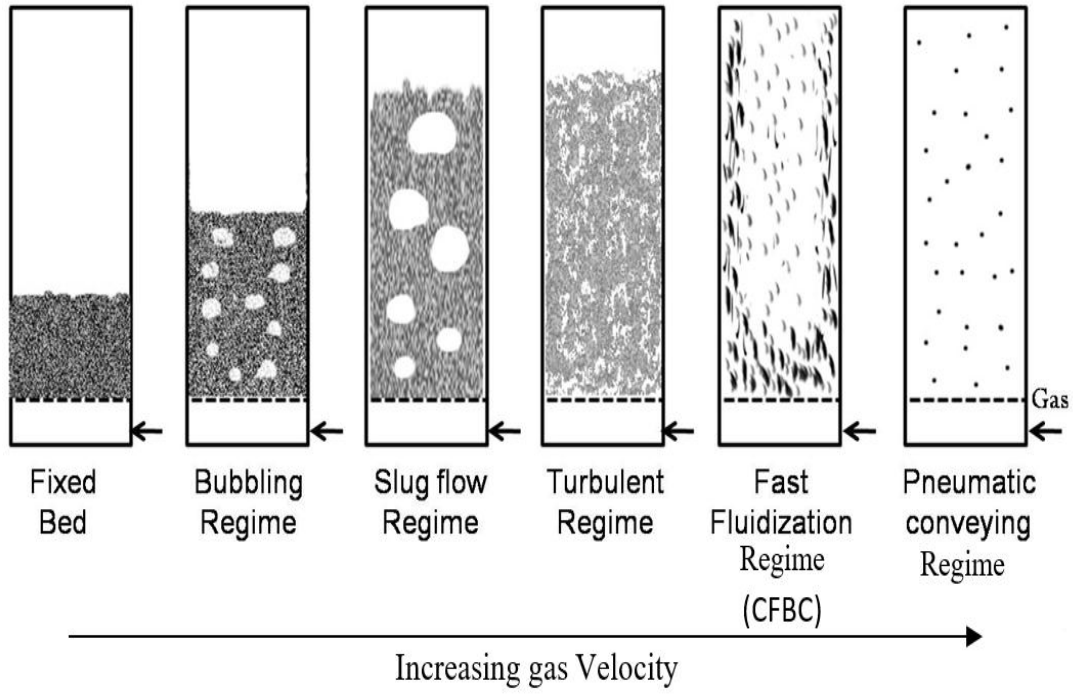

Fig. 3.5 Effect of fluidizing velocity on hydro–dynamic regimes [25]

The static pressure inside the bubbles is higher and constant while the pressure in the emulsion phase is lower and decreases with height. The bubbles erupt when they reach the surface of the bed ejecting solids to the free board. The solid concentration in the gas reduces along the height of the bed and remains unchanged beyond TDH. The minimum bubbling velocity can be found using the following relationship.

$$U_{mb} = 2.07 \exp(0.176\ F)\ d_p \frac{\rho_g^{0.06}}{\mu_g^{0.347}} \quad (3.4)$$

Where F is the mass fraction of the particles less than 45 μm

It is found that in case of particles with dp = 0.3 mm and above

$$U_{mb} \approx U_{mf} \quad (3.5)$$

The bubble size increases with increase in gas velocity. In deep beds when the bubble size reaches above 0.6 D (where D is bed diameter) the bed is called slugging. The larger bubbles, called slugs, because pressure unbalances in the bed and make the fluidization poor. The slugging velocity can be determined by the following equation:

$$U_{sl} = U_{mf} + 0.07(gD)^{0.5} \quad (3.6)$$

It is observed that slugging does not occur in all beds under normal operating conditions [25].

3.1.3 Turbulent Regime

Further continuous increase in the superficial velocity change the hydrodynamics of the bed from bubbling to turbulent regime. The bed expands further and the bubble phase loses its identity due to rapid breakup of bubbles. This transition starts at the superficial velocity U_c and completes at U_k. (Some restricted relationships for U_c and U_k are available in literature). So the terminal velocity is an average velocity of flow in a turbulent fluidized bed. A turbulent bed is highly active and expanded bed having a better gas–solid mixing. In turbulent regime the pressure drop across the bed fluctuates rapidly and the bed surface is highly diffused.

3.1.4 Fast Fluidization Regime

This is a regime that lies between the turbulent and pneumatic transport regime. In this regime one observes a non–uniform suspension of particles agglomerates moving up and down in a dilute upwardly flowing gas–solid continuum. Agglomerates or clusters are formed by temporary get–together of coal particles. They rise up in the core of the furnace with rising gas stream and move down along the walls of the furnace when they become larger and denser.

The above mentioned regimes are called captive regimes because majority of the particles remain within the combustor and there is no large scale migration of particles from the combustor along the outgoing gas.

3.1.5 Pneumatic Transport Regime

This is the hydrodynamic regime of pulverized coal combustion system where very fine coal particles are blown up by very high gas velocity and the particles burn under entrained condition leaving no bottom ash. The volume fraction of solids in the combustion zone is the lowest and the pressure of the gas is uniform throughout the combustor. The combustors are made long enough to ensure complete combustion of coal particles in a single pass.

Table 3.1 gives a comparison of combustion parameters of different coal firing systems. Amongst these, the circulating fluidized bed boiler which operates in an intermediate state between the bubbling and pneumatic transport regime has a number of unique features that make it more attractive than any other coal combustion systems.

Table 3.1 Comparison of fixed, bubbling, circulating and pulverized coal combustion systems [87]

Characteristics	Fixed Bed / Stoker fired	Bubbling Fluidized Bed	Circulating / Fast Fluidized Bed	Pulverized / Pneumatic Transport
Coal particles size av. diameter (mm)	6–30	0.03–3	0.1–0.5	<0.1
Air velocity through combustor (m/s)	1–2	1.5–2.5	3–12	15–30
Height of the bed (m)	0.2	1–2	10–30	27–45
Combustion efficiency (%)	85–90	90–96	95–99	99
Heat transfer coeff (W/m^2K)	50–150	200–550	100–250	50–100
NO_x emissions (ppm)	400–600	300–400	50–200	400–600
SO_2 capture (in furnace) percent	None	80–90	80–90	Small

3.2 Effect of Particle Size on Hydrodynamics

It is found experimentally that in a fluidized bed particles of different sizes behave differently under same operating conditions. So the particles have been classified into four groups A, B, C and D depending on their mean particle size.

Group A: 30–100 µm (Aeratables)

These particles fluidize well, expand considerably before bubbling. Many CFBC use this group of particles.

Group B: 100–500 µm (Sand like)

Majority of CFBC use these particles. The bubbles appear just after minimum fluidization i.e. $U_{mb} = U_{mf}$.

Group C: <30 µm (Cohesive particles)

Fine particles. Clump together and form agglomerates because of large cohesive forces, an attempt to fluidize results in channeling.

Group D: >500 µm (Spoutable)

Largest particles, require higher velocity to fluidize, used in spouted beds.

Table 3.2 Characteristics of four groups of particles [87]

Group	C	A	B	D
Size Range (µm)	<30	30–100	100–500	>50
Expansion of bed	Low	High	Medium	Medium
Minimum bubbling velocity U_{mb}	No Bubbles	> U_{mf}	= U_{mf}	= U_{mf}
Solid Mixing	Very low	High	Medium	Low
Channeling / Sputable	Severe channeling	Little Channeling	Shallow spoutable	Readily spoutable

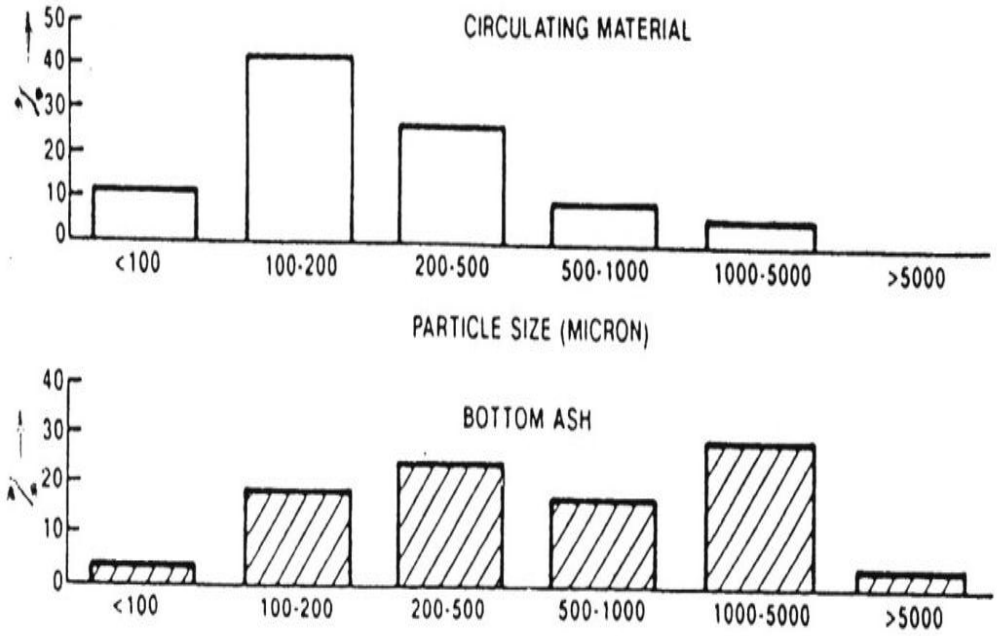

Fig. 3.6 Particle size distribution in a CFB plant [14]

Figure 3.6 shows particle size distribution in circulating material as well as in the bottom ash of a commercial CFB plant. The coarser particles tend to congregate near the bottom of the furnace while fine particles are entrained out of the cyclone as fly ash. Average bed solids i.e. from 100 microns to 500 microns (Group B) circulate through the bed and around the primary loop.

3.3 Pressurized FBC Systems

Majority of the circulating and bubbling FBCs operate under atmospheric pressure conditions. These are simpler in construction and operation. Their overall efficiency lies between 25 to 30 percent depending mainly upon the quality of fuel. For higher efficiencies both of these systems can be operated at higher pressures from 0.2 to 1.2 MPa and above. In case of pressurized CFBC the heat release rate increases manifolds depending on the pressure in the combustor while the overall efficiency rises from 30 to 42%.

The pressurized CFBC works on the principle of combined gas–steam cycle i.e. it produces high pressure high temperature gas to operate a gas turbine and it also produces high pressure steam to operate a steam turbine simultaneously. The combustion of coal takes place under high pressure in the CFB combustor and the hot gas produced is cleaned and expanded through a gas turbine. The exhaust gas from the gas turbine is used to generate steam in a waste heat boiler. The steam is also produced in water tube section placed in the CFB combustor. The steam generated partially in the waste heat boiler and partially in the pressurized CFB combustor is used to drive a steam turbine for developing mechanical power. The overall efficiency of such combined cycle is above 40%. The coal gasification combined cycle known as IGCC gives even higher efficiency up to 50 percent. But due to some operational problems occurring in the pressurized system (mainly the thermodynamics instability) these systems are not as successful in operation as Atmospheric CFBC.

3.4 Merits of Circulating Fluidized Bed Combustion (CFBC)

One of the major attractive features of CFBC is the fuel flexibility that is it can burn variety of solid fuels efficiently e.g. coal of any grade even with 60% ash, agriculture waste (biomass), municipal solid waste (MSW), used rubber tires and polythene bags etc. it has high combustion efficiency above 95% because of better gas solid mixing, higher burnout rate and particularly the recycling of un–burnt particles. Coarse fuel particles are recycled again and again until they are completely burnt.

The second major advantage is the favorable emissions characteristics. Over 90% of SO_2 is eliminated within the combustor by adding a small quantity of limestone which is a cheaper sorbent. The CFBC require smaller quantity of $CaCO_3$ than a BFBC because it provides a longer time contact of SO_2 and CaO. The quantity of limestone

can be further reduced by reducing their particle size thus allowing maximum utility of $CaCO_3$. Moreover, a CFBC generates lower NO_x when combustion air is distributed into two stages i.e. 60 to 90% of stoichiometric air in primary stage and the remaining makeup quantity in the secondary stage.

Another merit of the CFB boiler is the high heat release rate up to 4.5MW/m^2 of cross–sectional area; this is because of high superficial velocity and excellent gas–solid mixing. This will in turn reduce required grate area of the furnace as well as the number of feed ports. Moreover, it has quick response to load variation and a higher turn down ratio up to 4.0 without affecting the performance of the plant considerably. These are some of the reasons that make the CFBC technology widely accepted and one of the advanced environment–friendly coal combustion technology.

3.5 General Arrangement of a CFB Boiler

In a circulating fluidized bed boiler, the heat transfer surfaces are distributed into two sections.

i) The primary section comprising of combustor (furnace), boiler tubes, cyclone separator, solid recycling tube (return leg) with loop seal.
ii) The secondary section or back–pass that consists of super heater, economizer, and air–heater etc. It is also called convective section.

The boiler (evaporator) is sub–divided into water walls, cross tubes and wing walls as shown in Fig. 3.7. The water walls in the lower section of combustor are covered by the refractory material to protect their metal from the chemical attack (erosion) of prevailing environment. In some designs an external heat exchanger is employed that absorbs the load fluctuation without affecting the bed temperature. A part of the boiler tubes is placed in this heat exchanger. Some super heater tubes maybe distributed in the furnace and they are called Omega super heater.

The bed is pre–heated by a startup burner. The coal particles are continuously injected through the feed ports located in the lower section of combustor above the distributor. They are sometimes fed into the loop seal from which it enters the furnace along with returned hot solids. The bed solids are well mixed throughout the height of the combustor so the bed temperature is nearly uniform in the range of 850–900 °C.

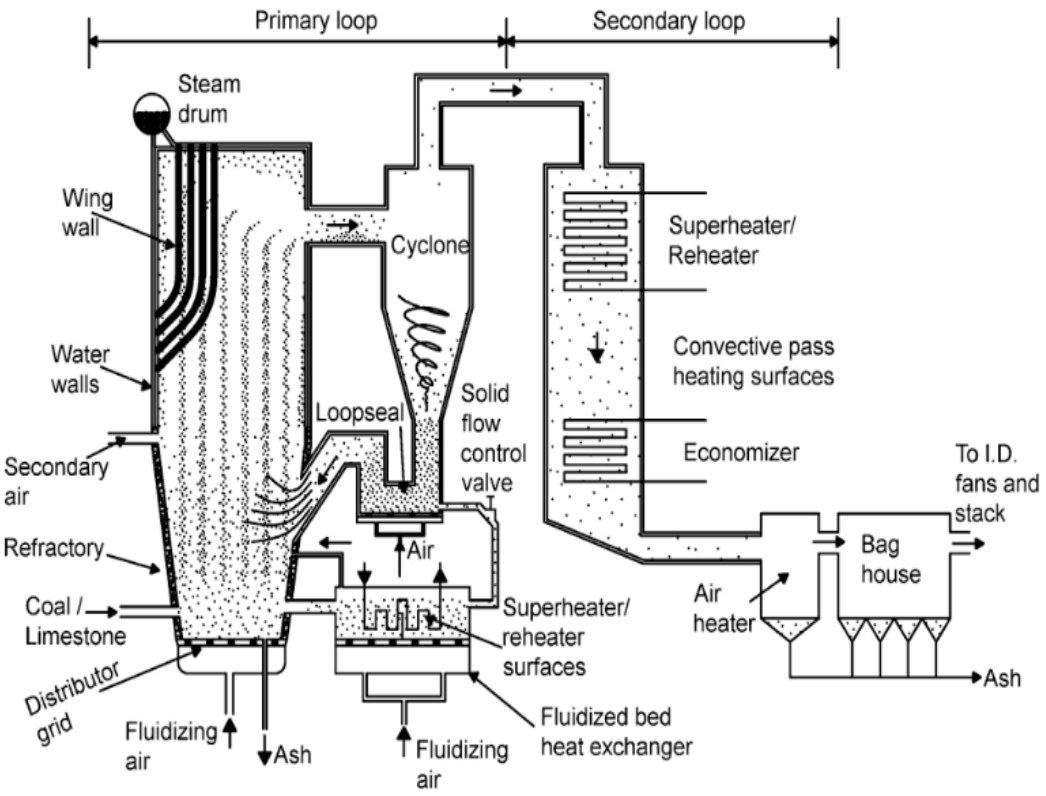

Fig. 3.7 General arrangement of a CFBC plant [25]

The majority of the coal fed into a CFB boiler is in the size range of 100 µm (0.1 mm) to 500 µm (0.5 mm) but there are some fine particles less than 0.1 mm and some coarse particles up to 5 mm size as shown in Fig. 3.6. The coarse particles of sorbent and un–burnt char are captured in the cyclone separator and recycled back near the base of the furnace. Finer solid residues i.e. fly ash and spent sorbent generated during combustion and desulfurization leave the furnace escaping through cyclone separator are collected by a bag house or an electrostatic precipitator located further downstream. The primary sub stoichiometric air is injected through the floor gate of the furnace and the secondary air is added at some height to complete the combustion.

The lower section of the combustor is potentially very erosive region as it contains large particles not elutriated from the bed. Hence the heat transfer tubes should not be installed in this section and the water walls should be protected by the refractory material. Ash is drained periodically from the drain port close to distributor.

As mentioned earlier that coal particles are a minor fraction about 3–5% of the bed material. Others are ash, used sorbent, silica sand etc. Some other inert materials are added to the combustor to maintain the bed inventory which is required for stable

CFB operation. It is found that higher suspension density is the major factor for the high heat transfer co–efficient.

Table 3.3 Hydrodynamic regimes in CFB power plants [25]

Components of the plant	Hydrodynamic Regimes
Combustor (below secondary air level)	Turbulent
Combustor (above secondary air level)	Fast
Standpipe (return leg)	Moving packed bed
Back Pass	Pneumatic transport
External Heat Exchanger	Bubbling

As mentioned earlier that coal particles are a minor fraction about 3–5 % of the bed material. Others are ash, used sorbent, silica sand etc. Some other inert materials are added to the combustor to maintain the bed inventory which is required for stable CFB operation. It is found that higher suspension density is the major factor for the high heat transfer co–efficient.

The circulating fluidized bed has a number of advantages over other firing system e.g. bubbling bed particularly in larger power plants using low grade fuels where control of NO_x and SO_x emissions is of prime importance.

CHAPTER NO. 4

COAL GEOLOGY, COMBUSTION AND EMISSIONS

4.1 Geology

Pakistani region under the current study is shown on geological map as given in the Fig. 4.1. The Salt Ranges and Trans Indus Ranges are situated in Kohat–Potwar geologic province, which is bounded by the Parachinar–Murree fault in the north, the Kurram fault in the west and the Jhelum fault in the east. Indus geologic province is located on the south of the Salt Range [33]. The Kohat–Potwar geologic province is characterized by regional geological structures as shown in Fig. 4.2. The mountains of Kohat and Potwar Plateau falls are known as Sub–Himalayas. The Himalayan orogeny is the outcome of collision between the mighty Eurasian Plate drifting southward with the Indo–Pak Plate drifting northward. The collision started somewhere in Eocene (less than 55 million years ago). Both the plateaus are separated by Indus River [88]. Structurally, these plateaus are fold and thrust belts. In the north they are bounded by Main Boundary Thrust (MBT), while in the south these are bounded by Main Frontal Thrust (MFT) [89]. Depositional record of the Kohat–Potwar geologic province is known from late Proterozoic to Holocene.

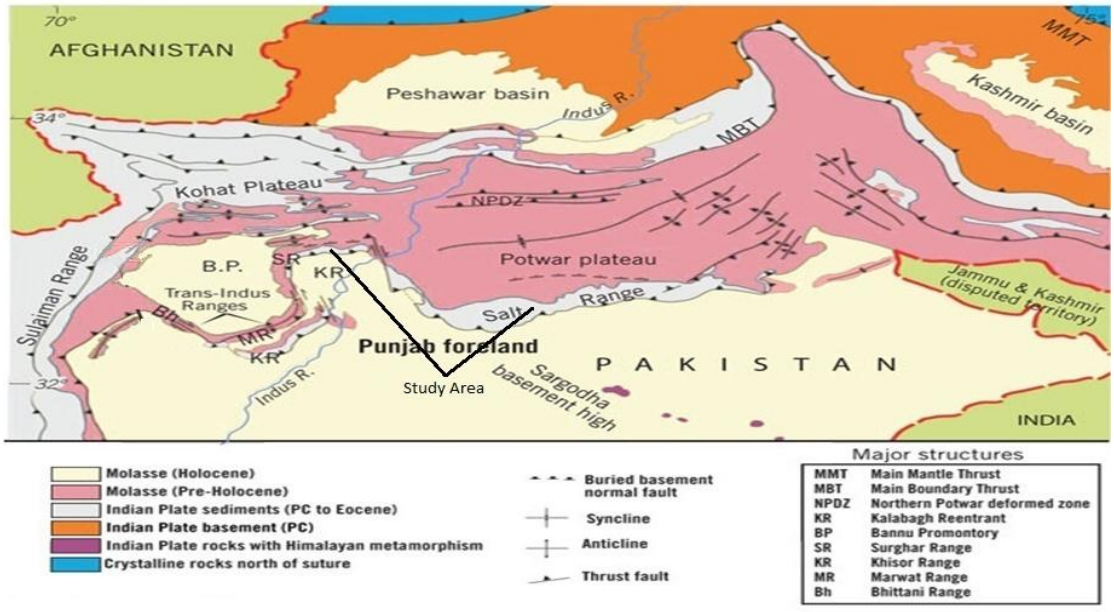

Fig. 4.1 Salt Range and Trans–Indus (Surghar) Range on geological map (Modified after Kazmi and Rana, 1982) [13]

The Salt Range as rightly said 'The Museum of Geology' extending about 250 km east–west and about 7–8 km north–south is the most southern part of the Himalayan orogeny. It is exposed along the Main Frontal Thrust (MFT). The ramp–like structure dipping north, verging south on the Indo–Pak Plate seems to be responsible for the Salt Range thrust (a part of MFT). On the east, the Salt Range terminates along the Jhelum Fault and in the west it terminates with the Kalabagh Fault and further it runs in north–south direction [90].

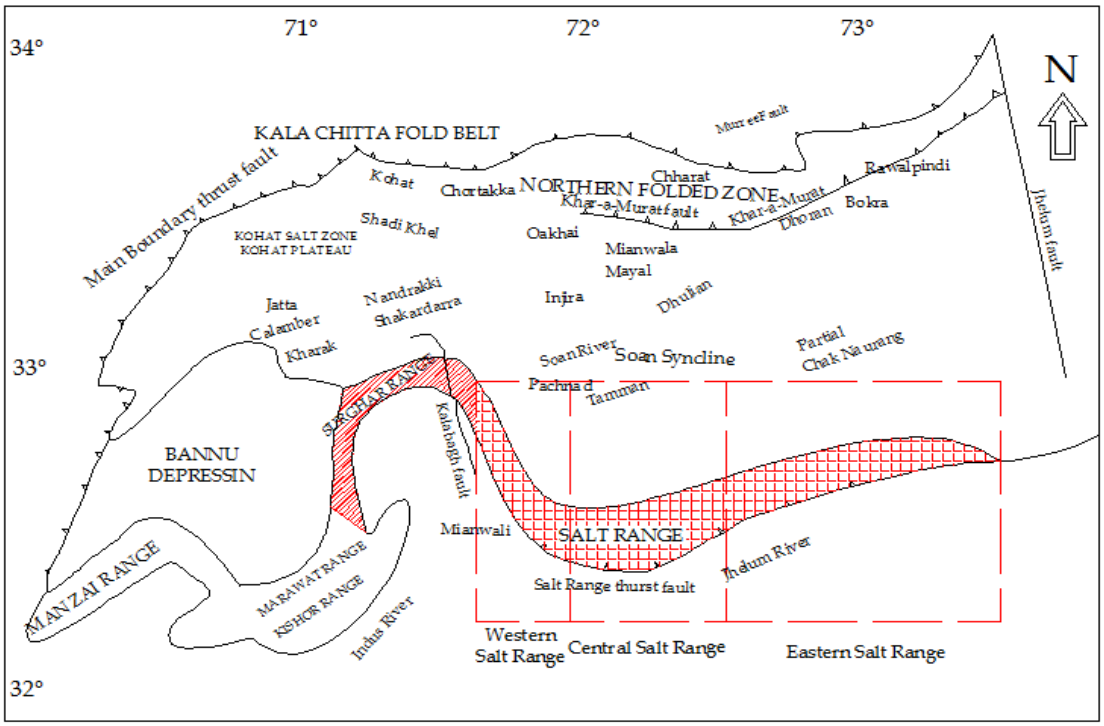

Fig. 4.2 Regional geological structures of the Kohat–Potwar geologic province (Modified after Wandrey et. al. 2004) [13]

4.2 Stratigraphy

Coal of Salt Range and Trans Indus Range is found at three different stratigraphic horizons, i.e. rocks of Permian age, Hangu and Patal formations of Palaeocene age. However, the age range of stratigraphic units of the Salt Range is from Precambrian to Quaternary as shown in Fig. 4.3. Permian coal is the oldest one, which is located in the Western Salt Range and is limited in quantity. Palaeocene coal is younger and is extracted from Hangu and Patal formations, and it is available in abundance. This coal is mined from Eastern and Central Salt Range and Trans Indus Range.

The coal seams, 18–20 m thick in this area, are generally developed in the middle part of the Patala Formation [13, 34].

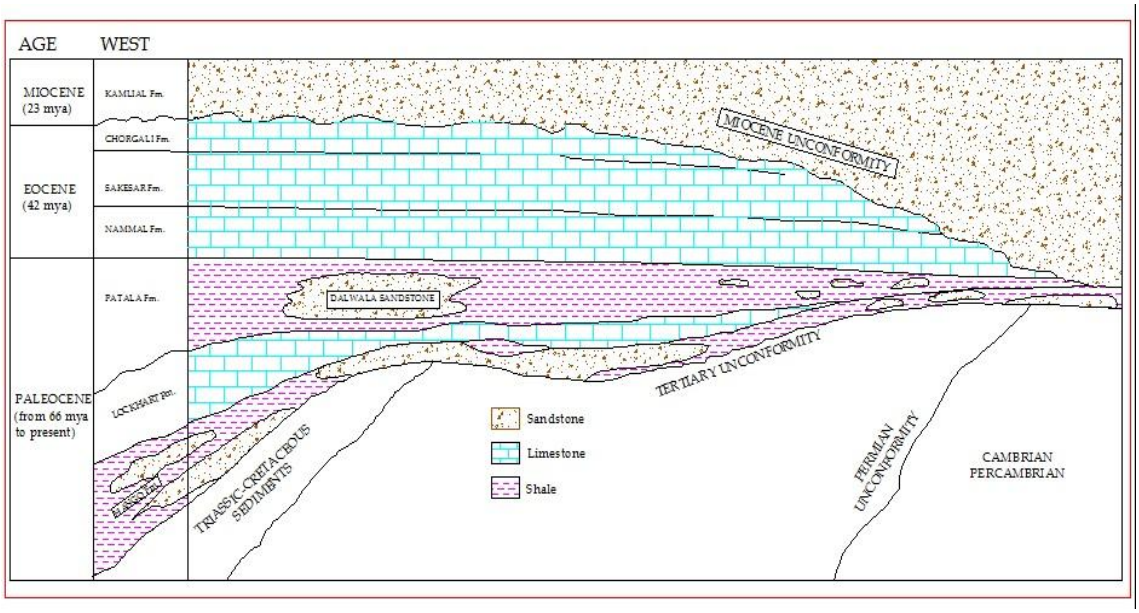

Fig. 4.3 Generalized east–west cross–section through the entire Salt Range (Modified after Snowden report, 2012) [13]

4.2.1 Eastern Salt Range

The coal mining in the Eastern Salt Range was started in the 1880's and the mines have been well developed with the passage of time. The area from Ara to Nilawahan shows the coalfields of the Eastern Salt Range as shown in Fig. 4.2. However, extensive mining activities are currently being carried out in Ara and Dandot. In previous literature, the workable coal seam of this area is known as 'Dandot coal seam'. Clay and sand partings split the coal bed into two or more coal benches/seams in some areas, but generally only one coal layer is worked. Coal seam of 1m thickness is being mined at some places, while thin coal seams ranging from 15–22 cm are also mined out at other few places. For example, a poor quality pyritic coal, with thickness bigger than 1.2 m, has been measured in the east of Khewra at Dalwal, thickness of coal seam ranges from 0.3 to 1.2 m and northwards, the coal seam varies from 15 to 22 cm. Eastwards, the coal seam is a few centimetres thick only in the Dalwal and Nilawahan area [91].

4.2.2 Central Salt Range

The coal mining in the Central Salt Range was started in the beginning of the 20th century at Katha collieries. The coal seams are not consistent in thickness ranging from 0.08 to 1.5m. The absence of the coal in certain areas is attributed to both tectonic and no depositional causes. Generally, the coal is the thinnest in the north and the thickest in the south of the coalfields. In the western part, siltstone and sandstone are at the base of the coal seam, while in the eastern part clay stone and shale form the coal floor. Facies change from sand and silt to clay stone is observed in the central part of the coalfield. The roof of the coal seams is mostly capped by shale, but sandstone and siltstone are also present in various locations. This coal seam is frequently inter–bedded with sand, silt and shale bands [91]. Such mineral intercalations, resulted in high ash content, reduce coal quality [31, 92, 93].

4.2.3 Western Salt Range

Permian coal is found at Buri Khel (32°41'N, 71^{o}38'E) in the Western Salt Range, at the top of the Tobra Formation. The Permian rocks in other parts of Salt Range are devoid of coal, although in some cases coal streaks are found in the upper part of the Tobra Formation and Warcha Sandstone. The maximum mineable coal seam in this area is 162 cm thick and the average thickness of the coal in Buri Khel area is 62 cm. Sandstone lies at the roof and floor of the coal seam, which laterally passes into the clay stone facies [91].

Coal is a heterogeneous mixture of organic and inorganic materials. Its characteristics vary widely between seams and within a seam at different elevations and locations in the coal mines. There are four well known grades of coal i.e Anthracite being the highest ranked, bituminous and Sub–bituminous the mediums and Lignite the lowest ranked coal. These types have further sub–classification and ASTM has classified coal in 13 grades based on the amount of volatile matter contained in, the fixed carbon and the calorific or heating value of the coal. The summary is given in table 4.1.

The volatile matters that may contribute up to 50 percent by weight in a coal sample are the gases and vapors released through the pores of a coal particle when it is heated by the hot environment in the combustor. The VM may consist of CO, CO_2, CH, CH_4, C_2H_6, C_3H_8 etc. and H_2, H_2S, HCN, NH_3, NH_2 etc. Most of these gases are combustibles and burn before the combustion of coal (char).The fixed carbon in a

sample of coal means the amount of carbon in solid form present in the sample. It varies from 30 to 93 percent in different grades of coal.

Table 4.1 ASTM Classification of coal (Summarized) [94]

Coal Types	Fixed Carbon (%)	Volatile Matter (%)	Calorific Value (MJ/Kg)
Anthracite (3 Grades)	85–93	0–13	33–35
Bituminous (5 grades)	69–85	14–30	26–32
Sub. Bituminous (3 grades)	55–68	30– 40	19–25
Lignite (2 grades)	30–54	30–40	12–15

The non–combustibles which contribute the residual ash may contain a large number of oxides of different metals listed in table 4.2. Some of these compounds are reactive during combustion process, some of them act as catalysts while some of them remain just inert. The knowledge of composition of coal ash is useful for estimating and predicting the fouling and corrosion/erosion characteristics of coal. More over trace element such as As, Pb, Cd, Se and Hg are also found in the coal and during combustion process their oxides are also emitted in vaporized or gaseous form [87].

Table 4.2 Composition of coal ash in different coal grades [87]

Oxides of Metals	**Composition (%)**
SiO_2	20–60
Al_2O_3	10–35
Fe_2O_3	5–35
CaO	1–20
Na_2O+K_2O	1–4
MgO	0.3–4
TiO_2	0.5–3
P_2O_5	0.01 –1

4.3 Combustion of Coal

Combustion of coal is a complex process because of variety of composition of its constituents in different grades of coal and the number of variable operating conditions. There are large numbers of chemical reactions taking place in the combustor during different stages of coal combustion. However the sequence of events when coal particles are injected into a CFB combustor, are (a) Heating and drying of the particles (b) Devolatilization of coal and volatile combustion (c) Primary fragmentation (d) Combustion of char & secondary fragmentation.

When a fresh coal particle is fed into a CFB combustor, it is surrounded by a large body of non–combustible hot solids. These solids pre–heat the coal particles close to bed temperature. The rate of heating may vary from 100 $^{\circ}$C/s to more than 1000 $^{\circ}$C/s depending on the coal particles size and the surrounding material characteristics [94].

4.3.1 Devolatilization of Coal

Devolatilization also called pyrolysis is the process in which the volatile matter is released from the coal particles. The VM contains combustible gases and vapors being decomposed at different temperatures. Hydrocarbon gases, water vapors, H_2S, CO and CO_2 are released at lower temperature from 500 °C to 600 °C while sulfur and nitrogen are released at higher temperature 700 °C to 850 °C. The rate of devolatilization from the coal particles depends mainly on the rate of heating, exposure time, particle size and temperature & pressure of the surroundings [25].

The process of devolatilization and volatile combustion occur almost simultaneously. The combustion of VM takes place in a diffusion flame, at the boundary between oxygen and unburnt volatiles i.e. processes controlled by the diffusion of volatiles and oxygen at their interface. Fraction of VM released x in time t can be estimated by the following empirical relation

$$t / T = 1 - 3(1 - x)^{\frac{2}{3}} + 2(1 - x) \qquad (4.1)$$

where T is the time for complete devolatilization

A coal particle of 0.5 mm diameter takes about 14 seconds to complete its devolatilization and combustion in a bed at 850 °C [87].

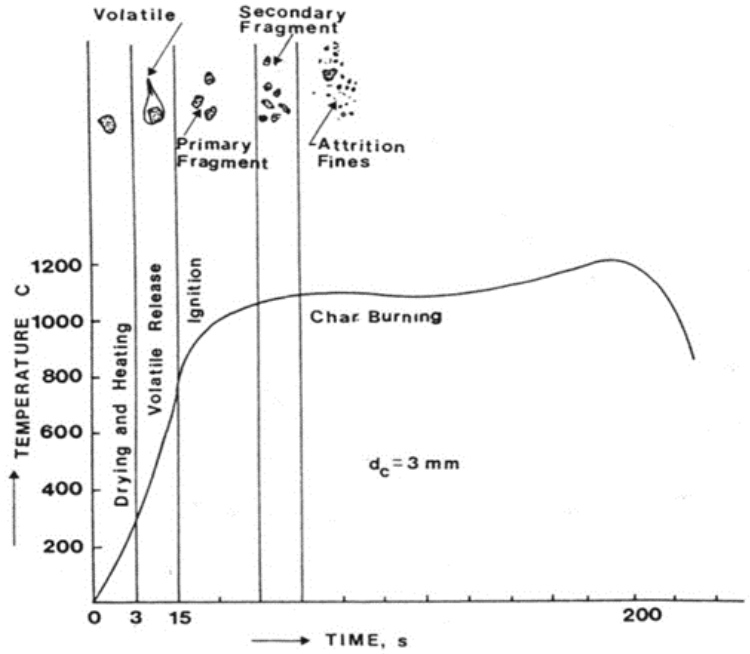

Fig. 4.4 Sequence of events in the combustion of coal particle [25]

4.3.2 Combustion of Char

The devolatilized coal known as char burns slowly and its combustion starts after the evolution of volatiles. Oxygen from the bulk stream of the combustion air enters through the pores of char particles as well as on the char surface to oxidize the carbon to produce CO & CO_2. The rate of production of these gases depends on the combustion temperature. Because of the complexity of the process, the combustion of char may be divided into three regimes.

In regime I that normally occurs between 400 °C to 600 °C the chemical kinetic rate is much slower than the diffusion rate. Oxygen diffuses rapidly into the char through its fine pores and the combustion occurs uniformly throughout the char at about 600 °C. In case of coarse and non–porous particles this regime occurs at higher temperature at about 800 °C. In regime II at temperatures from 600 °C to 750 °C the reaction rate and pore diffusion rates are comparable so most of the oxygen is absorbed in oxidizing carbon at the surface of char particle and the penetration of oxygen into the char particle is limited. In regime III that occurs at temperature from 750 °C to 900 °C, the kinetic rate is very high and pore diffusion rate is very slow so the amount of oxygen approaching the char particles is entirely consumed on the surface of the particle. This type of combustion is called diffusion controlled combustion and occurs at the surface of coarser particles [25].

In a circulating fluidized bed the coal particles of different sizes from 0.1 mm to 0.5 mm are subjected to high degree of mixing due to fast fluidization. When combustion proceeds the size of char particle reduces and mass transfer rate increases so the mechanism moves gradually from regime III to regime II and then to regime I conditions.

The mass transfer rate can be expressed as

$$q = h_m \ (C_g - C_s) \tag{4.2}$$

Where $C_g$and $C_s$is partial pressure of O_2 in the bulk stream and on the char surface and $h_m$is the coefficient of mass transfer.

The maximum mass transfer rate (as in regime III) called as diffusion limit can be obtained by putting C_s =0.

$$q_{max} = m_d = h_m C_g \tag{4.3}$$

The specific burning rate of carbon in oxygen;

$$q = R_c C_s^{\ n} \tag{4.4}$$

Where R_c = reactivity of the coal used i.e.

$$R_c = \frac{q}{[C_g(1-\frac{q}{m_d})]^n} \tag{4.5}$$

For a first order reaction i.e. n = 1, the burning rate q can be found by simplifying the above equation

$$q = \frac{C_g}{\frac{1}{h_m}+\frac{1}{R_c}} \tag{4.6}$$

The numerical values of h_m and R_c can be found by using empirical relations available in the literature [87, 94].

4.3.3 Fragmentation

During devolatilization process the coal normally passes through the plastic phase between 420 °C and 500 °C. In this phase the pores breakdown and the gases released from the interior of the coal particle cause it to swell. In some cases a balloon like censo sphere is formed due to uniform swelling. The volatile gases released inside the non–porous coal particles exert a high internal pressure that breaks the coal into fragments. This phenomena is called primary fragmentation.

When char burns under regime, I or II conditions the internal pores of the char increase in size that weakens the bridge connecting carbon islands inside the char.

When the bridge is too weak to withstand the hydrodynamic forces on the char it breaks up into lose fragments. This process is called secondary fragmentation.

4.3.4 Combustion Zones in CFBC

The combustion process in a CFB combustor takes place in three distinct zones.

a). The lower zone located below secondary air level.

b). The upper zone located above secondary air level.

c). The cyclone separator.

The lower zone of the combustion is fluidized by primary combustion air while this section receives fresh coal from the coal feeder as well as partially burnt char particles from the cyclone separator. Devolatilization and partial combustion occurs in this zone which is oxygen deficient but rich erosion environment so to protect the boiler tubes from the possible erosion attack this zone is refractory lined.

The upper zone is taller than the bottom zone and has oxygen rich environment. Most of the combustion of char particles takes place in this zone. The clusters of char particles are transported upward through the core of combustor and slide down along the wall of the furnace when they become heavy. In this way the char particles make many trips in the combustor before they are finally entrained to the cyclone separator. When the boiler load increases, the proportion of primary to secondary air is increased and a greater amount of hot solids are transported to the upper zone of combustor.

In the cyclone the extent of combustion is small as compared to the rest of the CFB loop, because of shorter residence time and low oxygen concentration. However the combustion of volatiles continues in the cyclone.

4.4 Parameters Affecting Combustion in CFBC

The parameters that may influence the combustion of coal in a CFBC are:

(i) Coal characteristics
(ii) Combustion temperature
(iii) Fluidizing velocity
(iv) Excess air
(v) Recirculation
(vi) Cyclone efficiency
(vii) Over–bed and under–bed feeding
(viii) Attrition

4.4.1 Coal Characteristics

i) Particle size: Small size coal particle has shorter burnout time but on the other hand a higher probability of entrainment with fluidizing air that increases the unburned carbon loss thus decreasing the combustion efficiency. While the coarse particles burn slowly and reduce the bed temperature that also reduces the combustion efficiency so to maintain a higher combustion efficiency the particle size should be optimized.

ii) Reactivity of coal: It is the mass of fuel oxidized per unit time per unit external area. More reactive coal gives higher combustion efficiency and vice versa.

iii) Calorific value or heating value: This parameter governs the coal feed rate.

iv) Fuel ratio: It is the ratio of fixed carbon to VM in a coal sample. It is observed that the coals with higher fuel ratio gives lower combustion efficiency and vice versa. The reason is that solid carbon particles require much more time to complete their combustion as compared to the volatile matter.

v) Ash content: Higher ash content gives lower combustion efficiency.

4.4.2 Combustion Temperature

Combustion temperature depends on the coal feed rate and the reactivity of coal. The higher is the temperature, higher is the combustion efficiency. This is because the higher temperature reduces the unburnt carbon loss.

Most of the CFBC furnaces are operated at about 850 ºC to have lower NO_x emissions and higher sulfur capture. Although higher temperature above 850 ºC has the advantage of reduced N_2O emissions and reduced unburnt carbon loss but it causes ash fusion and alkali metal deposition on boiler tubes. However, high temperature combustion is good for low volatile coals.

4.4.3 Fluidizing Velocity

High fluidizing velocity increases the entrainment of unburnt fine coal particles that reduces the combustion efficiency. It also increases oxygen bypass. While decreasing velocity of air causes de–fluidization in the bed and agglomeration of coal particles.

4.4.4 Excess Air

To ensure complete combustion of coal in FBC excess air is necessary because of some in homogeneity in solid gas mixture and the short residence time. The combustion efficiency increases with increase in excess air normally up to 25% percent above stoichiometric A/F ratio. Further increase in EA causes reduction in the bed temperature thus reducing combustion efficiency.

4.4.5 Recirculation of Solids:

Recirculation of solids reduces the unburnt carbon loss because these solids get another chance to complete its combustion. It also reduces the loss of unreacted limestone particles. Recirculation is particularly more important in case of less reactive coals because they need more residence time to complete their combustion.

4.4.6 Cyclone Efficiency

The char particles need multiple trips around the CFB loop to complete the combustion so if the cyclone is not efficient to capture the particles with burnout time larger than the single pass residence time the loss of combustibles increases and that reduces the combustion efficiency. Thus the cut–off size of cyclone must be smaller than the mean particle size.

4.4.7 Over Bed And Under Bed Feeding

In over–bed feeding the fine coal particles are readily entrained with the gas before reaching the bed surface, since the freeboard does not provide an environment for conductive combustion. While in under bed feeding the coal particles find adequate time to complete the combustion.

4.4.8 Attrition

It is the process of production of fine particles from the coarse particles through mechanical aberration with other particles when they cross each other moving with different velocities. So attrition results in size reduction of the particles and increases the reaction rate of coal and sorbent particles. The attrition rate of char is proportional to the slip velocities between the char and the bed material. The fine particles less

than 100 µm (0.1 mm) produced by attrition generally escapes through cyclone and constitute a combustion loss.

4.5 Emissions from CFBC

The combustion of fossil fuels in stationary power plants and transportation vehicles is the main source of environmental pollution. The pollutants emitted from these sources can be classified into two groups a) the regional pollutants which affect the region around the source and b) the global pollutants whose effects are not limited to the region around but span the entire globe [95].

The gases such as SO_2, NO_x, CO and organic compounds HC are the regional pollutants. They affect the human health adversely, change the plant metabolism of crops and trees and pollute the water reserves. Sulfur dioxide SO_2 has a complex chemical reaction with moisture when catalyzed by sunlight to form acids. These acids come down on the earth with rain. The acid rain damages the needles & leaves of the plants, washes away the nutrients in the soil and kills the inhabitants in the water reserves. Nitric oxide NO is harmful to human beings as it causes lungs infection. It also acidifies the rain. In the presence of oxygen some NO is converted to NO_2 which absorbs ultraviolet radiations from sun splitting itself into NO and atomic oxygen. This oxygen in turn produces ozone gas O_3. The presence of ozone at ground level is dangerous to the crops of wheat, cotton and soya bean etc. The volatile organic compounds HC are not poisonous but they react with nitrogen oxides to form number of secondary pollutants called photo chemical oxides. These oxides are the major contributor in smog formation.

Table 4.3 Regional pollutants emission from different sources [96]

Source	Emissions (millions ton /year)		
	SO_x	NO_x	HC
Stationary Thermal Plants (Boilers etc.)	18.2	9.1	1.1
Transportation Vehicles	0.8	8.5	8.0
Industrial Processes	4.3	0.7	11.1

The gases CO_2, N_2O, CH_4 etc. are called greenhouse gases and cause the changes in the global environment. They absorb a larger fraction of energy from the sun and cause global warming. The raise in temperature of atmosphere is the major reason for

the destruction of ozone layer that lies in the stratosphere at 15.5 miles above the ground surface. The depletion of this protective layer causes a number of skin diseases. The carbon dioxide has the least global warming potential but as it is emitted in large quantities from the combustion of all the fossil fuels so its control is gaining importance by some of the scientists. It is believed that increased carbon dioxide content in the atmosphere may cause change in the agro–climate and rainfall pattern. However no legislative measures for CO_2 have been imposed upon by any of the environmental protection agencies.

Table 4.4 Global warming potentials of greenhouse gases [97]

Gases	20 years GWP	100 years GWP
Carbon Dioxide CO_2	1	1
Methane CH_4	56	21
Nitrous Oxide N_2O	280	310
Chloro Fluoro Carbon CFC	–	4600

4.6 Sulfur Dioxide (SO_2) Emissions

It is the most harmful regional pollutant that damages the plants and the human health. It is normally produced by the combustion of fuels containing sulfur. The sulfur content of coal varies widely in the range from 0.10 to 10 percent and it may occur in coals in three different forms i.e. Pyritic, Organic and Sulfate. During combustion of coal the sulfur is oxidized to form SO_2.

$$S + O_2 \rightarrow SO_2 \qquad (4.7)$$

At high temperatures and in the presence of oxygen some SO_2 is converted to SO_3. When this gas gets in contact with the moisture in the flue gas, it forms sulfuric acid.

$$SO_3 + H_2O \rightarrow H_2SO_4 \qquad (4.8)$$

Limestone (mostly $CaCO_3$) and Dolomite ($CaCO_3 + MgCO_3$) are common sorbents used for elimination of SO_2in FBC. Some synthetic sorbents are also being developed to serve the purpose. Limestone decomposes into calcium oxide and carbon dioxide when heated and the reaction is known as calcination.

$$CaCO_3 \rightarrow CaO + CO_2 \qquad (4.9)$$

The calcination reaction creates and enlarges many pores in the limestone particles while emitting CO_2. These pores increase the exposed surface area for the subsequent

sulfation reaction. SO_2 enters the interior of the particles through these pores and react with calcium oxide to form calcium sulfate as shown in equation 4.10.

$$CaO + SO_2 + ½\ O_2 \rightarrow CaSO_4 \qquad (4.10)$$

It is evident from the Fig. 4.5 that this sulfation occurs on the exposed surface of CaO only. Due to sulfation the pores are plugged and only a fraction of calcined lime is utilized in capturing sulfur dioxide. The interior of the sorbent particle from 40 to 70 percent remain as unreacted. For this reason the FB combustors are supplied more than two times the quantity of limestone actually required for complete sulfation. To improve the utilization of limestone the particles should be ground to smaller sizes which have larger specific surface area or they may be hydrated by steam or water because the soft lime has higher capability of SO_2 capture. The limestone demand is also influenced by the quality of the solid mixing and the manner & location of feeding points [25].

It is interesting to note that calcination and sulfation reactions are much slower than the devolatilization and combustion of coal. A 0.5 mm coal particle takes 10–20 sec to complete the devolatilization and combustion processes while limestone particle of the same size can take about 50 seconds for calcination and 1200 seconds to complete sulfation reaction. It is the CFBC that provides sufficient time for such reactions by recycling it again and again.

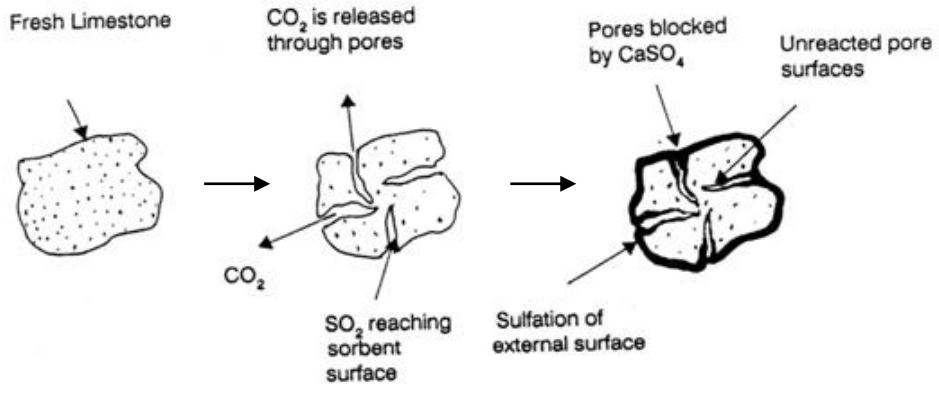

Fig. 4.5 Calcination and sulfation of a limestone particle [25]

It is observed that in the presence of CO the sulfation process may reverse and the calcium sulfate formed decomposes back to Calcium oxide as

$$CaSO_4 + CO \rightarrow CaO + SO_2 + CO_2 \qquad (4.11)$$

The lower section of CFBC is operated under sub stoichiometric conditions to reduce NO_x emissions, so this section is rich in CO concentration that favors the reaction 4.10 and hence increase SO_2 emissions so it is necessary that for the simultaneous reduction of SO_2 and NO_x both an optimized quantity of primary air should be supplied [25].

It is important to note that calcination reaction occurs only if the partial pressure of CO_2 in the combustor is less than its equilibrium partial pressure corresponding to the combustion temperature. In pressurized fluidized bed combustors the partial pressure of CO_2 is always higher than that mentioned above, so calcination does not occur in such conditions. Hence in PFBC one has to use Dolomite as sorbent for eliminating SO_2 during combustion.

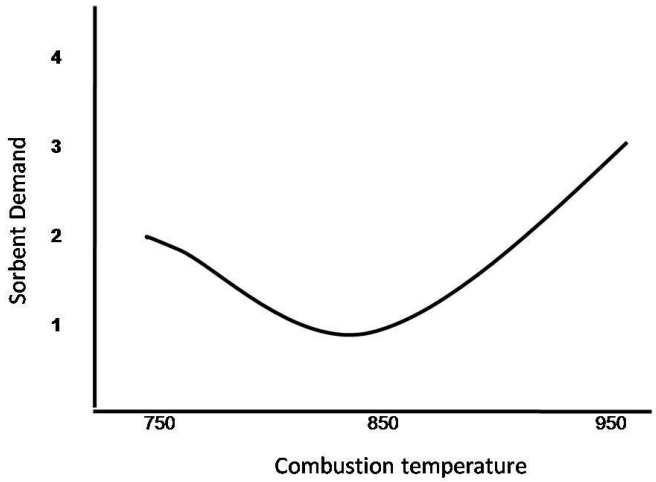

Fig. 4.6 Variation of sorbent demand with combustion temperature [25, 87]

It is a well–known fact that reactivity of the sorbent and pore characteristics are the major factors influencing SO_2 capture. The ferrous oxide Fe_2O_3 present in limestone is very effective catalyst in promoting the reaction between CaO and SO_2. It is found that dolomite with 30% $MgCO_3$ produces highest desulfurization of flue gas. This is because magnesium carbonate readily calcines at all temperatures and pressures [87].

The reactivity of the sorbent increases with increase in temperature reaching an optimum level at about 850 °C. Hence sorbent demand in CFBC is minimum at this temperature. At temperatures above 850 ºC the pores of sorbent are quickly plugged due to higher rate of sulfation. The sulfation efficiency reduces significantly below 780 °C and above 960 °C as shown in Fig. 4.6 [98]. Moreover at higher temperatures, the decomposition of $CaSO_4$ increases which increases the SO_2 emissions. The

experiments show that effect of Ca/S ratio in eliminating SO_2 is more pronounced from Ca/S = 0 to 3 and then the slope reduces as shown in Fig. 4.7.

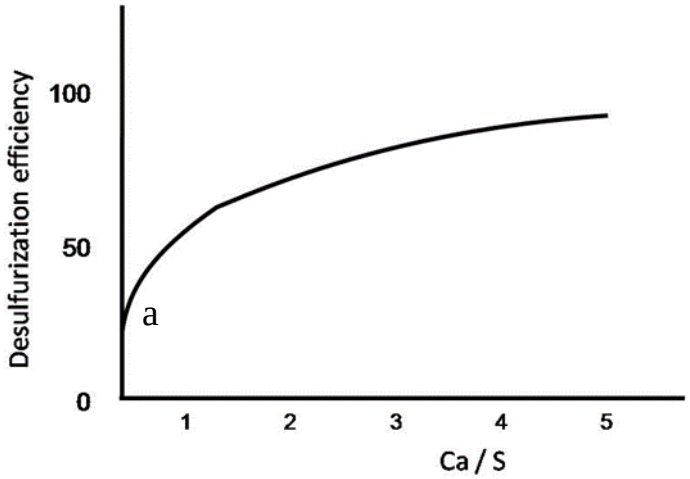

Fig. 4.7 Desulfurization efficiency and Ca/S ratio [87]

The calcium oxide contained in the coal (ash) eliminates considerable amount of SO_2, known as self–desulfurization as shown by point a, Fig. 4.7. Some other impurities also influence the limestone capacity for sulfur capture.

Two–stage combustion in CFBC is introduced to achieve lower NO_x emissions but reducing primary air causes increase in SO_2 emissions. It is observed that reducing primary air from 1.2 to 0.9 of stoichiometric air reduces SO_2 retention from 90 to 80 percent. However increase in excess air is advantageous in reducing SO_2 emissions. It is found that sulfur capture decays exponentially with furnace height. The detailed discussions on calcinations and sulfation reactions and ranking of limestone are available in literature [99].

4.7 Nitrogen Oxide (NO_x) & Nitrous Oxide (N_2O) Emissions

Oxides of nitrogen are the major air pollutants emitted by most of the combustion systems. In case of coal combustion the dominant source of NO_x and N_2O is the fuel nitrogen i.e. in the volatiles and char bound nitrogen. The nitric oxides produced by the atmospheric nitrogen called as thermal NO_x are negligible at temperatures below 1540 ºC [100].

The oxidation of volatile N and char bound nitrogen are complex processes. In the literature, more than 250 possible reactions have been proposed to simulate the formation and destruction of nitrogen oxides. Amongst those over 90 possible

reactions with HCN are believed to play a key role in the formation of these oxides. Most of these reactions are assumed to be homogeneous, some of these particularly related to char–N are heterogeneous, while for some of these reactions the kinetic data is not reliable [101].

Different schemes have been proposed to represent the formation and reduction of oxides of nitrogen. Johnson et al. proposed a scheme for the formation of NO from volatiles and char and its reduction back to molecular nitrogen N_2 as depicted in Fig. 4.8. According to this presentation 77% of fuel nitrogen is converted to NO. Catalysts CaO and char etc. for different reaction paths have been indicated as well [25].

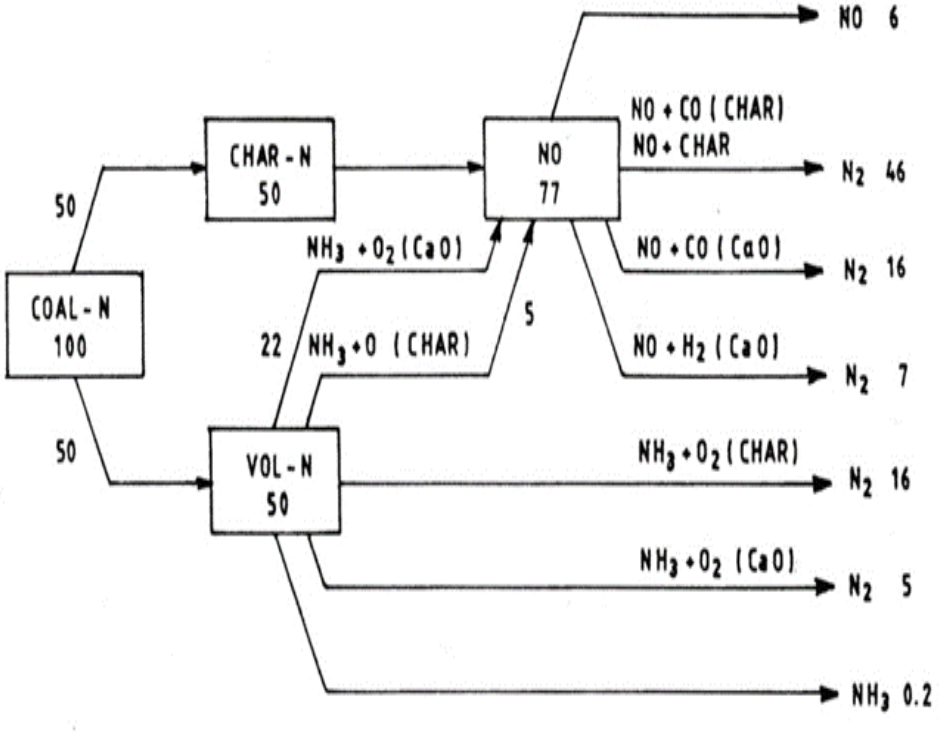

Fig. 4.8 A series of possible reactions of coal nitrogen, producing nitrogen oxide (NO) and its reduction to N_2 [25]

Hayhurst et al. [102] proposed another picture showing the step wise formation of NO and N_2O from coal volatiles and the char. Interaction of H, O and OH radicals and catalytic effect of CaO, CO and char in the formation of oxides of nitrogen have been presented. The configuration has been verified by the experimental evidences.

During devolatilization the gaseous matter emitted constitute compounds of nitrogen and hydrogen radicals. The most probable chemical reactions producing NO_x and N_2O from the volatile matter and the char have been presented by two different schemes proposed by the researchers.

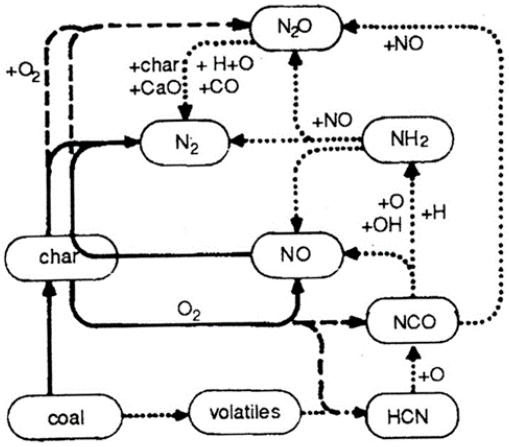

Fig. 4.9 Formation of oxides of nitrogen [25]

These schemes show different paths of chemical reaction for the formation & reduction of NO and N_2O. But it is agreed upon that major source of NO formation is the oxidation of ammonia contained in the volatile matter.

$$NH_3 + 5/4\ SO_2 \rightarrow NO + 3/2\ H_2O \quad (4.12)$$

In this reaction the concentration of NO is enhanced by the catalytic effect of CaO and char. The source of N_2O is an intermediate compound Hydrogen Cyanide HCN, produced by the coal volatiles.

$$CH + N_2 \rightarrow HCN + N \quad (4.13)$$

$$HCN + O \rightarrow NCO + H \quad (4.14)$$

The amines NCO decomposes to form N_2O

$$NCO + NO \rightarrow N_2O + CO \quad (4.15)$$

The N_2O thus formed is readily reduced by H & O radicals

$$N_2O + O \rightarrow N_2 + O_2 \quad (4.16)$$

$$N_2O + H \rightarrow N_2 + OH \quad (4.17)$$

The OH radicals react with animes and produce nitric oxide

$$NCO + OH \rightarrow NO + CO + H \quad (4.18)$$

It is found that high volatiles coals produce high NO_x and low N_2O emissions and vice versa.

Combustion of char takes place at 750 ºC and produce CO and CO_2 in significant amount depending on the concentration of NO.

$$C + NO \rightarrow CO + ½\ N_2 \quad (4.19)$$

$$C + 2NO \rightarrow CO_2 + N_2 \quad (4.20)$$

The CO is oxidized into CO_2 and molecular nitrogen is emitted

$$CO + NO \rightarrow CO_2 + ½ N_2 \quad (4.21)$$

There are many other relations of hydrocarbon radicals C_xH_y and compounds of nitrogen NH_i proposed by the researchers to determine the oxides of nitrogen. These reactions indicate the role of intermediate compounds NH_2, NH, CH_2 and H_2S in generating the oxides of nitrogen. However there are experimental evidence that conversion of coal–N into N_2O depends on the devolatilization process and nitrogen feeding the coal in the CFB loop may be useful in reducing N_2O [14, 25, 87].

4.8 Carbon Monoxide (CO) Emissions

Emissions of CO is the indication of incomplete combustion of carbon. The emission of CO from a combustor increases when combustion temperature decreases below 800 C or by the insufficient supply of oxygen. The combustion of coal volatiles CH_4 in the bottom zone of a CFB combustor produces CO in significant amount.

$$CH_4 + ½ O_2 \rightarrow CO + H_2O \quad (4.22)$$

And the combustion of char further produces CO

$$C + NO \rightarrow CO + ½ N_2 \quad (4.23)$$

The CO is oxidized to CO_2 on availability of oxygen from secondary level. The secondary air addition is helpful in good solid–gas mixing as well.

$$CO + ½ O_2 \rightarrow CO_2 \quad (4.24)$$

The ratio of production rates of CO and CO_2 is found dependent on the combustion temperature Ts only as

$$\frac{[CO]}{[CO_2]} = 2400 \exp\left[\frac{-51830}{8.31 T_s}\right] \quad (4.25)$$

Although staged combustion is favorable in reducing NO_x emissions but it causes increase in CO emission. However increase in excess air contributes to better combustion conditions and lower CO emissions. It is found that emission of CO from CFB is normally below allowable limits of environmental protection agencies [25].

4.9 Carbon Dioxide (CO_2) Emissions

CO_2 is produced in large quantities by the combustion of all fuels containing carbon. It is one of the greenhouse gas causing global warming and hence the depletion of ozone layer. With increasing energy demands and the number of coal power plants, CO_2 emissions are ever increasing.

Oxy–fuel combustion of coal is the technology gaining attention to protect the atmosphere from higher concentrations of CO_2. The most attractive aspect of oxyfuel combustion is its ability to achieve a carbon capture and storage (CCS) system [103]. A CCS involves producing nearly pure stream of CO_2 either by concentrating it in some manner from the flue gas or by using pure oxygen as combustion oxidant in place of air. The CO_2 level in the flue gas is further increased by recirculating the flue gas in the combustion zone. Pure CO_2 can be easily compressed and stored in for some industrial processes and hence the CO_2 emissions are made negative.

It is found by experimentation on lab–scale FBC coal combustors that this technology offers almost all the advantages of air fired FBC. A stable combustion condition can be obtained with CO_2 concentration up to 90 percent in the flue gas. In case of oxyfuel combustion of coal the emission of CO and NO_x are lower or comparable to that of air firing system. But the concentrations of N_2O and SO_2 are higher. The reason of higher SO_2 is the poor sulfation. It is proposed that addition of petroleum coke can improve the sulfation process [104].

Oxyfuel has been well studied for pulverized coal combustion as well as for CFBC using lab–scale coal combustor, the question is whether it will be economical to use pure oxygen in a commercial FBC [105].

4.10 Particulate Emissions

Particulate matter (PM) emissions from coal power plants in the form of fine ash (CaO & $CaSO_4$ particles) and inert bed material silica sand etc. contained in the flue gas pollute the environment around the plant. The permissible particulate emission limit is 50 mg/m^3 of flue gas. To clean the flue gas from these particles before it passes through the stack, different dust collectors are utilized in the flue gas circuit. The cyclone separators are the dust collectors used in CFB primary loop to capture the unburnt coal particles and unreacted limestone particles in the flowing gas for recycling. The fine particles normally escape through these separators. The cyclones can be used for high temperature gas but these are unable to capture very fine particles [106]. To remove such fine particles from the gas, following gas cleaning devices are used:

i) **Fabric or Bag House Filters**: A fabric filter or bag house collects the dry particulate matter as the cooled flue gas passes through the filter material. The fabric filter is comprised of multiple compartments containing very large number

of small diameter fabric bags. The gas passes through the porous bag material which separates the particulate from the flue gas. The layer of the dust accumulating on the bag is referred to as dust cake. These filters are used where the gas temperature is below 150°C but use if fiber glass in these filters is suitable up to 250 °C. These are economical devices but normally used in smaller power plants. In addition to fiber glass the synthetic materials having better abrasion to particles and resistance to acid attack are used in larger plants but these are expensive [107].

ii) **Electrostatic Precipitators (ESP)**: It is a particulate collection device that removes the fine particles from a flowing gas using the force of an induced electrostatic discharge. An ESP can capture very fine particles up to 0.1 µm very efficiently with separation efficiency above 99% and reduces the particulate emission below 10 mg/m^3. The voltage across the electrostatic field is in the range of 20 to 50 kV/cm. When the flue gas passes through an ESP the fly ash particles are charged in the electrostatic field and attracted by an electrode i.e. dust collector plate. The collectors are shaken to dislodge the dust. Depending upon dust characteristics and gas volumes to be treated, there are many designs of ESP described in the reference [108]. ESP collection range for different types of particles is given in Fig. 4.10.

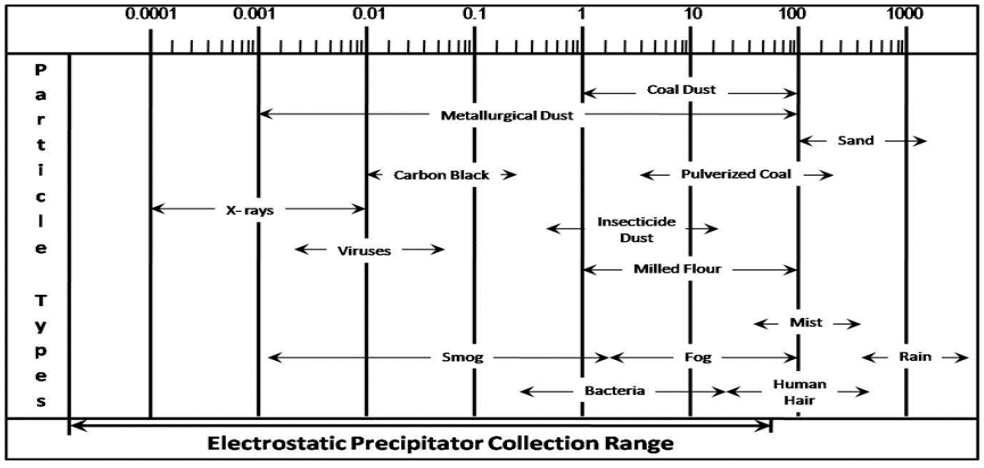

Fig. 4.10 Electrostatic Precipitator (ESP) [108]

CHAPTER NO. 5

MATERIALS AND METHODS

5.1 Introduction

The experimental work consists of following two phases.

Phase–I: Lab Scale Testing.

i) Phase–I (Part–I): Study of coal quality characteristics.
ii) Phase–I (Part–II): Study of coal combustion characteristics and performance indices.

Phase–II: Pilot Scale Testing.

i) Phase–II (Part–I): Study of major gaseous emissions (SO_2, NO_x, CO, CO_2) with limestone (L/s) addition during combustion in FBC.
ii) Phase–II (Part–II): Study of major gaseous emissions (SO_2, NO_x, CO, CO_2) with biomass addition during co–firing in FBC.
iii) Phase–II (Part–III): Optimization of process parameters (Ca/s ratio, bed temperature, Limestone particle size and biomass proportion) to reduce gaseous emissions.

5.1.1 Phase–I: Lab Scale Testing

i. Phase–I (Part–I): Study of coal quality characteristics.

Testing of following quality characteristics of 30 coal samples was carried out.

a. Proximate analysis
b. Ultimate analysis
c. Gross calorific value (GCV) / Net calorific value (NCV)
d. Ash fusion temperature (AFT)
e. Ash composition analysis

ii. Phase–I (Part–II): Study of coal combustion characteristics and performance indices.

Testing of following combustion parameters and characteristics of 30 coal samples was carried out.

a. Volatile initial separating temperature (T_s)
b. Ignition temperature (T_i)

c. Complete burning temperature (T_h)

d. Complete burning time (t_{rj})

e. Maximum combustion rate (w_{max})

f. Average combustion rate (w_{mean})

g. Temperature of maximum combustion rate (T_{max})

h. Temperature difference of DTG's half peak width (ΔT_h)

i. Temperature difference of DTG's total peak width (ΔT)

j. Ignition characteristics index (F_z)

k. Flammability index (C)

l. Stable firing index (M)

m. Combustion Characteristics Curves (TG and DTG)

5.2 Lab Scale Testing (Phase–I)

Thirty coal samples were collected for the experimentation from different coal mines of Salt Range and Trans Indus Range situated in the northern part of Punjab province of Pakistan. The location of the collected samples from different mine areas is given in the Fig. 5.1 and their detail is given in table 5.1 [13, 34].

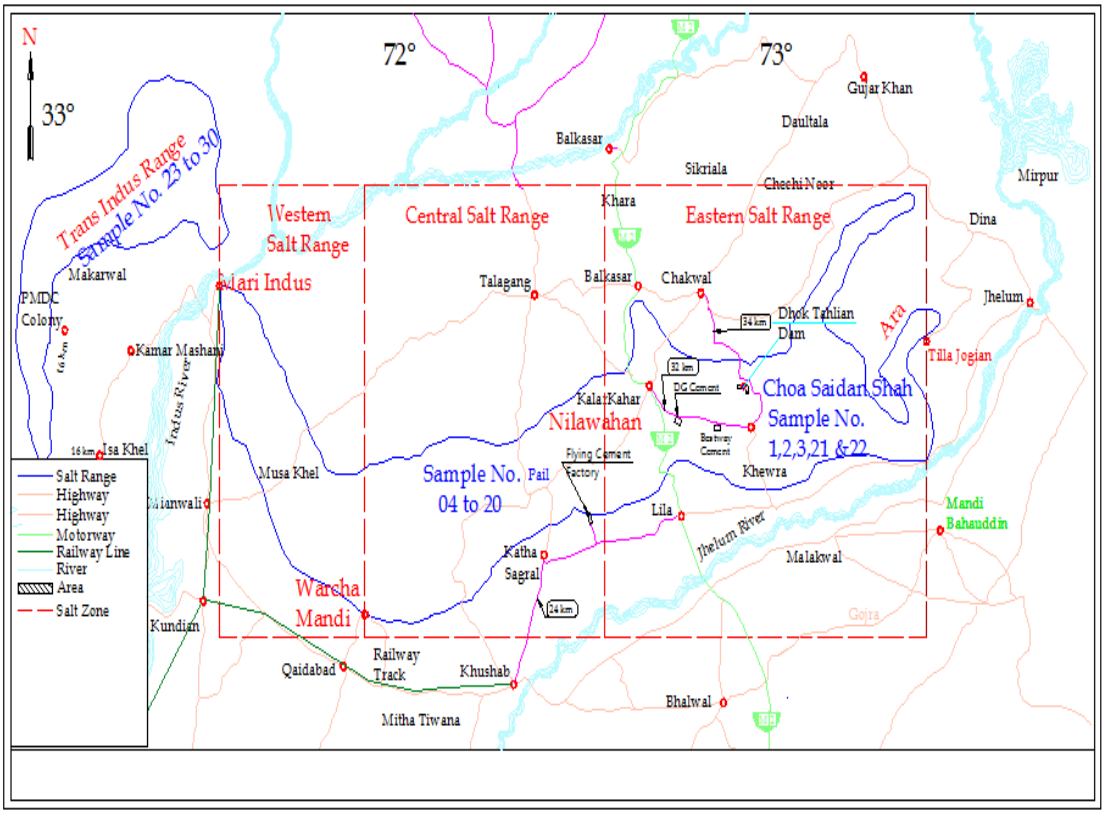

Fig. 5.1 Location of Salt Range and Trans Indus Range with geographic divisions [13]

Table 5.1 Detail of coal samples collected from Salt Range and Trans–Indus Range

Sample	Mine	Area/ District	Sample	Mine	Area/ District
1	Hashim Mine	Munara, Chakwal	16	Mine No.5	Kalial, Khushab
2	Mine“C”	Munara, Chakwal	17	Ehsaan Mine	Arrarah, Khushab
3	Habib Ullah Mine	Munara, Chakwal	18	Tariq Mine	Arrarah, Khushab
4	Shaft“A”	Padhrar, Khushab	19	Zia Mine	Kalial, Khushab
5	Sangha Mine	Padhrar, Khushab	20	Rehman Mine	Kalial, Khushab
6	Mine No.5	Padhrar, Khushab	21	Mine No.7	Kalar Kahar, Chakwal
7	Mine No.2	Khatta, Khushab	22	Abu bakar Mine	Kattas Raaj, Chakwal
8	Amina Mine	Nalli, Khushab	23	PC–1 Mine	Gula Khail, Mianwali
9	Old Bashir Mine	Kalial, Khushab	24	Majid Latif Mine	Gula Khail, Mianwali
10	Piari Mine	Kalial, Khushab	25	Tarkia Mine	Gula Khail, Mianwali
11	New Bashir Mine	Kalial, Khushab	26	Abaid–Ullah Mine	Makerwal, Mianwali
12	Sulman Mine	Kalial, Khushab	27	Maadin–e–Haq Mine	Makerwal, Mianwali
13	Mine No.3	Kalial, Khushab	28	Khatkiara, Section A	Makerwal, Mianwali
14	Mine No.1	Kalial, Khushab	29	Khatkiara, Section B	Makerwal, Mianwali
15	Mine No.4	Kalial, Khushab	30	Khatkiara, Section C	Makerwal, Mianwali

5.2.1 Study of Coal Quality Characteristics (Phase–I, Part–I)

This study was completed by conducting the following testing of 30 coal samples from SGS Pakistan and Changsha University of Science and Technology (CUST) Changsha, Hunan, China:

i. Proximate analysis (fixed carbon (FC), moisture, volatile matter (VM), ash)

ii. GCV

iii. Ultimate analysis (sulfur, carbon, hydrogen, nitrogen, oxygen)

iv. Ash composition

v. AFT

SGS used following equipment for different testing:

a) Furnace (make: carbolite, model AAF12/18 range: up to 1200 ºC) and oven (make: Memmet) were used for proximate analysis.
b) CHNS (carbon (C), hydrogen (N), nitrogen (N) and sulfur (S)), analyser was used for ultimate analysis.
c) LECO bomb calorimeter was used for GCV.
d) Global industry standards were used for AFT and ash composition analysis.

CUST used following equipment for different testing:

a) TGA–2000 (make: NAVAS Instrument USA) was used for proximate analysis.
b) Calorimeter (model: SDACM 4000, manufacturer: Hunan Sundy Industrial Co. Ltd. Chian) was used for GCV.
c) Elementar (model: vario macro manufacturer: Elementar Analysen systeme GmbH, donaustrasse 7, D–63452 Hanau Germany) was used for ultimate analysis.
d) Silicate's Chemical Component Analyzer, (model: GKF–VI, make: Hunan Huafeng, Equip. Manufact. Co. Ltd. China) was used for ash composition
e) Ash fusion tester (Model: SDAF 2000 d, Make: Hunan Sundy Industrial Co. Ltd. China) was used for AFT.

Detail of standards and equipment used for all above mentioned testing (i to v) by SGS and CUST is given in the table 5.2 and their pictorial views & principles of operation are shown in the Fig. 5.2 to 5.14.

Table 5.2 Standards and equipment used for coal testing by SGS and CUST

TESTS	**SGS**		**CUST**	
	Standards	**Equipment**	**Standards**	**Equipment**
Proximate analysis (Ash, VM, FC, TM, IM)	ASTM D3174, D4239, D5142, D3173	Make of Furnace: Carbolite, Model : AAF12/18 Range: up to 1200 °C For moisture : Oven make: Memmet	GB 483–98	TGA–2000, NAVAS Instrument, USA. Infra–Red moisture Balance Model AD–4712 A&D Tech Japan
GCV	ASTM D5865	Isoperibel Bomb Calorimeter Make: LECO Corporation	GB/T213–2008	Calorimeter Model SDACM 4000 Manufacturer: Hunan Sundy Industrial Co. Ltd Chian
Ultimate analysis (C, H, N, S, O)	ASTM D4239	CHNS Analyzer	GB476–91	Elementar, Model: vario Macro Manufacturer: Elementar Analysen systeme GmbH, Donaustraße 7, D–63452 Hanau Germany
Ash composition analysis	Global Industry Standards	N.A	N.A	Silicate's Chemical Component Analyzer, Model: GKF–VI Make: Hunan Huafeng, Equip. Manufacturing Co., Ltd. China
AFT	Global Industry Standards	N.A	GB/T219—1996	Ash Fusion Tester, Model: SDAF2000d Make: Hunan Sundy Industrial Co.,Ltd. China

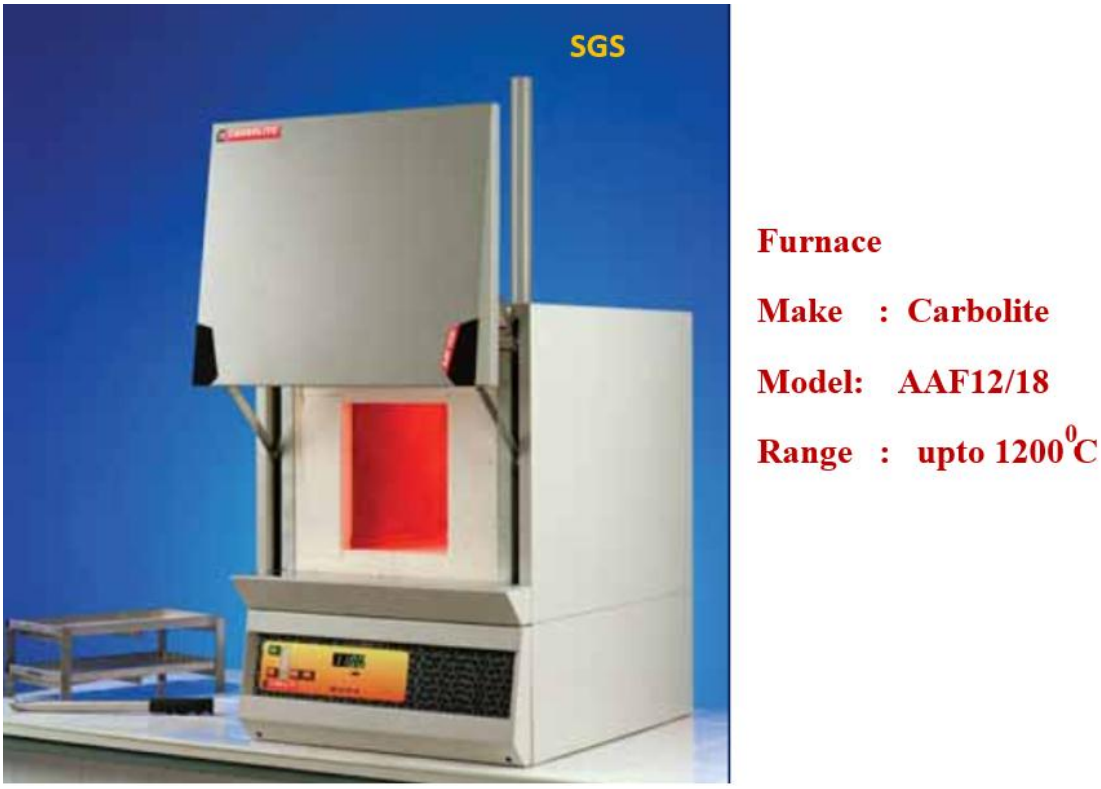

Fig. 5.2 Furnace used by SGS for proximate analysis

Fig.5.3 TGA used by CUST for proximate analysis

Oven

Make: Memmet

Fig.5.4 Oven used by SGS for proximate analysis

Fig.5.5 CHNS analyzer used for ultimate analysis

Fig.5.6 Internal parts of CHNS analyzer

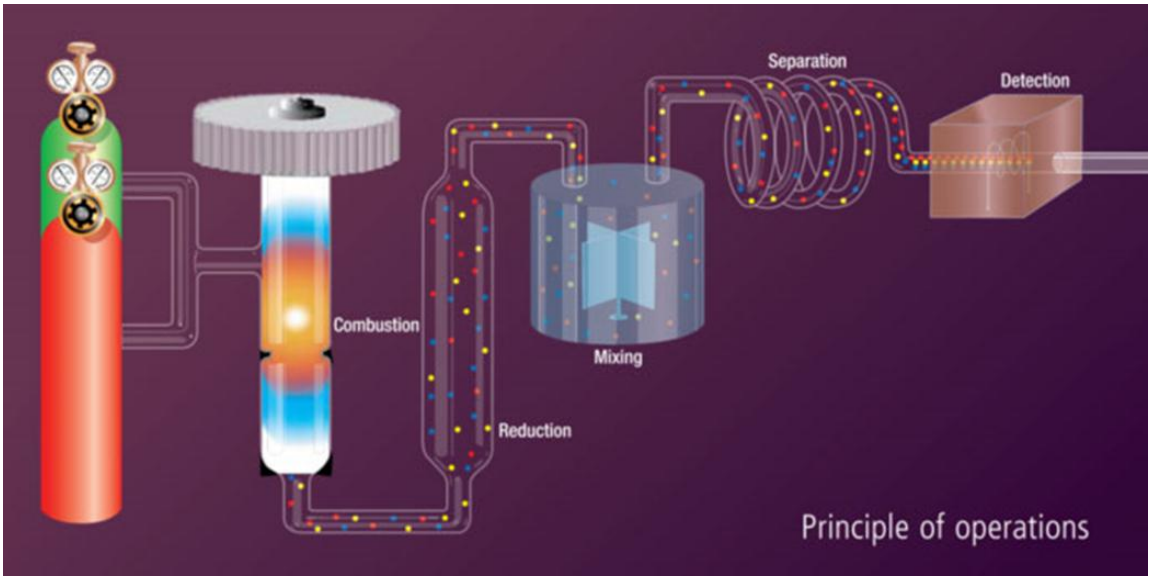

Fig.5.7 Principle of operation of CHNS analyzer

Fig. 5.8 Bomb calorimeter used for GCV

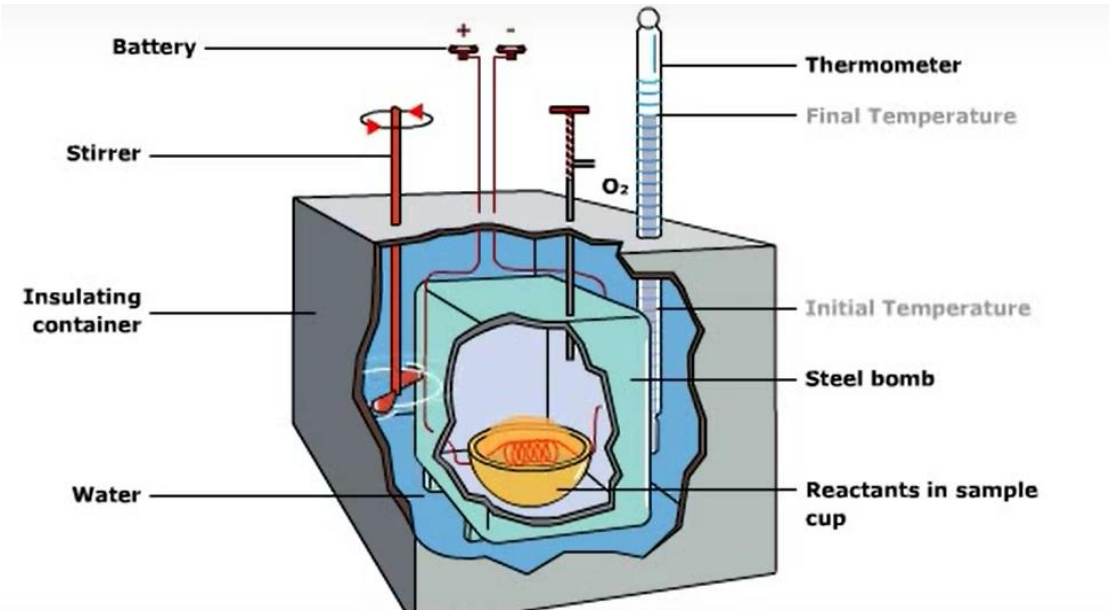

Fig.5.9 Principle of operationof bomb calorimeter

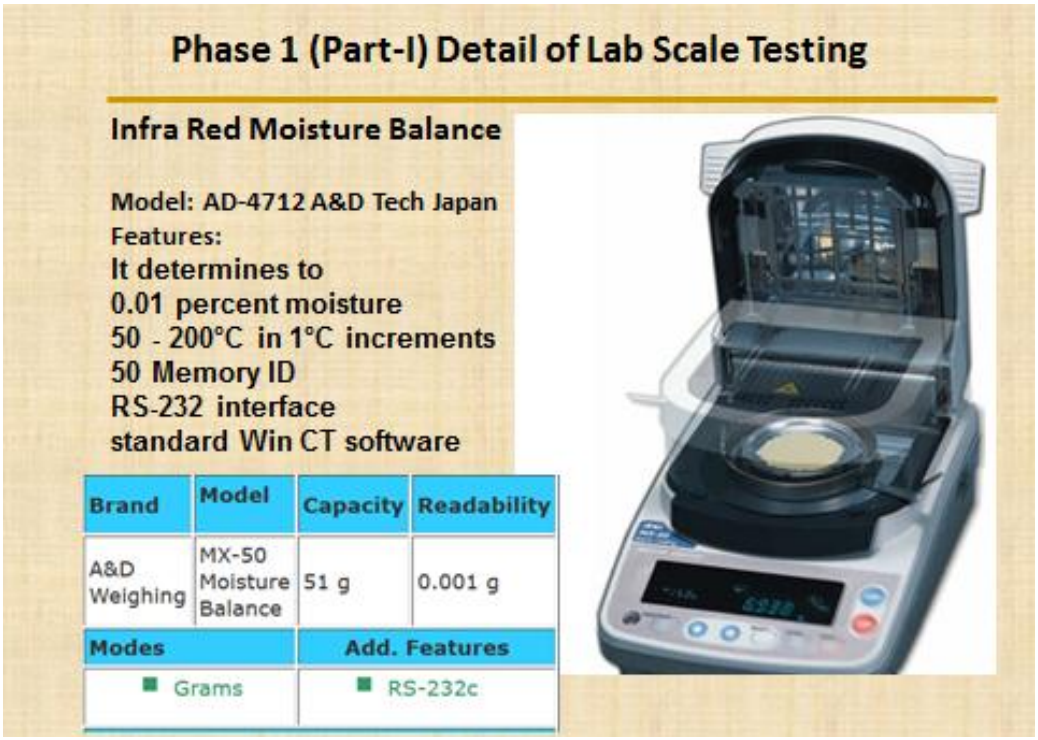

Fig.5.10 Infra red moisture balance

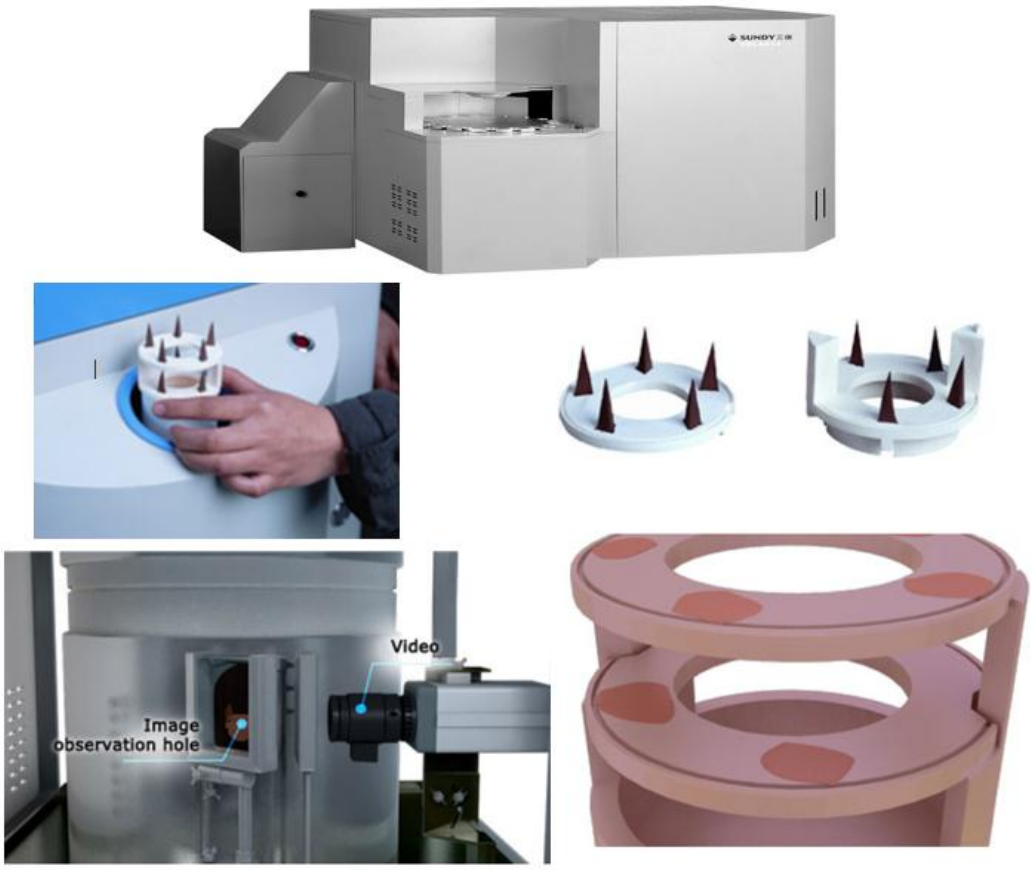

Fig. 5.11 Ash fusion tester used by CUST

Fig.5.12 Ash fusion tester used by SGS

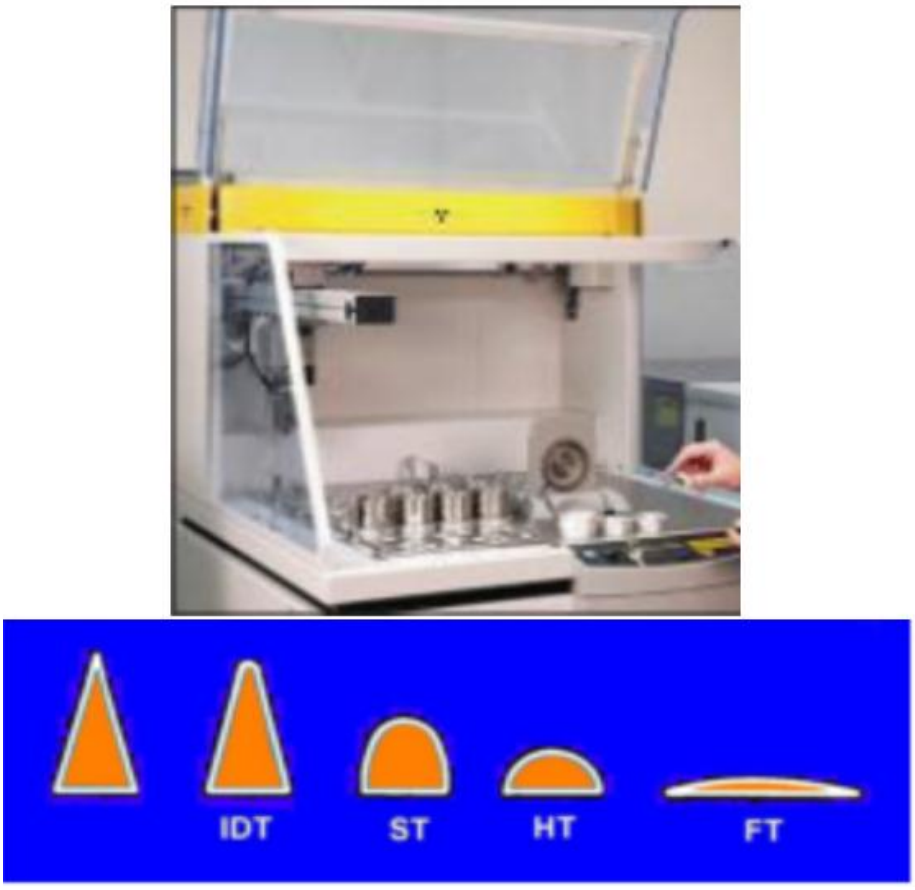

Fig. 5.13 Internal parts of Ash fusion tester

As given in Table 5.2, SGS used global industry standards for parameters of ash fusion testing.

IDT = Initial deformation temperature
ST = Softening temperature
HT = Hemispherical temperature
FT = Flow temperature

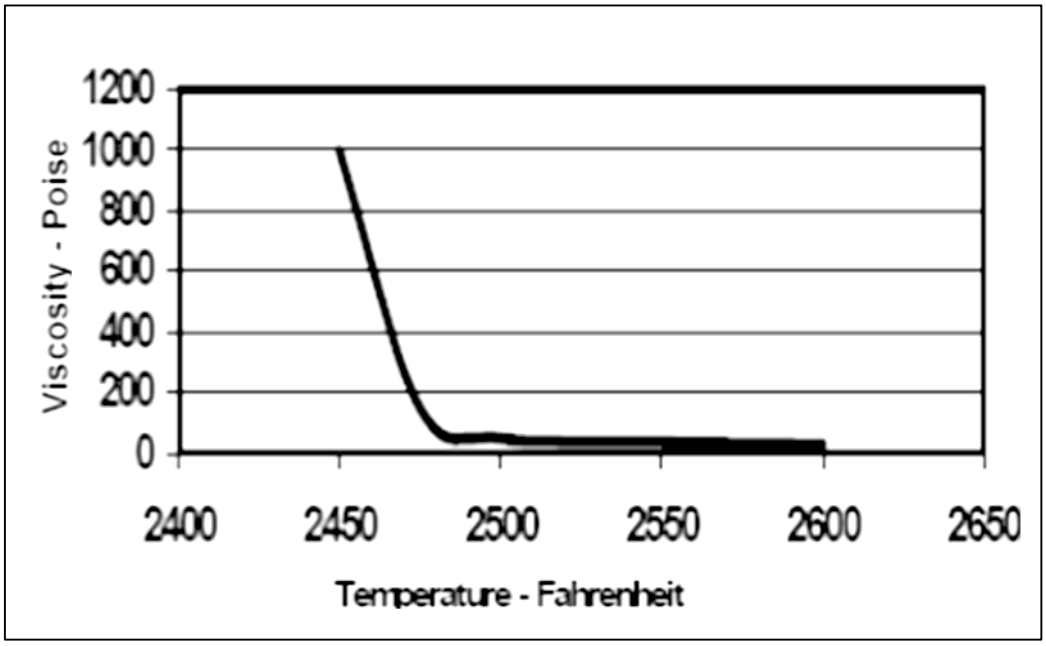

Fig. 5.14 Temperature and viscosity relationship

5.3 Study of Coal Combustion Characteristics and Performance Indices (Phase–I, Part–II)

Testing of 30 coal samples for following combustion parameters/characteristics was performed in CUST lab China.

a. Volatile initial separating temperature (T_s)
b. Ignition temperature (T_i)
c. Complete burning temperature (T_h)
d. Complete burning time (t_{rj})
e. Maximum combustion rate (w_{max})
f. Average combustion rate (w_{mean})
g. Temperature of maximum combustion rate (T_{max})
h. Temperature difference of DTG's half peak width (ΔT_h)
i. Temperature difference of DTG's total peak width (ΔT)
j. Ignition characteristics index (F_z)
k. Flammability index (C)
l. Stable firing index (M)
m. Combustion Characteristics Curves (TG and DTG)

5.3.1 Combustion Characteristics Indices

Followings are the important combustion characteristics indices [87].

a) Flammability index (C_b)

The flammability index represents the coal's sensitivity in the former combustion, defined as:

$$C_b = \frac{\left(\frac{dG}{d\tau}\right)_{max}}{T_i^{\,2}} \tag{5.1}$$

The larger the C_b, the more flammable is the coal.

b) Stable firing index (R_w)

The stable firing index is defined as:

$$R_w = \frac{560}{T_i} + \frac{650}{T_{max}} + 0.27\ DTG_{max} \tag{5.2}$$

The larger the R_w, the more stable is the coal when burning.

c) Complete combustion index (H_j)

The complete combustion index represents burning out degree during combustion, defined as:

$$H_j = \frac{\left(\frac{dG}{d\tau}\right)_{max}}{T_i . T_{max} . \frac{\Delta T_h}{\Delta T}} \tag{5.3}$$

The larger the H_j, the more complete is the coal burned.

d) Integration combustion index (S_n)

The Integration Combustion index represents the ignition and combustion characteristics of the coal, defined as:

$$S_n = \{d\omega|d\tau\}_{max}\{d\omega|d\tau\}_{mean}\frac{1}{T_i^{\,2}}\frac{1}{T_h} \tag{5.4}$$

The larger the S_n, the better comprehensive behavior of combustion of the coal.

5.3.2 Testing Methodology and Equipment Used for Combustion Characteristics Analysis

The combustion characteristics analysis was conducted on simultaneous thermal analyzer (STA) NETZSCH STA 449 F3 and Ignition Tester (Rui Hai).

Thermo gravimetric analysis (TGA) conditions was as follows:

i) Temperature range: RT to 1150 ℃
ii) Heating rate: 20 °C/min
iii) Atmospheres: Simulated air atmospheres

iv) Nitrogen flow: 20 ml/min and pressure: 0.05 mPa

v) Oxygen flow: 6 ml/min and pressure: 0.03 mPa

vi) Coal sample weight :10 ± 1 mg

vii) Coal sample size : <74 µm

A pictorial view and model of STA and "TG/DTG curves of coal samples from STA analysis" are given in the Fig 5.15, 5.16 and 5.17 respectively.

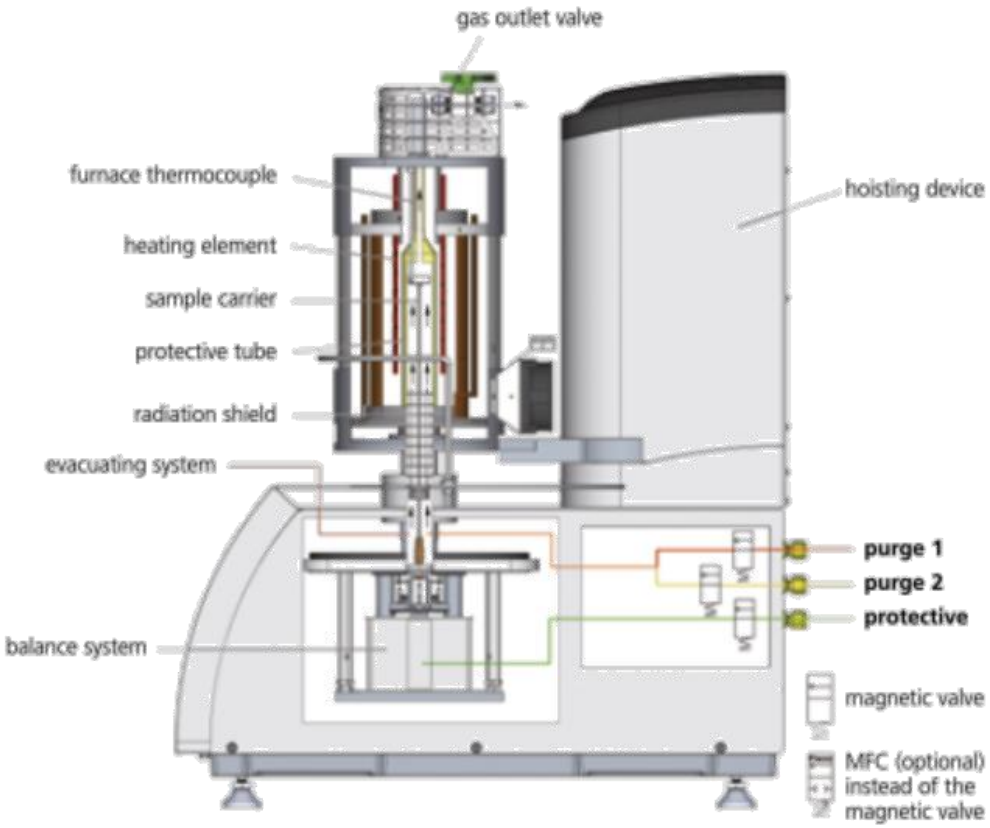

Fig. 5.15 Pictorial view of simultaneous thermal analyzer (STA)

Standard used in STA

ISO 11357, ISO 11358,

ASTM E 967, ASTM E 968

ASTM E 793, ASTM D 3895

DIN 51004, DIN 51006

DIN 51007

Fig. 5.16 Model of STA (NETZSCH STA 449 F3)

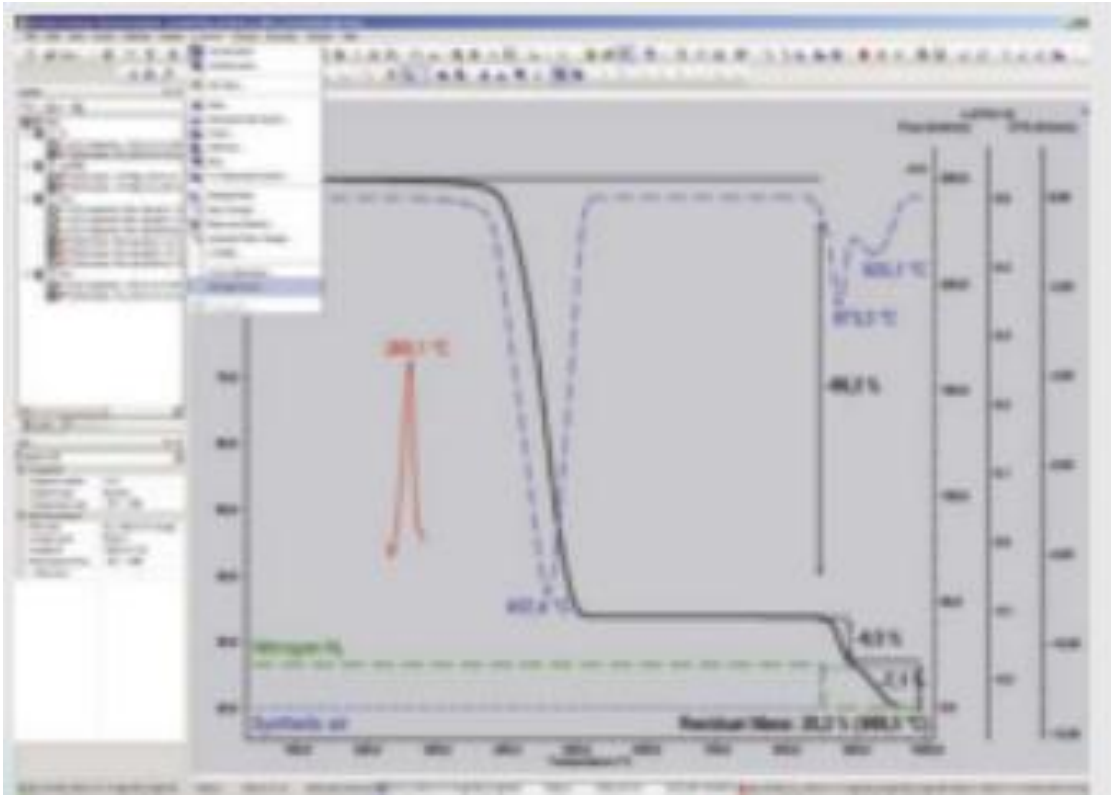

Fig. 5.17 TG and DTG curves of coal samples from STA analysis

5.4 Pilot Scale Testing (Phase–II)

Pilot scale testing has following three parts.

i) **Part–I.** Study of major gaseous emissions (SO_2, NO_x, CO, CO_2) with limestone (L/s) addition during combustion in FBC.

ii) **Part–II.** Study of major gaseous emissions (SO_2, NO_x, CO, CO_2) with biomass addition during co–firing in FBC.

iii) **Part–III.** Optimization of process parameters (Ca/s ratio, bed temperature, limestone particle size, biomass proportion) to reduce gaseous emissions.

Above mentioned pilot scale testing (Part I to Part III) was performed on FBC experimental rig at University of Leeds, Leeds UK.

For pilot scale testing coal mines were selected on the basis of lab scale testing results. Representative sample of Khatkiara Section Makerwal, Trans–Indus Range (samples 28–30) was taken as Coal A and that of Kalial section, Khusab, Salt Range (samples 9–16) as Coal B. Two tons coal was collected from the selected mines. Limestone (500 kg) was also collected from Salt Range area for desulfurization study. Coal and lime stone samples were transported to University of Leeds for experimental work at FBC Rig. GCV, proximate and ultimate analyses of coal, chemical analysis of limestone and proximate, ultimate and XRF analysis of biomass are given in table 5.3, 5.4 and 5.5 respectively.

Table 5.3 Results of GCV, proximate and ultimate analyses of coal samples

Coal	Moisture ARB (wt %)	VM ADB (wt%)	Ash ADB (wt %)	N ARB (wt %)	C ARB (wt %)	H ARB (wt %)	S ARB (wt %)	GCV ADB (kCal/kg)
A	5.46	35.5	34.71	1.17	44.00	3.46	7.23	4826
B	7.27	33.32	34.04	1.25	45.82	3.41	6.75	4949

Table 5.4 Chemical analysis of limestone

Parameters	SiO_2	Al_2O_3	Fe_2O_3	CaO	MgO	K_2O	Na_2O	SO_3	Cl
Results (%)	4.28	0.53	0.39	51.14	1.59	0.09	0.04	0.06	0.004

Table 5.5 Results of proximate, ultimate and XRF analyses of biomass

Proximate and ultimate analysis of biomass		Semi quantitative XRF Results	
Constituents	(wt %)	Elements	%
N	0.17	SiO_2	40
C	47.05	K_2O	8.81
H	5.39	P_2O_5	1.3
S	<0.1	MgO	4.79
O	47.39	CaO	22.9
Ash	1.14	Al_2O_3	8.46
Moisture	6.6	Na_2O	2.2
volatile matter	76.32	Br	3.21
Fixed carbon	11.83	Cl	0.0912
--	--	SO_3	0.292
--	--	Fe_2O_3	4.92
--	--	MnO	1.72
--	--	ZnO	0.174
--	--	NiO	0.0146
--	--	TiO_2	0.502

5.4.1 General Description of FBC Rig

The test facility is installed at the Low Carbon Combustion Centre, University of Sheffield, UK and it comprises a fluidized bed combustion (FBC) section, having overall dimensions of (1 x 1 x 5 m) with an extended freeboard section. Bed of sand, Garside Leighton Buzzard 14/25 range with nominal particle size of 1.18–0.60 mm in this case, was fluidized by air flowing through a stand pipe distributor. The internal dimensions of the fluidized bed and the combustion section above the fluidized bed are 0.42 x 0.38 m and 0.58 x 0.38 m, respectively. The combustion section is lined with castable refractory backed with ceramic fiber (having low thermal conductivity) based insulation. The bed having area of 0.16 m, is capable of accepting bio–fuels/ wastes feed rate up to 100 kg/h and mineral feed rate up to 500 kg/h depending on plant operating conditions and material type. The rig can be operated with fluidizing velocities of up to 3.5 m/s and fluidized bed heights of up to 700 mm, at combustion temperatures ranging from 750–950 ^{o}C.

There are three variable speed screws with feed hoppers to form the above–bed solid fuel feed system. All of them discharge into a high speed screw having 125 mm diameter which acts as a part–filled transfer screw and transfers the material onto the surface of the fluidized bed or into the splash zone. The system allows feeding of three different materials simultaneously and capable to handle variety of solid granular as well as powder materials.

The fluidized bed is instrumented with temperature and pressure ports for monitoring bed and freeboard conditions. Five thermocouples are arranged in vertical array at equal space, the bottom and top ones are at 30 mm and 450 mm from the top of the air distributor. In the access door, an off–take port is provided which allows overflow of bed material when nominal fluidized height reaches to 0.35m. To withdraw either a fraction of selected coarse size or the whole bed, an air classifier of 68 mm diameter is given in the base of the fluidized bed.

The positions of all thermocouples and pressure transmitters, to record temperature and pressure respectively, are shown in Fig. 5.21. The transmitters are connected to a National Instrument (NI) TBX–1303 module which is then linked to a NI SCXI–1102 (temperatures) and SCXI–1100 (pressures) and lab–view is used to read them via NI PCI–6035E card in the computer.

Manual control valves at primary air and secondary air lines as shown in Fig. 5.22 were used to regulate fluidizing air flow rate through the fluidized bed and above the bed, respectively. The Inverter control of the FBC exhaust fan enables the operator to maintain a negative pressure above the bed, in the mid freeboard and subsequent sections. Euro–therms PID controllers enable automatic and manual control of the fuel flow of each screw metering feeders into the bed.

Lab view software was used for logging the data of all the temperatures and pressures. The oxygen concentration was measured by a Portable Oxygen Analyzer (Servomex 570). A forced draught fan supplies fluidizing air which enters the bed through a standpipe distributor. A manual damper controls the air flow rate, while start–up is achieved by lighting the premixed gas at the primary burner.

The FBC consists of an air cooled heat exchanger to reduce the flue gases temperature, a bag filter and cyclone to clean the flue gas. The fluidized bed and freeboard sections are made of mild steel with interior refractory lining which results in a low outer casing temperature and consequently low heat losses.

The flue gases leaving the fluidized bed are cooled in the air cooled heat exchanger using forced draught air. The cyclone is used to separate most of the suspended solids from the flue gases leaving the heat exchangers. The solid particles are discharged into a sealed drum and can be collected for further analysis. The flue gases leaving the cyclone are passed either through the bag filter or discharged directly to atmosphere via the induced draft fan as shown in Fig. 5.22. The temperature of the flue gases is reduced down to 500 °C, depending on operating conditions.

All reported values of gaseous emissions like SO_2, NO_x etc. are corrected to 6% O_2 in the flue gas using the following equations.

$$SO_2 \text{ at } 6\%\ O_2(\%) = SO_2 \frac{(20.9\% - 6\%)}{(20.9\% - O_2\ \%)} \tag{5.5}$$

$$NO_x \text{ at } 6\%\ O_2(\%) = NO_x \frac{(20.9\% - 6\%)}{(20.9\% - O_2\ \%)} \tag{5.6}$$

The bag filter houses ceramic elements to enable the plant to be operated with a range of flue gas exit temperatures, and also to provide information on cleaning and cake properties for full scale plant proposing to use ceramic filters.

Flue gases and suspended solids exit the combustor via a refractory lined crossover duct at the top of the plant and pass into a metallic heat exchanger. This heat exchanger consists of 19 off 25 mm diameter air cooled stainless steel tubes. Flue gases pass through the tubes, while cooling air is ducted around them within a mild

steel outer casing containing internal baffles. The flue gases are reduced in temperature up to 500 °C, depending on operating conditions.

5.4.2 Rig Specification

Following are major specifications of FBC rig.

i) Overall dimension of FBC section = 1 x 1 x 5 m (extended free board section).
ii) Internal dimensions of FB Section = 0.42 x 0.38 m.
iii) Internal dimensions of Combustion Section = 0.58 x 0.38 m.
iv) The combustion section is lined with cast–able refractory (backed with low thermal conductivity ceramic fiber based insulation).
v) The bed is capable of accepting bio–fuels and wastes.
vi) Three variable speed screws with feed hoppers to form the above–bed solid fuel feed system.
vii) The fluidized bed is instrumented with temperature and pressure ports for monitoring bed and freeboard conditions.
viii) Five thermocouples are arranged in vertical array at equal space.

5.4.3 Operating Conditions

Following are major operating conditions of the rig.

i) Bed material = Sand, Garside Leighton Buzzard 14/25 range (with nominal particle size of 1.18–0.60).
ii) Fluidized bed height = 700 mm.
iii) Fluidizing velocities of up to 3.5 m/s.
iv) Typical combustion temperatures ranging from 750–950 °C.
v) Feed rate of coal = 150 to 300 g/min.
vi) Feed rate of limestone = 12–60 g/min.

5.4.4 Testing Procedure

The bed was continuously monitored during the experiments. All the measurements of temperature and gas composition were taken with the FBC reactor operating at pre–set steady conditions. At specified feeding conditions of air, coal and limestone, the steady state condition was evaluated by monitoring the temperature and the flue gas composition (in terms of O_2 and CO_2). The steady state condition was considered

when the temperature and the flue gas composition were stable, and then a complete set of measurements was obtained. Coal and limestone were continuously added to the bed, keeping the control on the bed height. The bed was continuously monitored during the experiments. Gas samples were withdrawn from the bed through water cooled probes and were passed through a non–dispersive IR (CO_2, CO, N_2O) and chemi–luminescence (NO) analyzers. Due to the existence of radial concentration gradients, the tip of each water–cooled probe was positioned at the distance of 0.07 m from the inner wall. For SO_2 (non–dispersive IR), the samples were taken from the freeboard through a non–cooled movable probe and a heated sampling line. This process restricted the sampling at certain locations in the freeboard, at 0.45, 0.65 and 1.68 m respectively above distributor plate. Coal A was taken from Trans Indus Range and coal B from Salt Range and their specifications are given in table 5.3.Coals and limestone were sieved to 5–15 mm size and 0.1–5.6 mm size respectively. Limestone used for desulfurization was taken from Salt Range area and its specifications are given in table 5.4. While white wood was used as a biomass for co–firing with coal and it was taken from Drax Power Plant UK. The results of proximate analysis, ultimate analysis and semi quantitative XRF analysis of biomass are given the table 5.5.

5.4.5 Materials Handling

The above–bed solid feed system consists of three variable speed screws, each with its own feed hopper. These all discharge into a 125 mm diameter screw, which is set to run at a constant high speed and act purely as a part–filled transfer screw. The transfer screw discharges material onto the surface of the fluidized bed or, depending on bed height, into the splash zone. The metering screws are 100 mm, 125 mm and 200 mm in diameter shown in Fig. 5.19. This system has proved to be capable of handling a wide range of solid materials including fine powders and granular materials, and also allows three different materials to be fed simultaneously with independent control of each. Granular materials can be fed directly into the bed using a 125 mm diameter variable speed screw feeder with a sealed hopper; this screw discharge point is at the hot face of the refractory lining, Centre line 130 mm above the air distributor. The plant is also capable of simple modification to allow liquids or fine solids to be pneumatically conveyed directly into the fluidized bed. The FBC rig is equipped with

three types of screw feeders connected to the main 125 mm screw feeder which runs at a constant speed. The three types of screw feeders are as follow (Table 5.6).

Table 5.6 Description and use of screw feeders

Variable Screw Feeder	Description
200 mm	Manual screw metering control up to 70% load and used mainly for feeding low density materials (turkey litter, paper, etc.)
125 mm	Manual screw metering control up to 100% load and used mainly for blending various materials with higher densities (china clay, turkey bones etc.)
100 mm	Manual screw metering control up to 100% load Supply high CV fuels into the burning bed (coal, biomass, etc.)

5.4.6 Schematic Diagram and Pictorial Views of FBC Rig

Figure 5.18 is a schematic diagram of the FBC showing the position of all thermocouples and pressure transducers which is also presented in table 5.7 and table 5.8 respectively. Figures 5.19–5.23 are showing the different pictorial views of major parts of the FBC rig.

Table 5.7 Thermocouples location and labels

Thermocouples	Label	Thermocouples	Label	Thermocouples	Label
Plenum temp	T101	FB Mid temp	T108	Glosfume in temp	T115
Bed A temp	T102	FB top temp	T109	Glosfume out temp	T116
Bed B temp	T103	FB exit temp	T110	Cooling air in temp	T117
Bed C temp	T104	HX in temp	T111	Cooling air out temp	T118
Bed D temp	T105	HX out temp	T112	FD temp	T119
Bed E temp	T106	Cyclone in temp	T113	2ndary air temp	T120
Sight temp	T107	Cyclone exit temp	T114	---	---

Table 5.8 Pressure transducers location and labels

Transducers	Label	Transducers	Label	Transducers	Label
FD Orifice Upstream	P302	2ndry air orifice	P305	Above bed P	P308
FD Orifice	P303	Plenum	P306	Mid Freeboard	P309
2ndry air orifice upstream	P304	Bed P	P307	Glosfume dP	P310

5.4.7 Controls and Instrumentation

All the temperatures and pressures were recorded using thermocouples or pressure transmitters connected to a National Instrument (NI) TBX-1303 module which is then linked to a NI SCXI-1102 (temperatures) and SCXI–1100 (analog signals i.e. pressures) which can be read through lab view via a NI PCI–6035E card in the computer.

5.4.8 Controls

Manual control valves shown as primary and secondary air in Fig. 5.21 and Fig. 5.22 were used to control the flow rate of fluidizing air through the fluidized bed and above bed respectively. The exhaust fan of the FBC was fitted with an Inverter control which enables the operator to increase assist in maintaining a negative pressure above the bed, the mid freeboard section and subsequent sections. Each of the screw metering feeders are connected to eurotherms PID controllers which enables automatic and manual control of the fuel flow rate introduced into the bed.

5.4.9 Instrumentation

i) Labview

A Labview software was designed to log data for all the temperatures and pressures as listed in table 5.7 and table 5.8 shown in Fig. 5.23. A screen capture from the commissioning test is shown in Fig. 5.18.

ii) Oxygen Analyzer

A Servomex 570 Portable Oxygen Analyzer was used to measure the oxygen concentration located at the Top Freeboard of the FBC.

iii) Emissions Testing

The current location of the FBC benefits from the possibility of online emissions measurement using the Mobile Emissions Laboratory. This unit is equipped to monitor smoke, carbon dioxide (CO_2), carbon monoxide (CO), oxygen (O), nitrogen oxides (NO_x) and unburned hydrocarbons. It has heated line controls to enable accurate control of sample line temperatures.

iv) Post–test Analysis

Aside from the emission measurement during tests, the facility is able to carry out a wide range of post–test analysis such as weighing of the ash collected from the cyclone, bag filter, bottom of the bed, size distribution of sand particles, chemical analysis on samples collected as well as electron microscopic analysis is required.

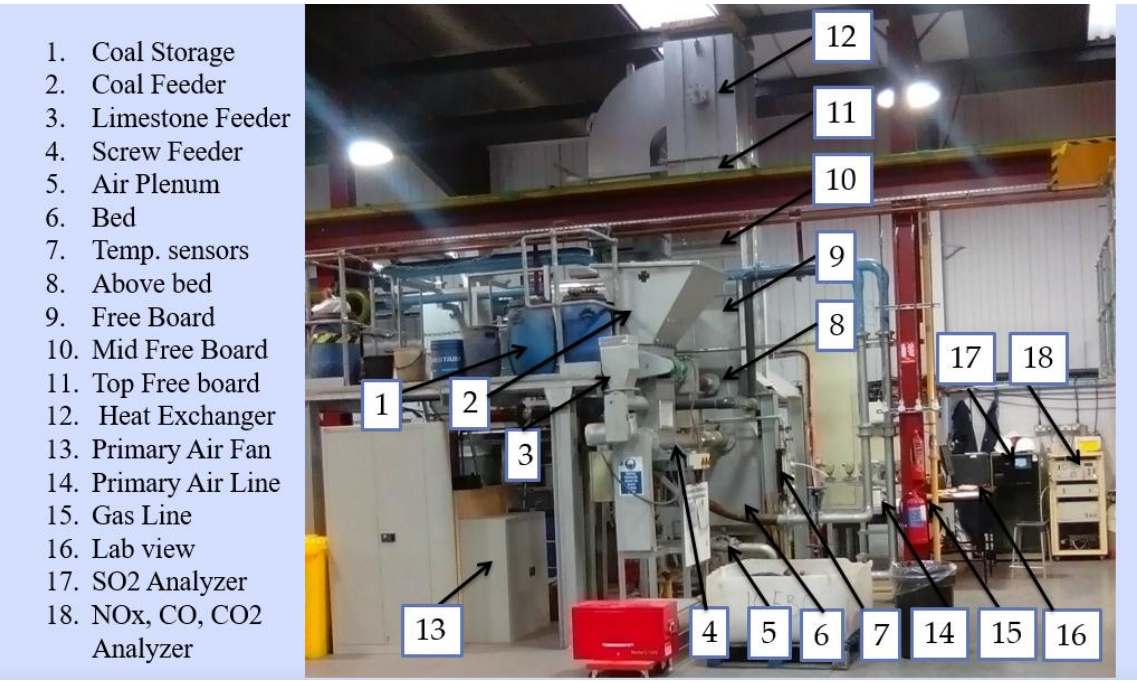

Fig. 5.18 Main parts of FBC

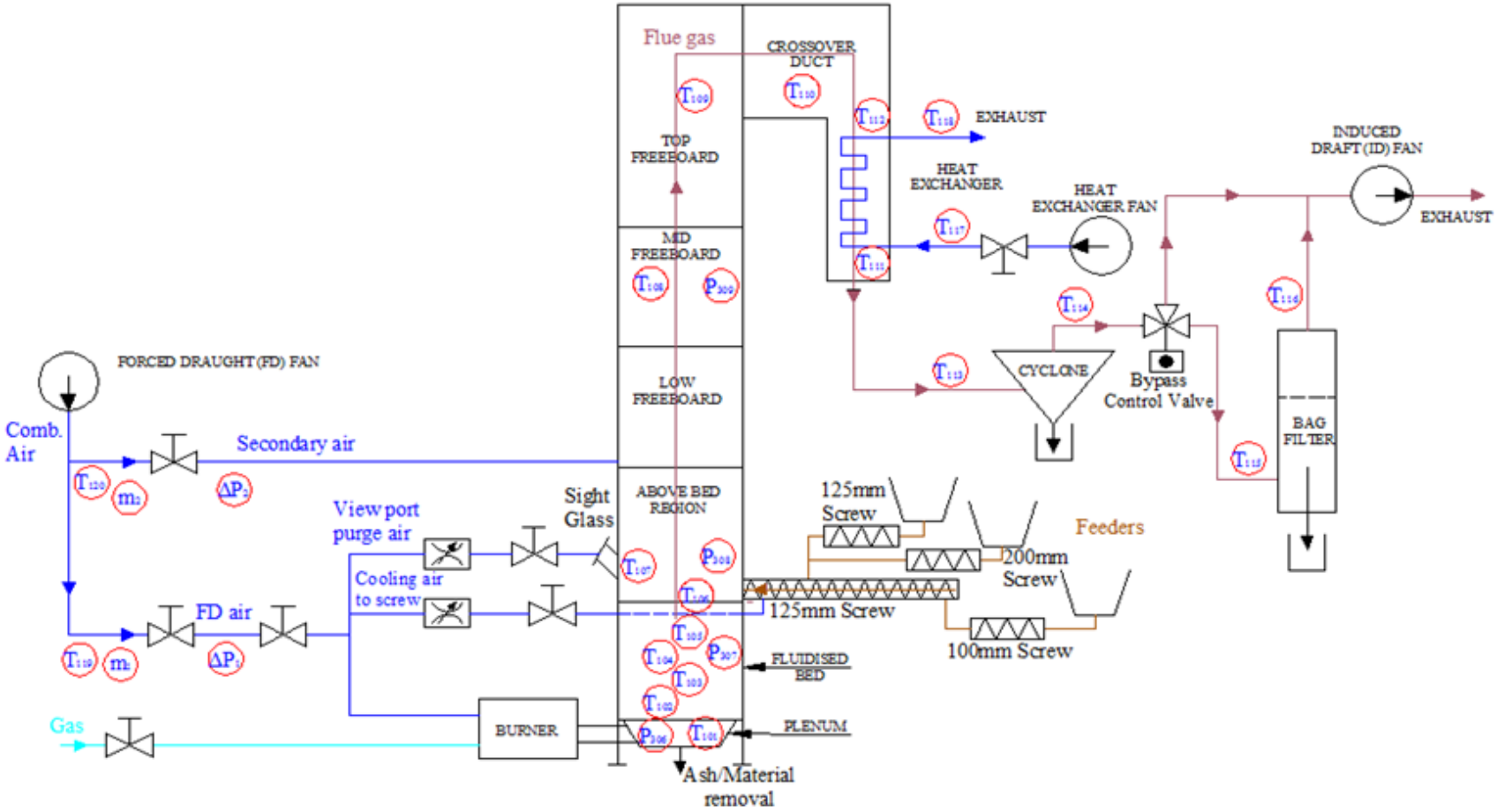

Fig. 5.19 Schematic diagram of FBC with instrumentation and control equipment

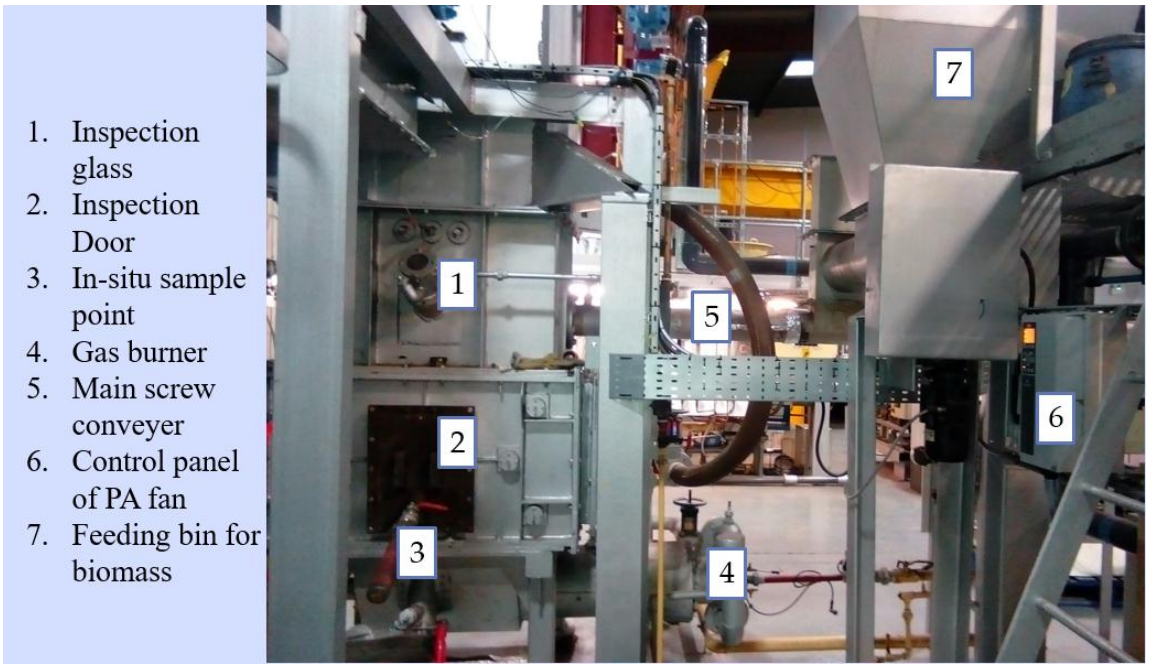

Fig. 5.20 Rear view of FBC

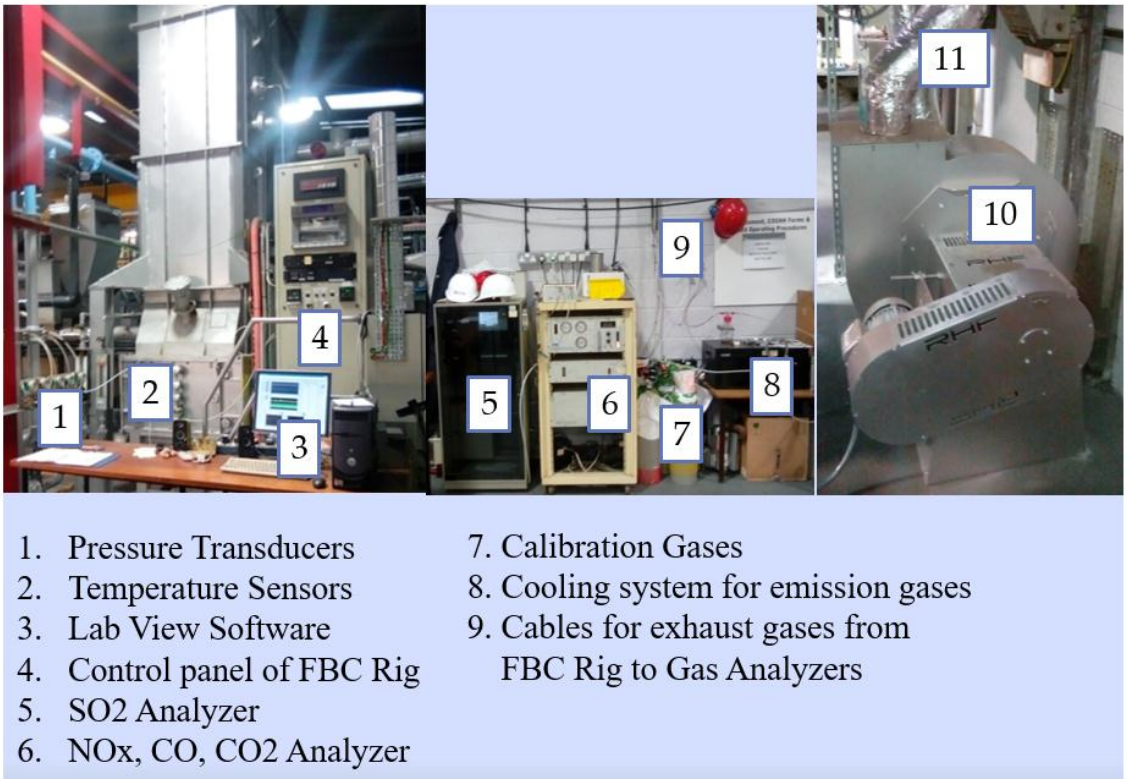

Fig. 5.21 Control panel, sensors and gas analyzers

1. Gas Line
2. Gas Burner
3. Primary Air(PA) Line
4. PA regulating Valve
5. Secondary Air (SA)Line
6. PA Flow valve
7. Cyclone (Ash Collection)
8. Ash collector

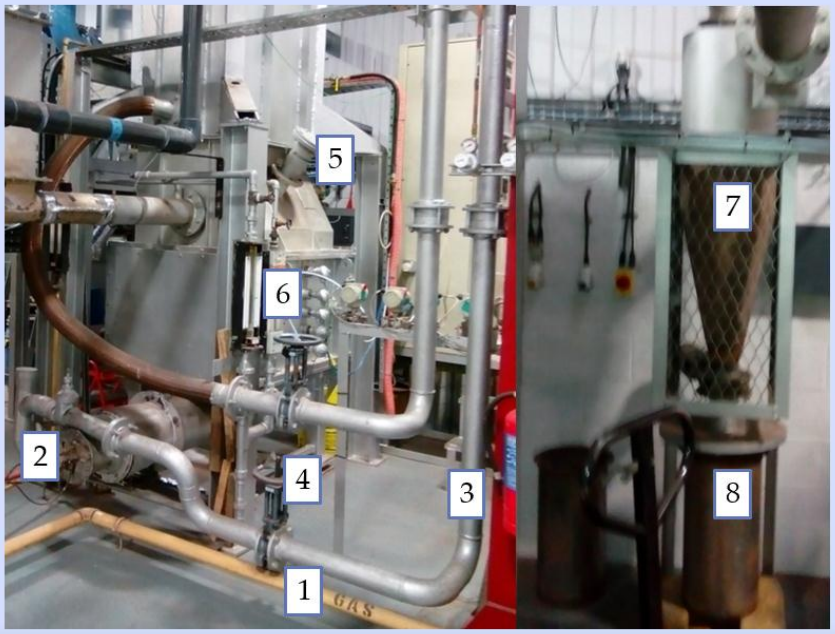

Fig. 5.22 Pipe lines of primary air, secondary air, natural gas and gas burner

Fig. 5.23 Screen short of lab view readings

CHAPTER NO. 6

EXPERIMENTAL WORK AND RESULTS

6.1 Introduction

Before presenting the results and their detailed discussion, here is the brief summary of experimental work which consists of the following two phases.

i. Phase–I: Lab Scale Testing

iii) **Part–I:** Study of coal quality characteristics.
iv) **Part–II:** Study of coal combustion characteristics and performance indices.

ii. Phase–II: Pilot Scale Testing

- Phase–II (Part–I): Study of major gaseous emissions (SO_2, NO_x, CO, CO_2) with limestone (L/s) addition during combustion in FBC.
- Phase–II (Part–II): Study of major gaseous emissions (SO_2, NO_x, CO, CO_2) with biomass addition during co–firing in FBC.
- Phase–II (Part–III): Optimization of process parameters (Ca/s ratio, bed temperature, Limestone particle size, biomass proportion) to reduce gaseous emissions.

6.1.1 Phase–I: Lab Scale Testing.

i. Part–I: Study of coal quality characteristics

This study was completed by conducting the following testing from SGS Pakistan and Changsha University of Science and Technology (CUST) Changsha, Hunan, China.

f. Proximate Analysis
g. Ultimate Analysis
h. Gross Calorific Value (GCV) / Net Calorific Value (NCV)
i. Ash Fusion Temperature (AFT)
j. Ash composition Analysis

ii. **Part –II:** Study of coal combustion characteristics and performance indices.

Following combustion characteristics and testing was performed in CUST lab China.

a. Volatile initial separating temperature (T_s)
b. Ignition temperature (T_i)
c. Complete burning temperature (T_h)
d. Complete burning time (t_{rj})
e. Maximum combustion rate (w_{max})
f. Average combustion rate (w_{mean})
g. Temperature of maximum combustion rate (T_{max})
h. Temperature difference of DTG's half peak width (ΔT_h)
i. Temperature difference of DTG's total peak width (ΔT)
j. Ignition characteristics index (F_z)
k. Flammability index (C)
l. Stable firing index (M)
m. Combustion Characteristics Curves (TG and DTG)

6.1.2 Phase–II: Pilot Scale Testing

Following studies were carried out at FBC experimental Rig, University of Leeds, Leeds UK. The Rig is located at Low Carbon Combustion Center, Crown Works Industrial Estate Unit 2, Rotherham Road Beighton S20 1AH, UK.

i. **Part–I.** Study of major gaseous emissions (SO_2, NO_x, CO, CO_2) with limestone (L/s) addition during combustion in FBC.

ii. **Part–II.** Study of major gaseous emissions (SO_2, NO_x, CO, CO_2) with biomass addition during co–firing in FBC.

iii. **Part–III.** Optimization of process parameters (Ca/s ratio, bed temperature, Limestone particle size, biomass proportion) to reduce gaseous emissions.

A schematic diagram showing process flow of lab scale and pilot scale testing is given in Fig. 6.1.

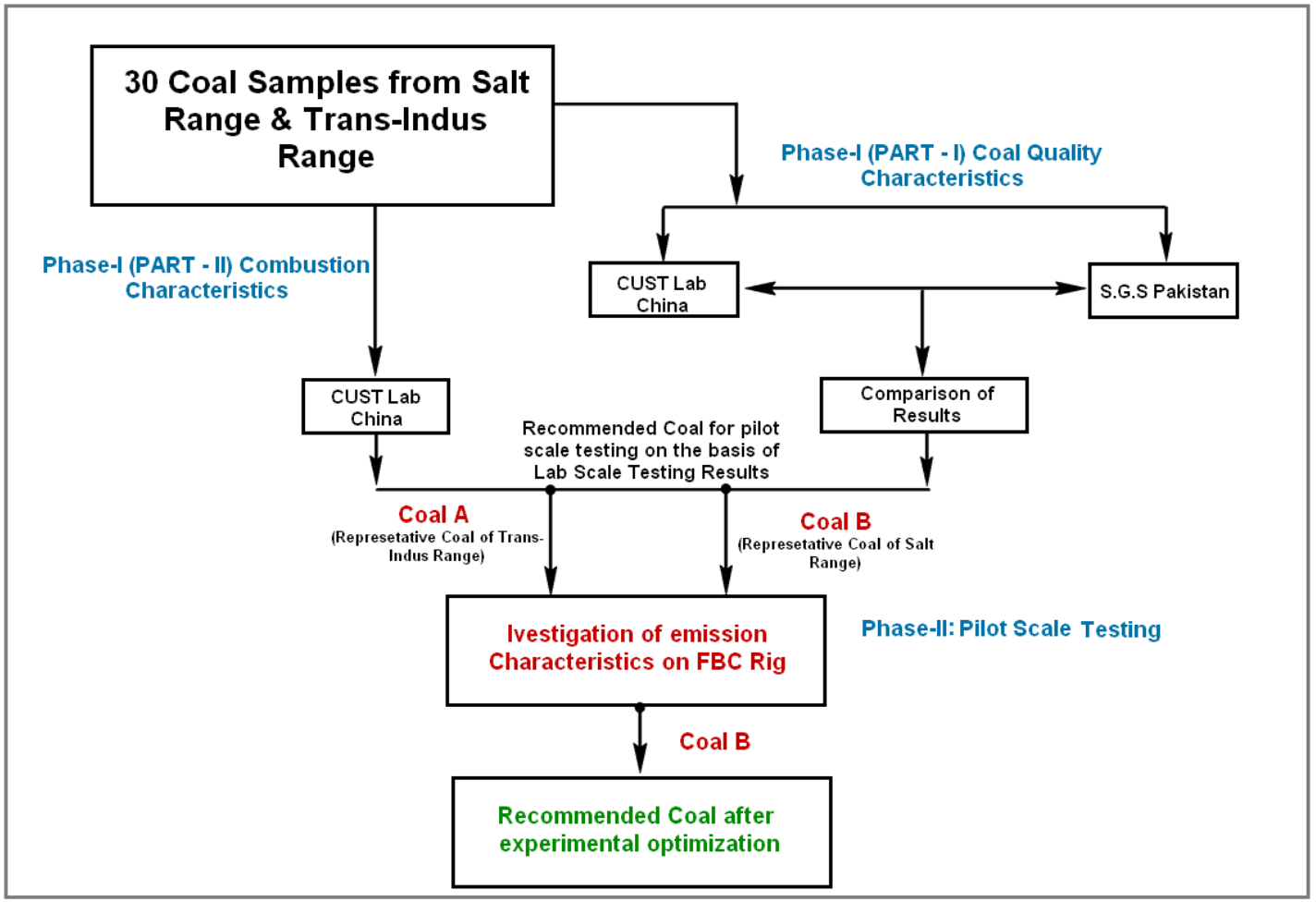

Fig. 6.1 Process flow diagram of lab scale and pilot scale testing

6.2 Results and Discussion

Testing of Salt Range and Trans Indus Range coal was carried out to investigate the different quality parameters, combustion characteristics and emission characteristics as given below. This testing is divided into two phases, i.e. lab scale testing and pilot scale testing of the coal.

6.2.1 Phase–I: Lab Scale Testing, Part–I: (Study of Coal Quality Characteristics)

6.2.1.1 Proximate Analysis and GCV

As proximate analysis determines the fixed carbon (FC), volatile matter (VM), moisture and ash percentages in the coal, results of proximate analysis and calorific values of the thirty coal samples are compared in this study as shown in table 6.1. For further insight into this experimental work, average results are also presented in table 6.2 and Fig. 6.2. There is no major difference in the results of two the aforementioned Labs. However, the results of CUST for proximate analysis are more conservative as compared to SGS. Therefore, they have been considered for further discussion.

Table 6.1 Proximate analysis and calorific value from CUST China and SGS Pakistan

Sr. #	TM (%) (arb)		IM (%) (adb)		VM (%) (adb)		Ash (%) (adb)		FC (%) (adb)		GCV MJ/kg (arb)		NCV MJ/kg (arb)	
	CUS	SGS	CUS	SGS	CUS	SGS	CUS	SGS	CUS	SGS	CUS	SGS	CUS	SGS
1	5.1	6.5	2.9	3.4	24.3	36.1	47.0	27.2	25.8	30.3	13.3	21.9	12.6	20.9
2	8.4	7.4	2.3	3.3	24.2	28.0	47.1	42.4	26.4	22.3	12.9	15.3	12.0	14.6
3	8.4	8.1	2.5	3.5	24.3	30.9	44.3	33.1	29.0	28.0	13.4	18.6	12.6	17.7
4	5.7	5.7	3.0	3.2	30.0	33.8	32.7	32.3	34.3	28.3	18.8	19.8	17.8	18.9
5	6.4	6.9	2.9	3.2	28.5	34.6	36.9	28.7	31.9	29.9	17.0	21.1	16.3	20.1
6	8.8	7.6	3.2	3.6	24.3	30.3	50.3	35.7	22.2	26.4	10.1	17.9	9.4	17.0
7	10.3	8.3	4.4	3.8	36.4	34.6	25.2	26.7	34.1	30.4	20.4	21.2	19.3	20.2
8	5.9	7.3	2.5	3.5	25.2	28.3	42.0	38.2	30.4	26.2	15.2	16.5	14.5	15.7
9	7.5	7.2	3.2	4.0	35.5	38.0	25.0	23.5	36.4	31.3	21.3	22.4	20.2	21.4
10	8.6	7.0	3.4	2.7	33.1	27.5	34.1	42.3	29.4	23.2	18.0	15.7	17.1	15.0
11	9.7	9.5	3.0	3.9	34.6	34.8	23.5	23.4	39.0	32.3	21.5	21.7	20.3	20.6
12	6.9	5.5	2.6	3.3	27.0	27.7	44.6	44.4	25.8	22.5	14.1	14.9	13.3	14.2

13	10.0	9.2	2.6	3.7	35.3	35.2	23.3	23.7	38.9	31.9	21.3	22.0	20.2	21.0
14	8.1	8.2	2.5	3.5	25.8	29.0	44.9	41.3	26.8	21.5	13.1	15.3	12.2	14.4
15	10.0	8.7	3.2	3.7	33.8	33.2	34.0	32.7	29.1	25.5	17.6	18.6	16.6	17.7
16	9.0	9.0	3.0	3.5	29.8	32.5	39.1	35.0	28.1	23.5	15.3	17.5	14.5	16.6
17	10.4	10.1	2.8	3.7	32.9	34.5	28.2	25.9	36.1	29.6	19.4	20.4	18.3	19.4
18	8.2	7.6	3.6	3.0	31.0	30.0	36.0	37.4	29.5	25.0	16.8	17.2	16.1	16.3
19	9.6	8.5	4.2	3.6	37.4	33.6	21.8	24.7	36.6	33.2	22.4	21.3	21.3	20.3
20	8.7	7.8	3.9	3.5	39.2	32.9	25.6	29.8	31.4	29.5	21.0	19.8	20.0	18.9
21	6.5	6.5	2.4	2.8	30.4	32.6	36.3	34.7	30.9	26.3	17.4	18.5	16.5	17.6
22	9.5	7.1	3.3	3.1	37.8	35.1	24.3	28.3	34.6	29.4	21.5	20.9	20.5	19.9
23	8.5	6.6	3.6	3.4	40.5	37.2	24.3	26.5	31.7	29.7	21.0	20.6	19.9	19.6
24	7.7	6.0	3.3	2.7	37.8	33.7	29.1	34.8	29.8	25.6	19.3	18.1	18.3	17.2
25	5.3	3.8	2.7	2.4	33.1	32.7	38.1	40.2	26.0	23.3	16.6	16.6	15.8	15.7
26	6.6	6.3	3.2	4.3	40.4	41.5	14.2	13.1	42.2	39.2	24.1	25.3	22.9	24.2
27	3.2	4.0	2.4	2.3	33.5	31.1	38.7	42.6	25.4	22.4	16.1	15.8	15.3	15.1
28	5.3	3.9	2.6	2.7	39.5	38.4	29.2	30.8	28.8	27.0	19.7	20.3	18.7	19.4
29	6.8	5.5	2.8	2.6	39.4	37.0	28.7	30.9	29.2	26.5	19.8	19.9	18.8	18.9
30	7.7	6.4	3.2	2.7	32.7	37.3	34.6	30.8	29.5	25.5	19.3	19.5	18.3	18.6

adb: air dry basis arb: as received basis

Table 6.2 Proximate analysis and GCV (range, mean, std. deviation & variance)

Characte –ristics	No	Range		Minimum		Maximum		Mean		Std. Dev.		Variance	
	N	CUS	SGS	CUS	SGS	CUS	SGS	CUS	SGS	CUS	SGS	CUS	SGS
TM (%) (arb)	30	7.2	6.3	3.2	3.8	10.4	10.1	7.8	7.1	1.8	1.6	3.3	2.5
VM (%) (adb)	30	16.2	13.9	24.2	27.5	40.5	41.5	32.6	33.4	5.3	3.5	28.4	12.1
Ash (%) (adb)	30	36.1	31.3	14.2	13.1	50.3	44.4	33.4	32.0	9.1	7.2	82.0	52.2
FC (%) (adb)	30	20.1	17.7	22.2	21.5	42.2	39.2	31.0	27.5	4.7	4.0	21.8	15.7
GCV (MJ/kg) (arb)	30	14.0	10.4	10.2	14.9	25.7	25.3	18.8	19.2	3.4	2.5	11.5	6.4

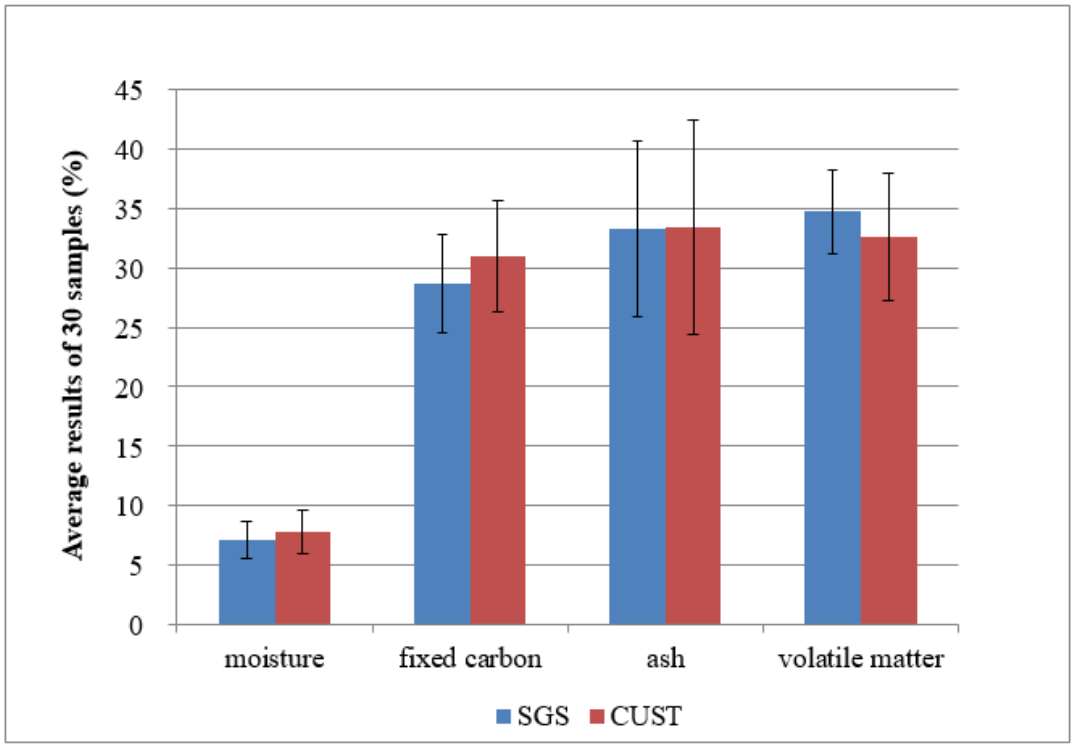

Fig. 6.2 Comparison of average values of proximate analysis for 30 coal samples (SGS vs CUST)

6.2.1.2 Ultimate Analysis

Ultimate analysis has a great importance in design, performance analysis and combustion control of a coal–fired combustion system. The results are useful in determining the quantity of air required for combustion and the volume composition of the combustion gases. This information is also used for the calculation of flame temperature and flue duct design. Gaseous emissions like SO_x, NO_x, CO and CO_2 can be calculated in the flue gas. $DeSO_x$ and $DeNO_x$ systems are designed on the basis of these results. Results and their average values of ultimate analysis, based on thirty coal samples from SGS and CUST, are given in table 6.3 and table 6.4, respectively. Moreover, figure 6.3 offers detailed comparison of the average results. It is clear from the Fig. 6.3 that there is no considerable difference in the values of carbon, hydrogen and sulfur as investigated from SGS and CUST. However, there is great disagreement in the results of nitrogen from these Labs (i.e. CUST: average value >4% and SGS: average value <1%). CHNS analysis of the coal has been repeated in the laboratory of University of Leeds, UK and the results of nitrogen are in the range of 1.07% to 1.33% (average value = 1.19%). Similarly, average results of carbon, hydrogen and sulfur are 43.4%, 3.4% and 7.61% respectively which are close to the SGS results.

Thus, for ultimate analysis, SGS results have been taken as a reference for further discussion.

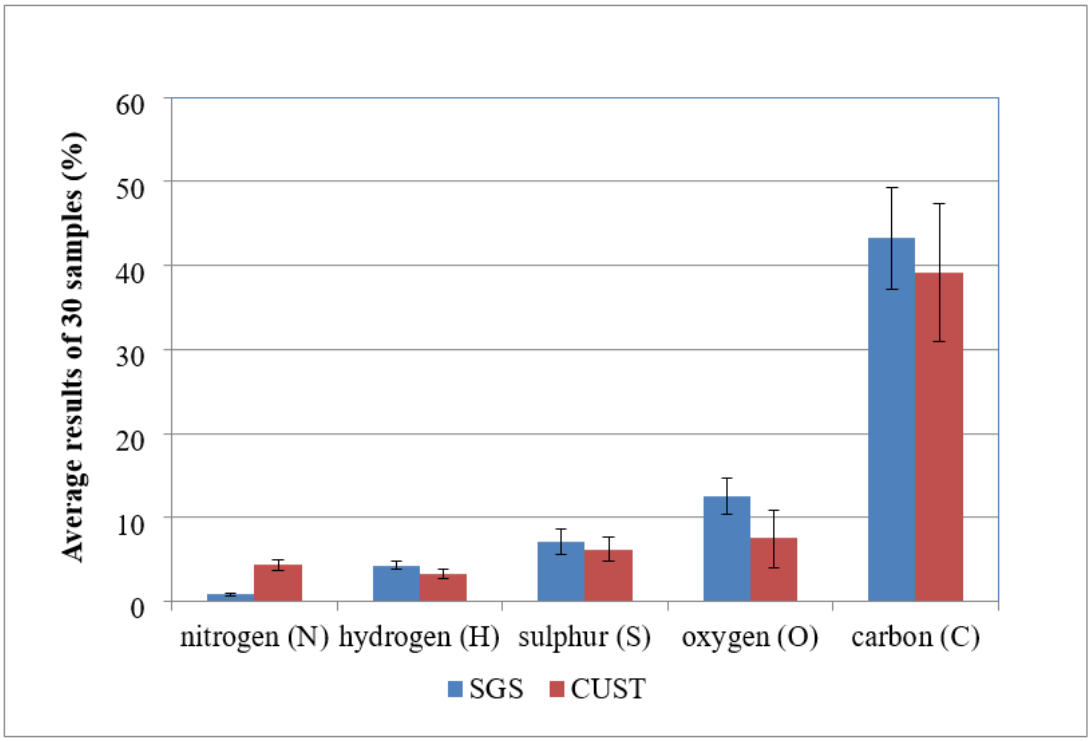

Fig. 6.3 Comparison of average values of ultimate analysis for 30 coal samples (SGS vs CUST)

Table 6.3 Results of ultimate analysis by SGS Pakistan and CUST China

Sample No.	Carbon (C) % (arb)		Hydrogen (H) % (arb)		Nitrogen (N) % (arb)		Sulfur (S) % (arb)		Oxygen (O) % (arb)	
	CUST	SGS	CUST	SGS	CUST	SGS	CUST	SGS	CUST	SGS
1	27.6	48.0	2.7	4.3	3.8	1.3	5.4	8.7	9.5	10.5
2	29.4	34.0	2.8	3.7	4.1	0.9	6.6	7.8	4.6	11.3
3	30.1	41.6	2.8	4.1	4.1	1.1	6.9	7.6	6.1	12.5
4	41.8	42.9	3.5	4.1	4.4	1.0	6.7	11.1	6.1	8.7
5	32.7	44.9	2.8	4.4	4.4	0.9	8.7	8.8	9.6	12.3
6	23.3	40.7	2.2	4.1	4.2	0.9	8.7	8.3	5.6	10.4
7	43.7	47.0	3.7	4.6	4.1	1.0	7.8	10.3	6.8	10.3
8	32.5	38.2	2.7	3.8	4.3	0.7	3.4	6.7	10.7	12.4
9	49.5	50.7	4.2	4.8	4.6	1.0	6.0	7.0	4.4	13.1
10	35.5	34.3	3.0	3.4	3.9	0.7	5.3	7.9	11.5	11.5
11	51.3	49.7	4.1	4.8	4.6	0.9	5.0	5.0	3.6	16.2

12	31.7	33.5	2.7	3.3	4.4	0.7	6.8	6.6	4.9	11.4
13	47.0	48.6	3.7	4.7	4.0	0.9	4.2	6.3	9.6	15.8
14	30.3	33.8	2.8	3.8	3.8	0.8	7.2	7.0	5.5	13.4
15	38.3	40.6	3.3	4.3	4.2	0.6	6.3	7.2	6.3	14.7
16	30.4	39.2	2.8	4.2	3.7	0.7	4.4	5.5	13.4	15.4
17	44.4	47.6	3.6	4.8	4.1	0.8	6.2	6.3	5.4	14.5
18	30.6	39.0	2.6	4.0	3.9	0.8	7.0	5.9	13.5	13.0
19	48.2	49.4	3.8	4.6	4.0	0.9	6.8	6.9	6.9	13.5
20	46.4	45.5	3.9	4.4	4.1	0.8	6.3	5.7	6.5	13.8
21	40.2	42.6	3.5	4.3	4.2	0.7	3.9	3.3	6.9	14.6
22	39.0	46.3	3.1	4.5	4.2	0.8	3.8	7.0	17.7	13.0
23	47.1	47.8	3.9	4.6	4.4	0.8	5.5	6.2	7.6	14.1
24	44.4	44.4	3.8	4.5	4.3	0.7	6.7	8.2	5.3	7.5
25	37.3	38.5	3.3	3.8	5.2	0.6	5.8	6.8	6.1	10.1
26	57.3	60.2	4.4	5.2	4.4	1.0	4.7	4.8	8.9	15.8
27	33.6	35.5	3.1	3.6	4.0	0.5	7.1	8.3	10.6	9.6
28	44.3	45.5	3.8	4.4	6.0	0.6	7.9	7.7	4.2	11.0
29	44.4	44.6	3.7	4.3	6.5	0.6	7.5	7.5	3.7	12.1
30	41.6	43.8	3.7	4.4	4.2	0.7	6.8	7.3	3.0	13.1

Table 6.4 Ultimate analysis from CUST and SGS (range, mean, std. dev & variance)

UA % (arb)	Range		Minimum		Maximum		Mean		Std deviation		Variance	
	CUST	SGS	CUST	SGS	CUST	SGS	CUST	SGS	CUST	SGS	CUST	SGS
C	34.0	26.7	23.3	33.5	57.3	60.2	39.1	43.3	8.2	6.1	67.8	36.6
H	2.2	1.9	2.2	3.3	4.4	5.2	3.3	4.3	0.6	0.4	0.3	0.2
N	2.8	0.7	3.7	0.5	6.5	1.3	4.3	0.8	0.6	0.2	0.4	0.0
S	5.3	7.8	3.4	3.3	8.7	11.1	6.2	7.1	1.4	1.6	2.0	2.4
O	14.7	8.7	3.0	7.5	17.7	16.2	7.5	12.5	3.4	2.2	11.7	4.7

6.2.1.3 Ash Fusion Temperature

This analysis is normally used to assess the coal quality for effective utilization, ash fusibility and its melting behavior during combustion. It could be used as a guide for coal blending, optimizing the use of coal resources and operational parameters of coal–fired power plants. It helps to predict the true combustion conditions and suitability of coal for the combustion [109]. The comparison of average AFT results conducted by SGS and CUST is depicted in table 6.5 and Fig. 6.4.

Fig. 6.4 Comparison of average values of ash fusion temperatures (SGS vs CUST)

Table 6.5 Ash fusion temp (AFT) from CUST and SGS (Range, mean, standard deviation and variance) using SPSS–20

AFT Red(R) / Oxid(O)	Range		Minimum		Maximum		Mean		Std. Deviation		Variance	
	CUS	SGS	CUS	SGS	CUS	SGS	CUS	SGS	CUS	SGS	CUS	SGS
IDT (R)	315	348	1015	1075	1330	1423	1229	1192	61	100	3740	10056
ST (R)	175	351	1245	1078	1420	1429	1367	1211	37	106	1398	11340
HT (R)	156	345	1331	1096	1487	1441	1406	1252	31	97	952	9397
FT (R)	111	459	1389	1141	1500	1600	1446	1304	44	99	1906	9737
IDT (O)	204	150	1154	1321	1358	1471	1269	1359	47	35	2177	1214
ST (O)	117	276	1319	1324	1436	1600	1390	1372	30	51	909	2618
HT (O)	160	252	1340	1348	1500	1600	1435	1388	48	48	2285	2309
FT (O)	98	237	1402	1363	1500	1600	1488	1405	31	47	948	2234

6.2.1.4 Ash Composition

Ash content of coal represents the remains of mineral matter after the carbon, oxygen, sulphur and water are driven off during combustion. Main purpose of this analysis is to calculate fouling and slagging indices, estimate of slag viscosity against temperature, modelling environmental impact of the ash, reference for ash utilization and estimation of corrosion in the boiler against K_2O, NaO, CaO_2 in ash [110, 111]. Average results of important constituents of ash (i.e. Al_2O_3, SiO_2, Fe_2O_3) obtained by SGS and CUST are compared in Fig. 6.5. Average values of slagging and fouling indices calculated on the basis of ash composition results, are given in table 6.6.

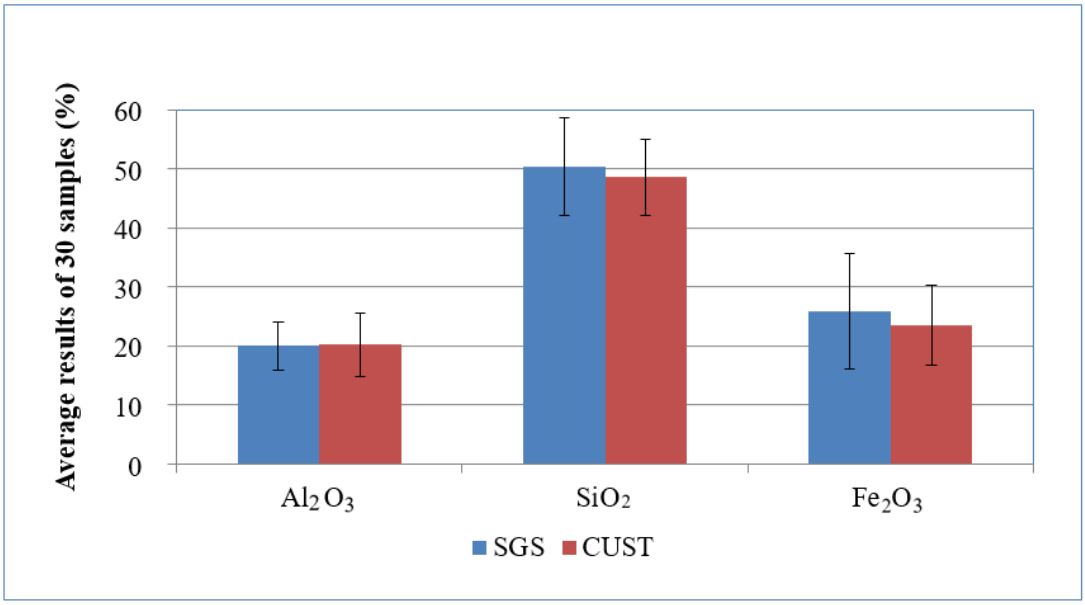

Fig. 6.5 Comparison of average values of ash composition (SGS vs CUST).

Table 6.6 Average slagging and fouling indices of coal using SPSS–20

Indices	Samples	Range	Minimum	Maximum	Mean	Std. deviation	Variance
Slagging	30	0.89	0.04	0.93	0.25	0.20	0.04
Fouling	30	21.00	1.00	22.00	2.13	3.79	14.33

6.2.2 Phase–I: Lab Scale Testing, Part–II:

Study of Coal Combustion Characteristics and Performance Indices;

Following combustion characteristics and testing was performed in CUST lab China.

n. Volatile initial separating temperature (T_s)
o. Ignition temperature (T_i)
p. Complete burning temperature (T_h)
q. Complete burning time (t_{rj})
r. Maximum combustion rate (w_{max})
s. Average combustion rate (w_{mean})

The coal combustion consists of de–volatilization of the coal and the heterogeneous combustion of the char. The ignition rate is important combustion characteristics of the coal. Evolution and ignition of volatiles occur simultaneously with higher heating rates however de–volatilization will start before ignition and combustion with low heating rates [112, 113]. Mean values of important combustion parameters and the results of ignition temperatures and combustion characteristics indices are given for thirty coal samples (Table 6.7, 6.8). Moreover, the classification of coal combustion characteristics is given in table 6.9.

Table 6.7 Combustion parameters from CUST China (range, mean, std. dev, variance)

	Range	Minimum	Maximum	Mean	Standard deviation	Variance
T_s	59.0	221.0	280.0	256.4	13.2	173.8
T_h	95.0	547.0	642.0	603.2	22.9	524.4
t_{rj}	5.0	8.8	13.8	11.6	1.3	1.8
w_{max}	0.1	0.6	0.7	0.6	0.0	0.0
T_{max}	51.0	471.0	522.0	484.9	9.6	92.3
w_{mean}	0.1	0.5	0.6	0.5	0.0	0.0
ΔT_h	95.0	45.0	140.0	92.3	24.7	609.3
ΔT	117.0	141.0	258.0	204.2	29.8	885.7

where,

T_s = the volatile initial separating temperature, ℃

T_h = the complete burning temperature，℃

t_{rj} = the complete burning time, min

w_{max} = the max combustion rate $[(dw/d\tau)_{max}]$，mg/min

w_{mean} = the average burning rate $[(dw/d\tau)_{mean}]$，mg/min

T_{max} = the temperature of maximum combustion rate，℃

T_h = the temperature difference of DTG's half peak width，℃

ΔT = the temperature difference of DTG's total peak width，℃

Table 6.8 Ignition temp and combustion characteristics indices of 30 coal samples

Sample	T_i (°C)	F_z	C	M	Sample	T_i (°C)	F_z	C	M
1	384	1.913	2.702	3.668	16	366	3.019	2.838	3.812
2	392	1.851	2.675	3.638	17	356	4.607	2.666	3.629
3	381	2.066	2.570	3.526	18	355	3.519	2.826	3.800
4	372	3.724	2.619	3.578	19	366	6.337	2.796	3.768
5	380	3.153	2.590	3.548	20	359	5.818	3.019	4.006
6	371	1.681	2.817	3.791	21	358	3.323	2.751	3.720
7	356	5.660	2.845	3.820	22	363	5.855	2.868	3.845
8	375	2.319	2.561	3.517	23	371	6.143	3.043	4.031
9	372	5.437	2.743	3.711	24	369	5.029	3.037	4.025
10	361	3.920	2.901	3.880	25	380	3.340	3.041	4.029
11	365	5.498	2.635	3.596	26	368	8.016	2.720	3.687
12	369	2.262	2.814	3.787	27	376	3.274	3.080	4.071
13	361	5.579	2.663	3.626	28	383	5.086	3.123	4.116
14	370	2.148	2.726	3.693	29	371	5.185	3.105	4.097
15	380	3.966	2.935	3.916	30	368	3.422	2.951	3.933

T_i = ignition temp, F_z = ignition characteristics index, C = flammability index, M = stable firing index

Table 6.9 The classification of coal combustion characteristics [13, 114]

Rank	Flammability Index (C)	Stable Firing Index (M)	Ignition Characteristics Index (Fz)
Extremely Difficult	≤ 0.9	<1.8	≤ 0.5
Difficult	0.9 ~ 1.4	1.8 ~ 2.3	0.5 ~ 1.0
Medium	1.4 ~ 1.75	2.3 ~ 2.6	1.0 ~ 1.5
Easy	1.75 ~ 2.3	2.6 ~ 3.3	1.5 ~ 2.0
Very Easy	>2.3	>3.3	>2.0

The ignition temperatures (T_i) and Flammability Index (C), Ignition Characteristics Index (F_z) and Stable Firing Index (M) are used for evaluating combustion performance of different fuels. F_z indicates the ignition performance of fuels, which means how fast or slowly the fuel gets ignited (Table 6.7). Ignition temperatures of all the coals are (355–392 °C) which are <400 °C indicating that the coal is easy for

ignition. Value of F_z is 1.5–2.0 for the coals 1, 2 and 6, and > 2.0 for all the remaining coals. It shows that all these coals have very good ignition characteristics.

Value of C of all the coals is (2.6–3.1) which is >2.3, indicating that these coals have very good flammability characteristics. The value of M is (3.5–4.1) which is >3.3 leading to the fact that these coals have ideal characteristics of stable firing.

TG and DTG curves of some representative coal samples are given in the Fig. 6.6 to 6.16 which is graphical presentation of the data of table 6.7 and table 6.8.

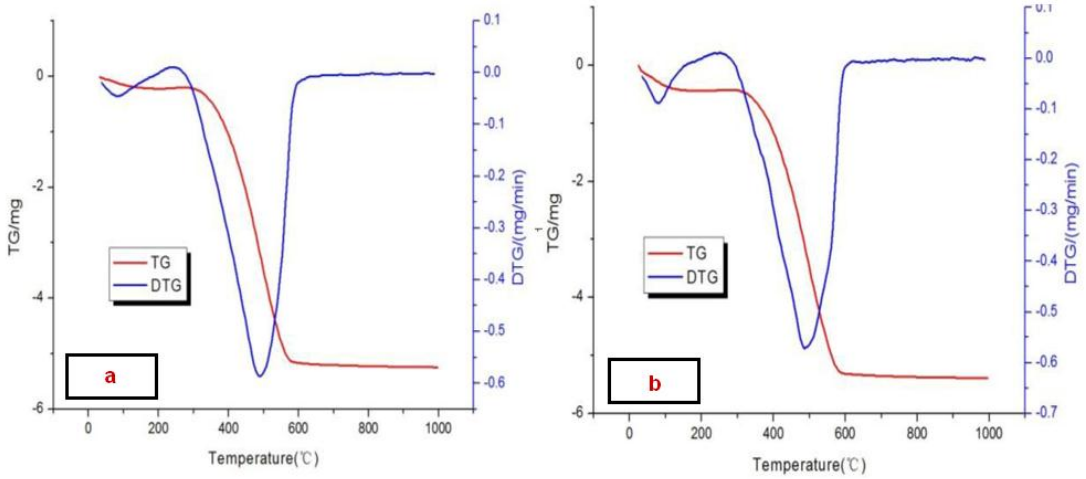

Fig. 6.6 (a) TG and DTG curves of sample 1 (b) TG and DTG curves of sample 2

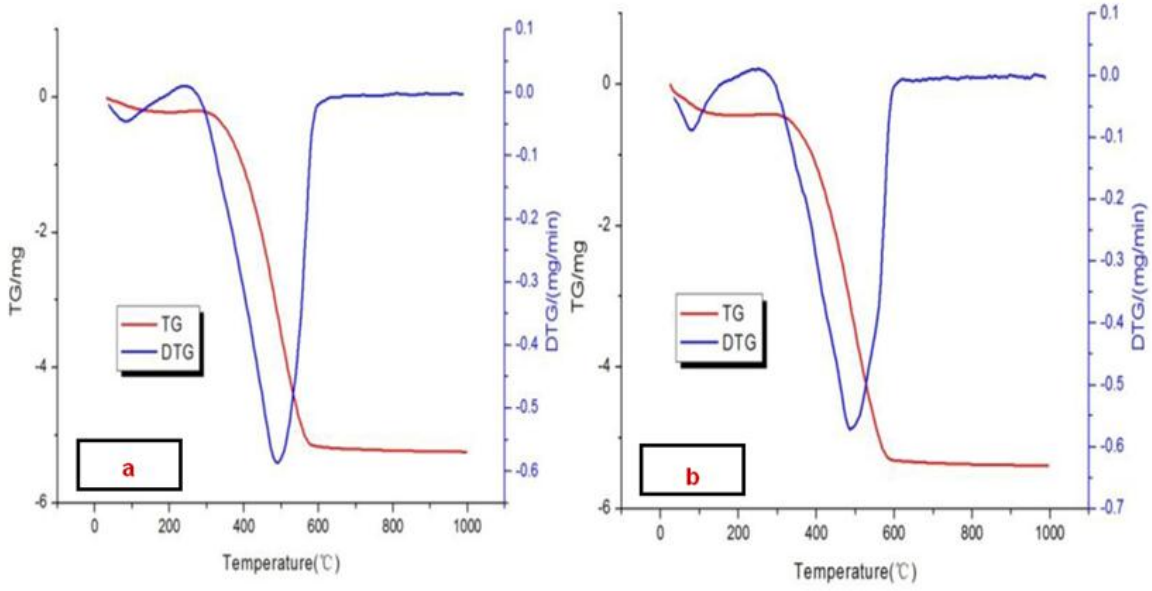

Fig. 6.7 (a) TG and DTG curves of sample 3 (b) TG and DTG curves of sample 4

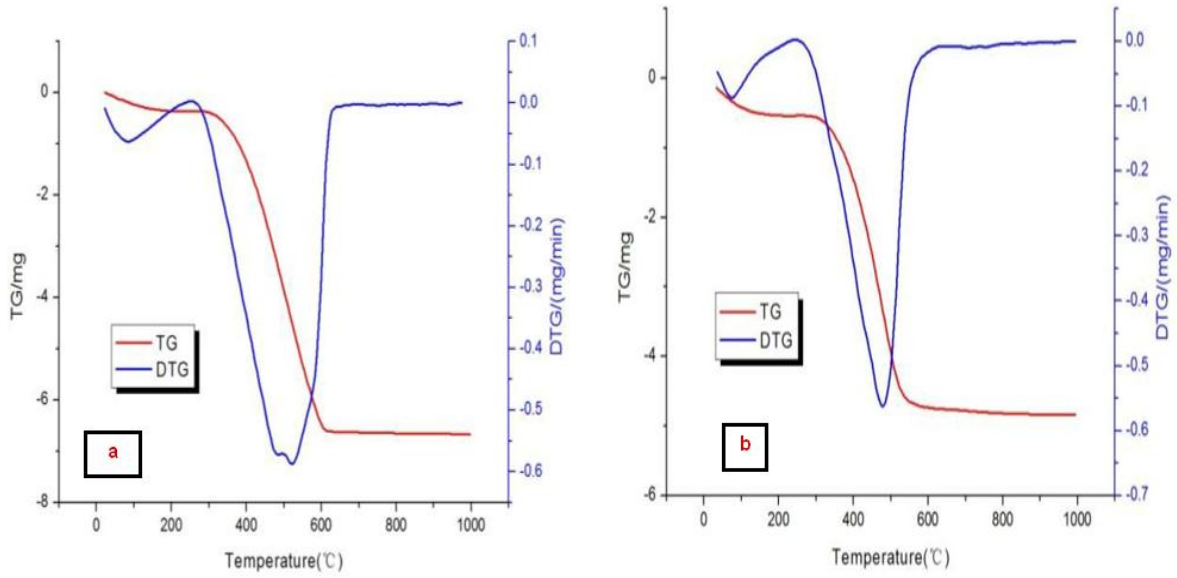

Fig. 6.8 (a) TG and DTG curves of sample 5 (b) TG and DTG curves of sample 6

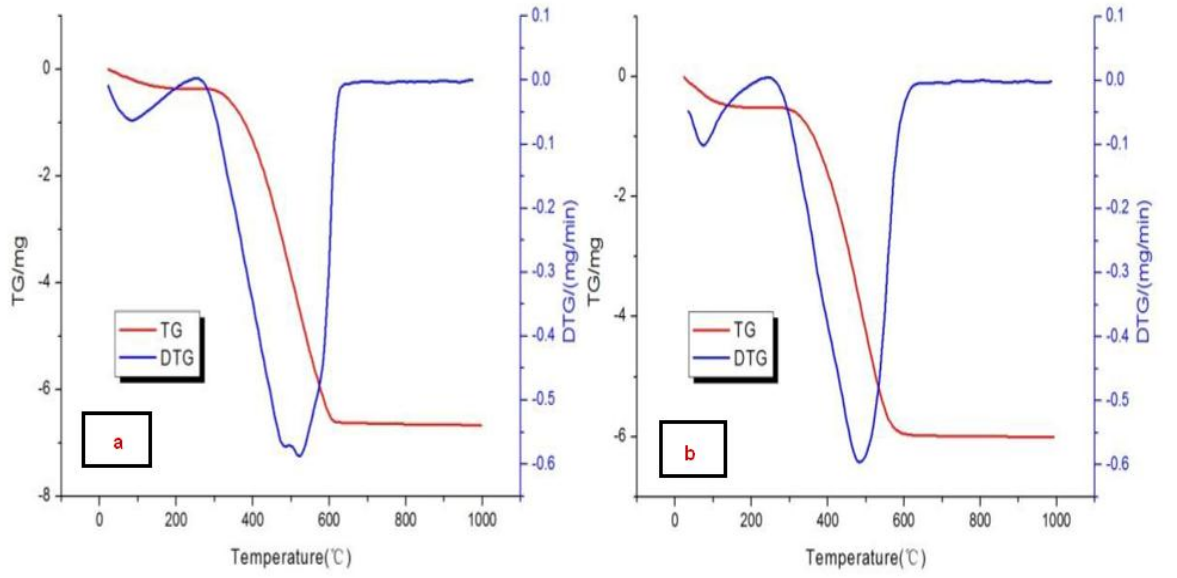

Fig. 6.9 (a) TG and DTG curves of sample 7 (b) TG and DTG curves of sample 8

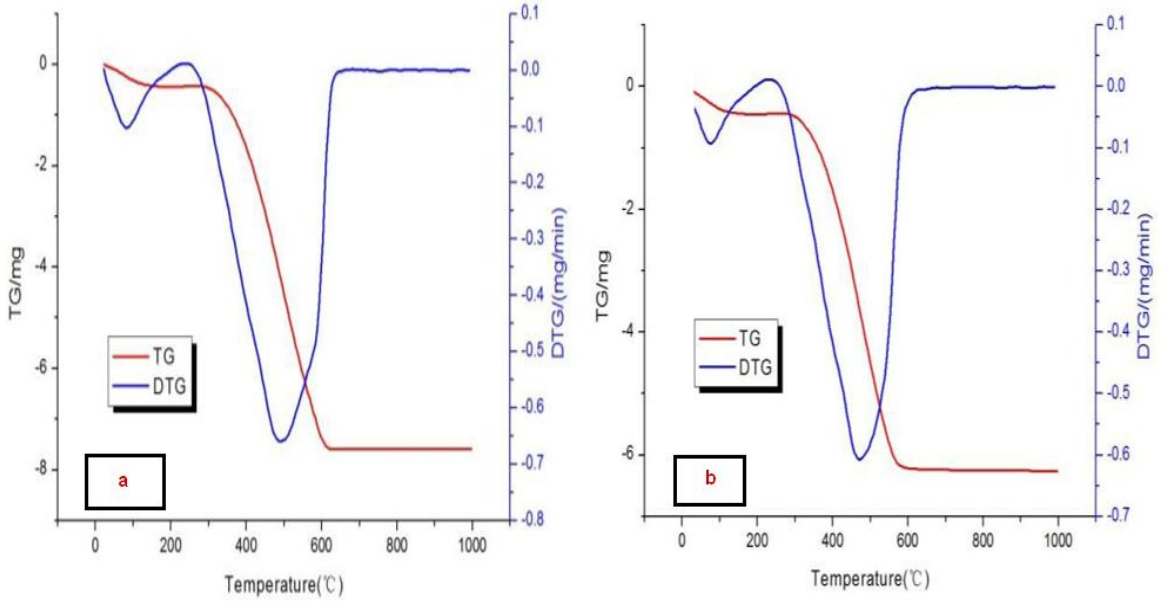

Fig. 6.10 TG and DTG curves of sample 9 (b) TG and DTG curves of sample 10

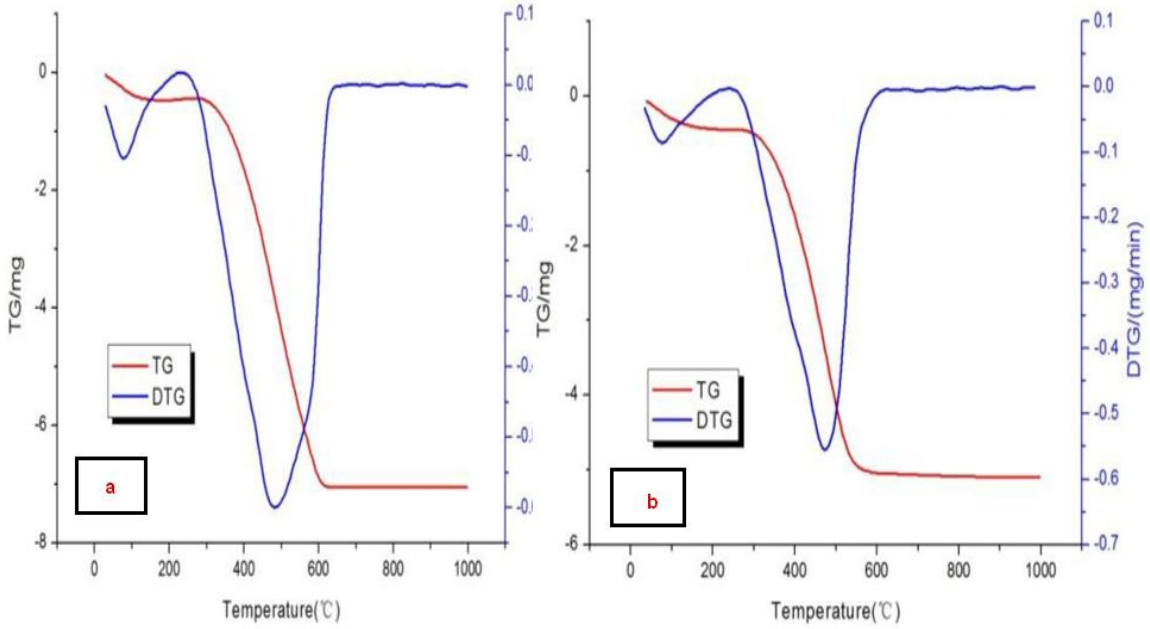

Fig. 6.11 TG and DTG curves of sample 11 (b) TG and DTG curves of sample 12

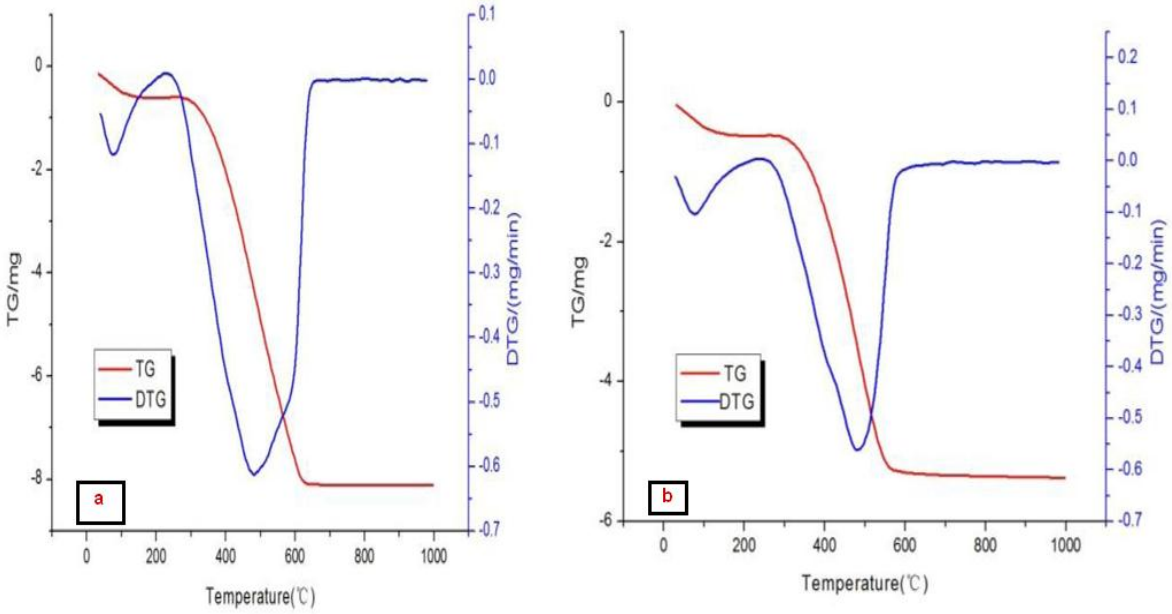

Fig. 6.12 TG and DTG curves of sample 13 (b) TG and DTG curves of sample 14

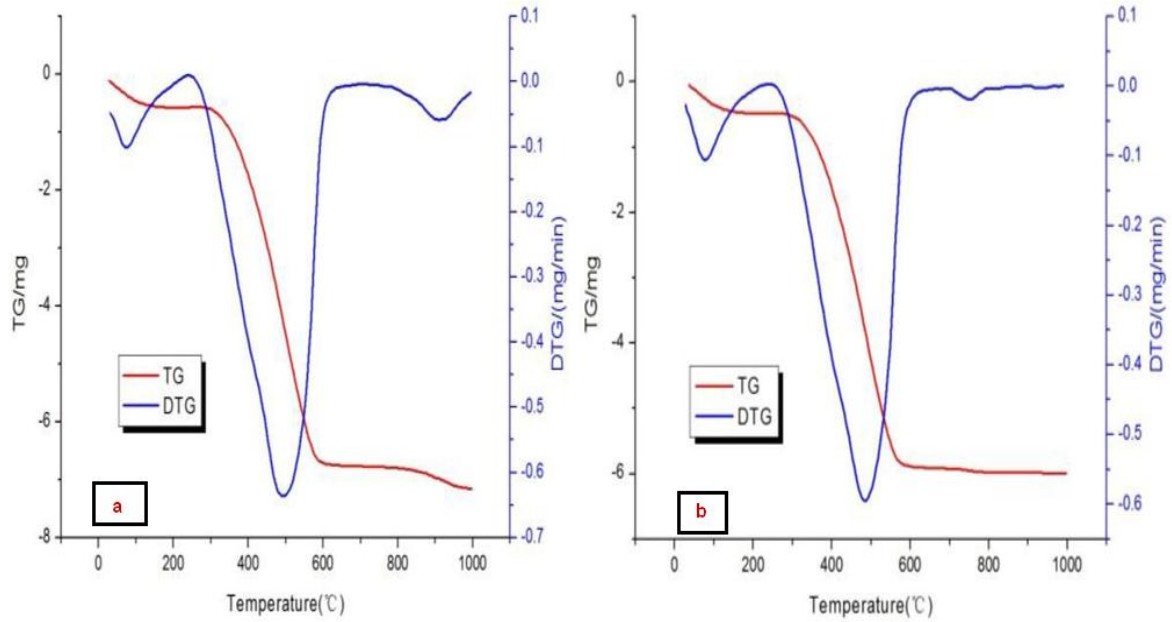

Fig. 6.13 TG and DTG curves of sample 15 (b) TG and DTG curves of sample 16

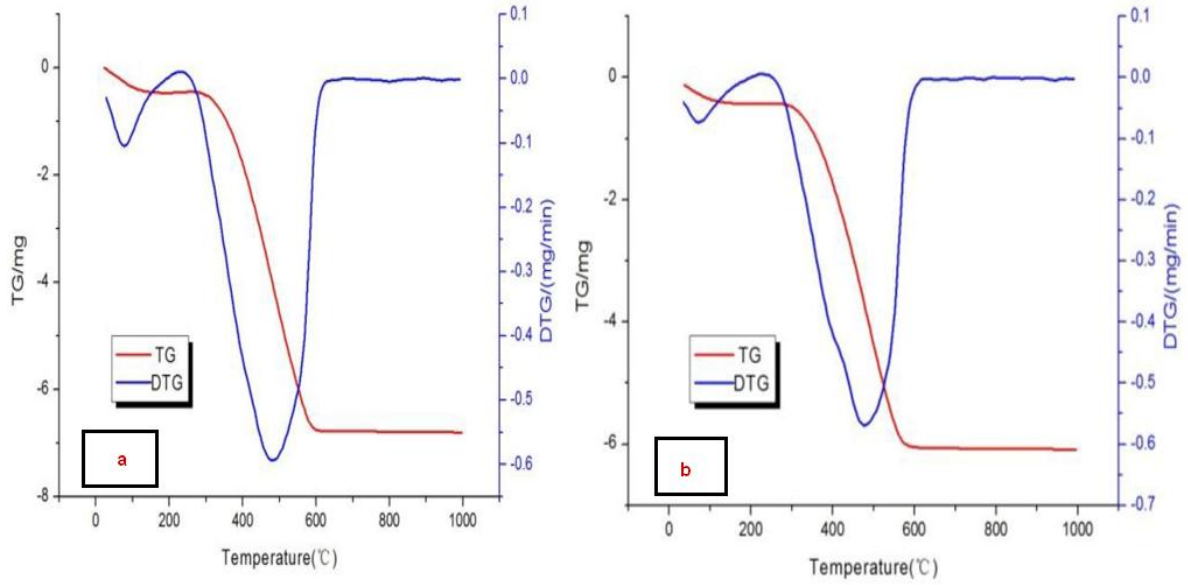

Fig. 6.14 TG and DTG curves of sample 17 (b) TG and DTG curves of sample 18

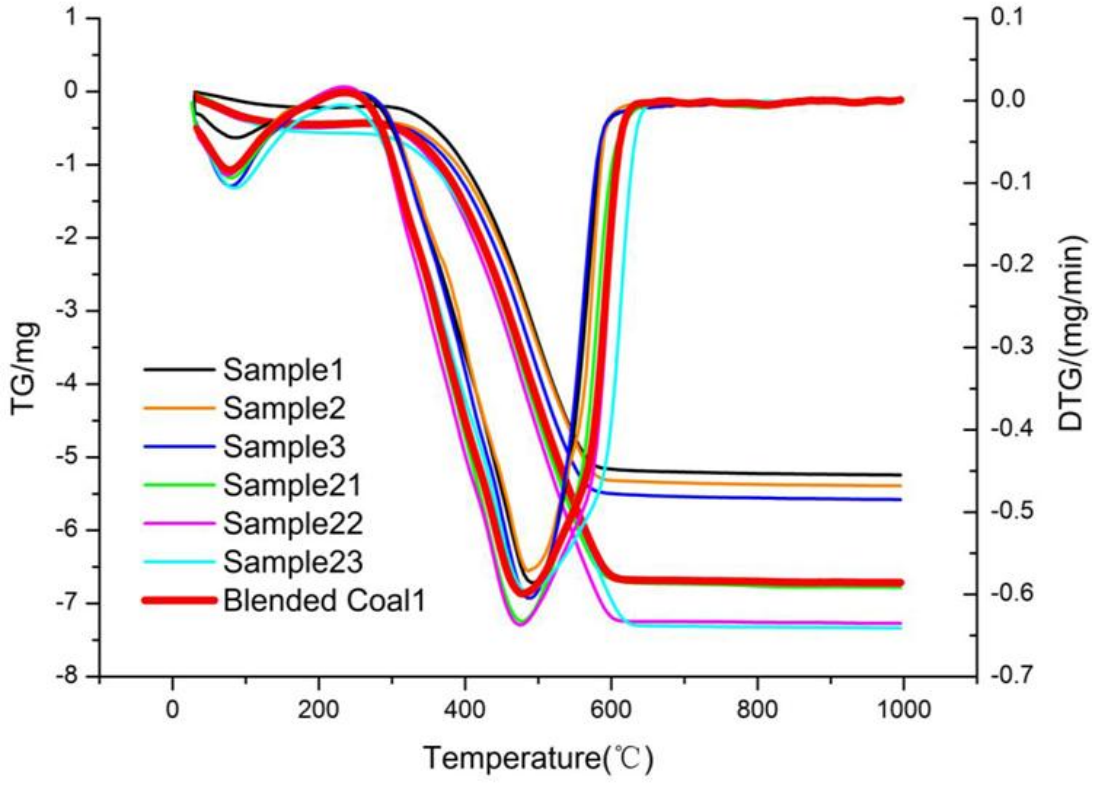

Fig. 6.15 TG and DTG curves of blended coal 1 compared with other coals

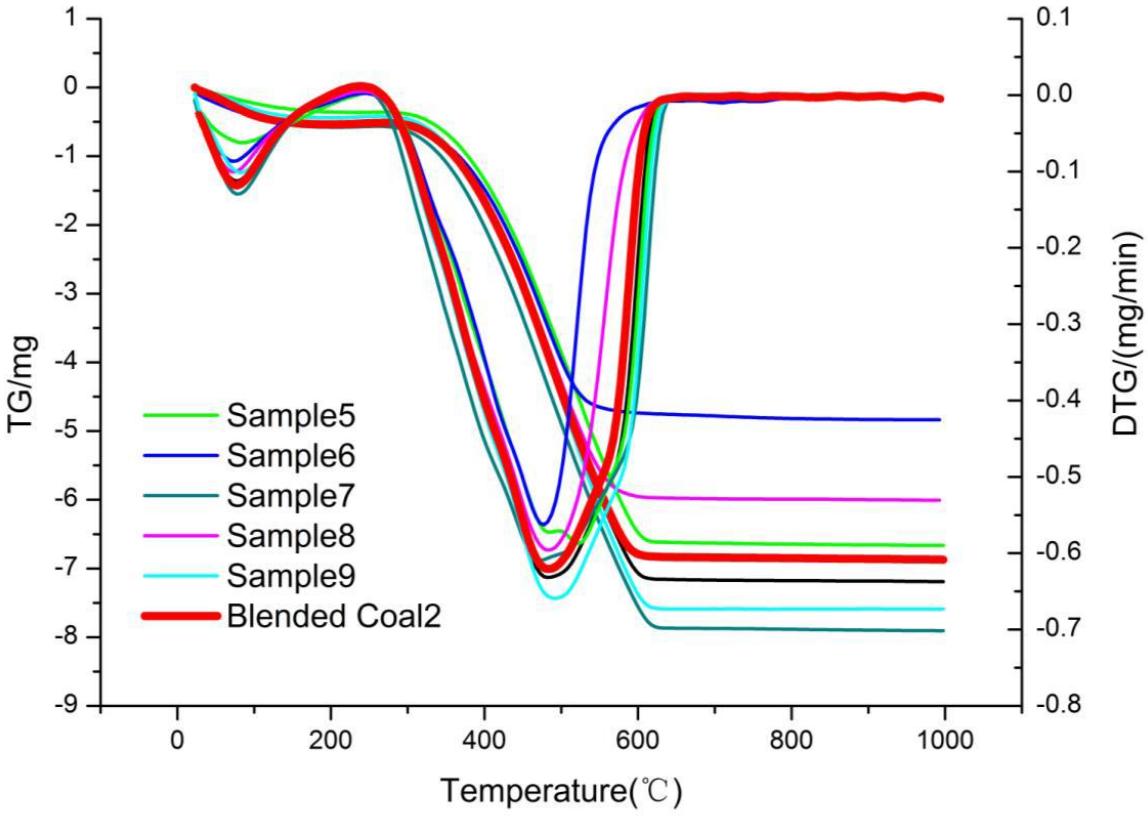

Fig. 6.16 TG and DTG curves of blended coal 2 compared with other coals

6.2.3 Discussion and Recommendation of Lab Scale Testing (Part–I and Part–II)

Some coal characteristics have great effect on the combustion and emissions of the coal. Comparison of these characteristics for the investigated coal of Salt Range and Trans Indus Range with other local coals (i.e. from Baluchistan and Sindh) and imported coal (i.e. high calorie thermal coal, PINANG 6150) from Indonesia [7]; (Table 6.10). In Pakistan, major coal resources and their mining activities are in Sindh, Baluchistan and Punjab. Quality of local coal is of low grade, i.e. lignite in Thar and Lakhra, and subbituminous in Punjab and Baluchistan. Good quality coal is being imported from Indonesia, South Africa, Australia and Afghanistan. Indonesian coal contributes to major share of the imported coal; hence it has been taken as representative of the imported coals and compared with local coal in this study (table 6.10).

Table 6.10 Comparison of coal characteristics of Salt Range and Trans– Indus Range coals with local and imported coals.

Coal Characteristics	Sample Coal			Imported Coal			Local Coal							
	Punjab			Indonesia			Baluchistan				Sindh			
	Salt Range and Trans Indus Range			PINANG 6150			Duki		Degari		Lakhra		Thar	
	Min.	Max.	Mean	Min	Max.	Mean	Min.	Max.	Min.	Max.	Min.	Max.	Min.	Max.
Total Moisture (%) (arb)	3.2	10.4	7.8 ±1.8	--	10.0	9.0	3.5	11.5	3.9	18.9	9.7	38.1	29.6	55.5
Volatile Matter (%) (adb)	24.2	40.5	32.6 ±5.3	38	45	42.5	32	50	20.7	37.5	18.3	38.6	23.1	36.5
Ash (%) (adb)	14.2	50.3	33.4 ±9.1	--	14	14.0	5.0	38	4.9	17.2	4.3	49	3.9	11.5
Fixed Carbon (%) (adb)	22.2	42.2	31.0 ±4.7	--	---	40.2	28	42	41	50.8	9.8	38.2	14.2	34
Sulfur (%) (arb)	3.3	11.1	7.1 ±1.6	--	1.0	0.7	4.0	6.0	0.6	5.5	1.2	14.8	0.4	2.9
GCV (MJ/kg) (daf)	16.0	36.6	26.3 ±4.9	34.4	35.5	35.2	23.6	32.9	26.2	32.3	12.9	21.3	14.5	25.7

adb: air dry basis arb: as received basis daf: dry ash free

Table 6.11 Uncertainty of the test results from CUST and SGS Labs [13]

Properties measured			NCV (kJ/kg) (adb)	GCV (kJ/kg) (adb)	VM (%) (adb)	Moisture (%) (arb)	Ash (%) (adb)	Sulfur (%) (adb)	IDT (°C)	ST (°C)	HT (°C)	FT (°C)
CUST	Uncertainty Measurement (±)	Percentage (%)	0.2	--	0.8	0.2–0.3	0.2–0.3	0.05–0.1	--	--	--	--
		Values	--	120	--	--	--	--	60	40	40	40
SGS	Uncertainty Measurement (±)	Percentage (%)	--	--	--	0.20	0.19	0.18	--	--	--	--
		Values	--	88 -159	--	--	--	--	--	--	--	--

Thar coals are 38.1% and 55.5%, respectively. Simply speaking, they include 4 to 5 times more the moisture than the investigated coal. Therefore, the moisture in the investigated coal is almost equal to high calorie thermal imported (Indonesian) coal and less than good quality coal from Baluchistan and far less than Lakra and Thar coals. Higher moisture in the coal causes spontaneous combustion during transportation and storage of the coal [115]. Moisture also plays an important role in combustion of the coal. Higher moisture in coal decreases the furnace temperature and eventually reduces the boiler efficiency. Higher moisture coals also have significant difference between GCV and NCV. Thus, low moisture coal is considered obviously most suitable for combustion [116, 117].

Volatile matter (VM) in the coal ranges from 24.2% to 40.5% with mean value of 32.6% on air dry basis (adb), which is in line with the values of VM of Degari (20.7–37.5%), Lakhra (18.3–38.6%) and Thar (23.1–36.5%). However, values of VM for Duki and Indonesian coals are 32–50% and 38–45%, respectively. They both have good thermal qualities. Average value of VM for the investigated coal is 33.6% on dry basis (db) and 49.69% on dry ash free (daf) basis. It belongs to the category of high volatile sub–bituminous coal. Normally, high VM coal gets easily spontaneous combustion. Extra care is required during the transportation and storage of such coal. It may also cause slagging, which disturbs the air flow inside the furnace.

Ash content in the investigated coals ranges from 14.2% to 50.3% with mean value of 33.4% on air dry basis (adb), which is close to the ash content of Duki (5–38%) and Lakhra (4.3–49%). On the other hand, ash content in Degari (4.9–17.2%) and Thar (3.9–11.5%) coals is quite smaller and comparable to Indonesian coal (14% max.). Average value of ash in the investigated coals on dry basis (db) is 34.6%, which is higher than in good quality coals. Higher ash content in the coal reduces the efficiency of the boiler. Ash also causes serious erosion of the boiler parts and it is a big challenge to keep the boiler in long–term continuous operation with high ash coals. However, the heat from bottom ash could be utilized, by means of different waste heat recovery technologies, to improve heat rate of the power plant.

Fixed carbon in the investigated coals ranges from 22.2% to 42.2%. Its mean value of 31%is less than Duki (28–42%), Degari (41–50.8%) and Indonesian (40.2%) coals, and is greater than Lakhra (9.8–38.2%) and Thar (14.2–34%) coals. If the carbon content in the coal is low, its GCV will be lower and ash will be higher and vice versa in the case of high carbon value. For complete combustion, carbon needs sufficient

time and temperature having good mixture with air. If carbon residence time is not sufficient, it could not be combusted completely. Coal particle size should be according to design and of the required distribution ratio. If the coal particle size is too small, it may blow off with fluidizing velocity and causes an increase of the carbon in fly ashes. If size of coal particles is too large it might not be combusted perfectly even after circulation of multiple times in FBC boiler and it may increase carbon in bottom ashes. Such cases will increase non–complete combustion loss [14].

Sulfur in the investigated coals ranges from 3.3% to 11.1% with mean value of 7.1% (adb). It is greater than the sulphur content in the coals from Duki (4–6%), Degari (0.6–5.5%), Indonesia (1% max.) and Thar (0.4–2.9%). Conversely, it is smaller than the sulfur in Lakhra coal (1.2–14.8%). Sulfur is a combustible substance and can be completely converted to SO_2. Due to higher SO_2 concentration, the moisture content in the flue gas will condense and combine with SO_2 to form sulfuric acid. To avoid the acid formation in the flue gas duct, it becomes necessary to increase the exit temperature of flue gas, which causes an increase in flue gas loss. If SO_2 is emitted to the atmosphere, it will combine with the moisture in the clouds and causes acid rain, which may destroy the structures of the crop lands. For elimination of SO_2 in flue gases, limestone is mixed with the coal. Thus, the Ca/S ratio could be 1–5 in FBC boiler [41]. Its efficiency depends of course on limestone quality, particle size, the quality of solid mixing, combustion temperature, degree of fly ash recirculation in case of CFBC and schematic of coal and limestone feeding points [44]. To get the same desulfurization efficiency, the Ca/S ratio should be higher than 4 for grate boiler and higher than 6 for pulverized fuel boiler [69].

Addition of more limestone for higher sulfur coals may form calcium sulfide (CaS) that is one kind of catalyst, which facilitates nitrogen to be converted to NO_x. Hence, FBC boiler burning high sulfur coals, with in–furnace desulfurization may cause an increase in NO_x emission. Therefore, it is necessary to optimize the combustion with desulfurization to avoid increase in NO_x over the emission limits [118]. Normally, nitrogen is found in the organic form inside the coal and it is converted to NO_x during coal combustion. NO_x is harmful mixture of NO and NO_2 gases. This is the most common case in FBC boiler. Other source of nitrogen is the air, which is required for coal combustion. The conversion of nitrogen via the thermal NO_x formation mechanism is relatively less significant especially in case of FBC boiler. Therefore, for high nitrogen coal fuel, FBC is the best choice [23].

GCV of the investigated coals ranges from 16.0 to 36.6 MJ/kg with mean value of 26.3 MJ/kg (daf). This value is less than the heating values for the coals from Indonesia (35.2 MJ/kg), comparable up to some extent for the coals from Duki (23.6–32.9 MJ/kg) and Degari (26.2–32.12 MJ/kg) and greater than for the Lakhra (12.9–21.3 MJ/kg) and Thar (14.5–25.7 MJ/kg) coals.

Mean values of key combustion characteristics including initial volatile separating temperature (T_s), the complete burning time (t_{rj}), the complete burning temperature (T_h), the average burning rate (w_{mean}), the maximum combustion rate (w_{max}), the temperature of maximum combustion rate (T_{max}), the temperature difference of DTG's half peak width (ΔT_h) and the temperature difference of DTG's total peak width (ΔT) are depicted for thirty coal samples (Table 6.7).

Coal characteristics index (F_z), flammability index (C) and stable firing index (M) are also very important during the process of the coals combustion. Ignition temp. of all the coals are less than 400 ºC (355–392 ºC) indicating that the coal is easy for ignition. Value of F_Z is 1.5–2.0 for the coals 1, 2 and 6, and greater than 2.0 for the remaining coals. It shows that all these coals have very good ignition characteristics. Similarly, value of C of all the coals is greater than 2.3 (2.6–3.1), which indicates that these coals have better flammability characteristics. The value of M is greater than 3.3 (3.5–4.1), leading to the fact that these coals have excellent characteristics of stable firing [119].

The coals of Salt Range and Trans Indus Range have: low slagging index, medium to high fouling index, good combustion characteristics parameters and better combustion characteristics indices. Summarizing all the aforementioned quality parameters, it must by concluded that the coals of Salt Range and Trans Indus Range are suitable for combustion in coal–fired power plants for power generation and FBC technology, which could be the best choice for combustion of these coals.

Three different scenarios have been discussed for different mines/areas based on quality of coal, combustion prospects and sites for blending facilities of the coals.

Scenario I. Use of representative (average) coals from Salt Range and Trans Indus Range for combustion. These coals have: low moisture, high ash, ultra–high sulfur,

Table 6.12 Recommended blends to get average coals of Salt Range and Trans Indus Range [13]

Blends	Coals						GCV (MJ/kg) (adb)	Ash (%) (adb)	Sulfur (%) (adb)	TM (%) (arb)	VM (%) (adb)	F.C (%) (adb)
1	2	6	15	19	22	26	19.2	32	7	8.8	33	31.9
2	7	11	12	13	14	27	18.8	33.4	7.3	8	32.1	31.7
3	4	8	9	16	18	20	18 .9	33.4	7	7.5	31.8	31.7
4	1	3	17	23	29	30	18.6	34.5	7.3	7.8	32.4	30.2
5	5	10	21	24	25	28	18.7	34	7.1	6.6	33.7	29.5
Average coals of Salt Range/Trans Indus Range							18.8 ± 0.23	33.5 ± 0.94	7.1 ± 0.15	7.7 ± 0.8	32.6 ± 0.76	31 ± 1.08

high VM and low GCV. Thus, the blends are recommended to get the average coal (Table 6.12). To burn such kind of coal, FBC technology seems to be one of the best choice.

Values of moisture, VM and GCV in the studied coal seams are suitable for combustion, but sulfur and ash are the most challenging problems. Average value of sulfur is 7.1%. Therefore, to resolve this great problem the following two methods are applied for desulfurization of coal to reduce SO_2 gas emissions:

a) In Furnace Desulfurization

Normally limestone is fed into the furnace with coal for desulfurization during combustion. Salt Range territory has huge resource of good quality limestone, which is being used by many cement factories operating in this area. It is available on the cheaper rates and can be used with coal for desulfurization purpose. Ca/S ratio can be set from 1 to 5 depending on quality and particle size of limestone to achieve maximum desulfurization efficiency [43]. However, desulfurization during combustion process cannot achieve the higher environmental protection requirements for such high sulfur coal. Therefore, post–combustion desulfurization is also required.

b) Post–Combustion Desulfurization

This method is also known as flue gas desulfurization (FGD). There are two types of FGD Process, i.e. wet flue gas desulfurization (WFGD) and dry flue gas desulfurization (DFGD) [116]. Both technologies have their own advantages and disadvantages. Any technology can be adopted according to requirement and priority of the end user. Using the listed above desulfurization technologies, SO_2 limits in gas emissions can be achieved up to 200 mg/Nm^3, which meets European Standard of gaseous emission from coal fired power plants. Average ash content in the investigated coals is 33.4%. It is higher than ash content of any good quality coal. So, combustion of the coal having high ash needs huge amount of water to cool down the bottom ashes. However, heat from these ashes can be utilized through different waste heat recovery technologies to increase the efficiency of the steam generation and its consumption processes. Ash is a huge by–product of coal–fired power plant burning high ash coals and it must be properly utilized to improve the economics of the plant.

Some common uses of ash from coal combustion are given below:

i) The resultant ash could be utilized for manufacturing of ash bricks of different sizes, density and shapes according to market requirement. These ash bricks might be cheaper than the normal clay bricks in Pakistan. Complete feasibility

study could be done for installation of ash bricks manufacturing plant on the basis of ash from a coal–fired power plant.

ii) The by–product ash could be sold to cement plants that are operating in the vicinity of Salt Range. The cement plants should be located very close to the coal–fired power plants. Therefore, transportation of by–product ash to cement plants will be obviously convenient and cheaper.

iii) The ash could also be subjected for the use in the construction and maintenance of roads as a binding and foundation material. This direction of utilization should especially be useful in areas where soil quality is poor, for example, in the Salt Range area because of land sliding and presence of salt in the soil.

iv) The ash may also be used in the construction of dams to increase their life and avoid the possible sliding. It is caused by the fact, that the ash has strong binding characteristics,

v) Finally, the ash from the coal–fired power plants could be also used for leveling of the land surface.

Average coal being representative coal of Salt Range and Trans Indus Range could be used as design coal for coal–fired power plant. All the performance guarantees regarding heat rates and thermal efficiencies of the plant should be based on this coal.

Scenario II. Use of different blends of local coals and imported coals for combustion. The different blends of Salt Range and Trans Indus Range coals are calculated on the basis of GCV, sulfur and ash (Table 6.13). Blends 1, 2 and 3 have better quality than average coals from Salt Range and Trans Indus Range and could be used directly for combustion using FBC technology. Quality of the coal blends 4 and 5 is poorer than that the average coals and they could be mixed with good quality imported coal, i.e. Indonesian coals, to improve their quality. Five different mixing schemes of imported coal (from 10% to 50%) with low quality local coals (blends 4 and 5) to improve their quality and make them suitable for combustion in coal–fired power generation systems are given in table 6.12. For blend 4 any mixing scheme from (10–50%) could be used depending on the required quality of the coal. Mixing of 10% imported coal make its quality equal to average coal of Salt Range, while 50% mixing makes it equal to or even better than the best coal of Salt Range [13].

Table 6.13 Recommended blends of local coals on the basis of GCV, sulfur and ash [13]

Blends	Coals						GCV (MJ/kg) (adb)	Sulfur (%) (adb)	Ash (%) (adb)
1	11	13	19	21	22	26	22.68	5.55	23.90
2	9	17	18	20	23	29	20.95	6.43	27.97
3	4	10	15	16	24	30	18.98	7.03	33.93
4	3	5	12	25	27	28	16.72	7.77	38.63
5	1	2	6	7	8	14	14.90	8.8	42.75

Table 6.14 Recommended blends of low quality coals of Salt Range and imported coals [13]

Blends of local coal	Quality parameters (adb)	Imported (100%)	Local (100%)	Different blends of imported and local coal (%Imported + %local)				
				(10 + 90)	(20 + 80)	(30 + 70)	(40 + 60)	(50 + 50)
Blend 4	GCV (MJ/kg)	27.5	16.72	17.80	18.88	19.95	21.03	22.11
	Ash (%)	14	38.63	36.14	33.68	31.22	28.76	26.30
	Sulfur (%)	0.7	7.77	7.09	6.38	5.67	4.96	4.25
Blend 5	GCV (MJ/kg)	27.5	14.90	16.16	17.42	18.68	19.94	21.20
	Ash (%)	14	42.75	39.92	37.04	34.16	31.28	28.40
	Sulfur (%)	0.7	8.80	7.99	7.18	6.37	5.56	4.75

For blend 5, mixing of 30% imported coal is required to get the coal quality comparable of the average coal of Salt Range (Table 6.14). Further increase in percentage of imported coal may be made according the required quality with consideration of economic feasibility.

Scenario III. (Use of different blends of local coals for combustion on the basis of geographical location).

Taking into consideration the discussion in Scenario I and Scenario II, it would be worth to get the blends of coal on geographical basis. It is more convenient, economical and feasible to use coal blends. The five blends of local coals and their characteristics are presented in this contribution on geographical basis in table 6.15 blends 1 and 2 have low GCV, higher ash and sulfur, which shows that the coals from Eastern Salt Range (i.e. Chakwal) and Central Salt Range (PEL/Padhrar) have high sulfur as compared to the average coal. GCV of blends 3 and 4 of Central Salt Range (Chamble Zone) and blend 5 from Trans Indus Range is higher, while their sulphur and ash are lower than the average coal. Thus, the coal quality of this area is better than the average coal and can be used directly for combustion in coal–fired power plant. Conversely, coal quality of blends 1 and 2 is lower than the average coal of Salt Range, and it could be mixed with imported coal to improve its quality for better combustion results (Table 6.15).

Table 6.15 Recommended blends of coals on geographical basis [13]

Blend	Mines Areas	Coals								GCV (MJ/kg) (adb)	Sulfur (%) (adb)	Ash (%) (adb)
1	Eastern Salt Range (Chakwal)	1	2	3	21	22	–	–	–	16.6	6.9	39.8
2	Central Salt Range (PEL/ Padhrar)	4	5	6	7	8	–	–	–	17.0	9.0	37.4
3	Central Salt Range (Chamble Zone 1)	9	10	11	12	13	14	–	–	19.4	6.6	32.6
4	Central Salt Range (Chamble Zone 2)	15	16	17	18	19	20	–	–	20.0	6.3	30.8
5	Trans Indus Range (Mianwali)	23	24	25	26	27	28	29	30	20.2	7.1	29.6

Average coal of Salt Range and Trans–Indus Range has been selected for pilot scale testing as given in the process flow diagram (Fig. 6.1).

6.2.4 Results and Discussion of Pilot Scale Testing

6.2.4.1 Effect of Limestone Quantity on SO_2

Figure 6.17 shows the influence of different quantities of limestone (added in the bed) in terms of Ca/S molar ratios (MRs) on SO_2 emissions during combustion of the coal A from Trans Indus Range and coal B from Salt Range.

Different values of MR were used depending on limestone particle size and operational parameters. It is clear from Fig. 6.17 that with increase in MR, SO_2 emissions decrease significantly for both coal A and coal B, reaching up to 40% and 41% at MR = 2 and 49% & 52% at MR = 3, respectively. However, maximum decrease of 72% for coal A and 78% for coal B (i.e. maximum desulfurization) was observed at MR = 3.5, With further increase in MR to 4, sulfur capture level decreased to 69% for coal A and 70% for coal B. It shows that increase in limestone quantity beyond MR = 3.5, is not feasible for SO_2 retention, and thus 3.5 is the optimum value of MR to get the maximum reduction in SO_2 in case of both coals.

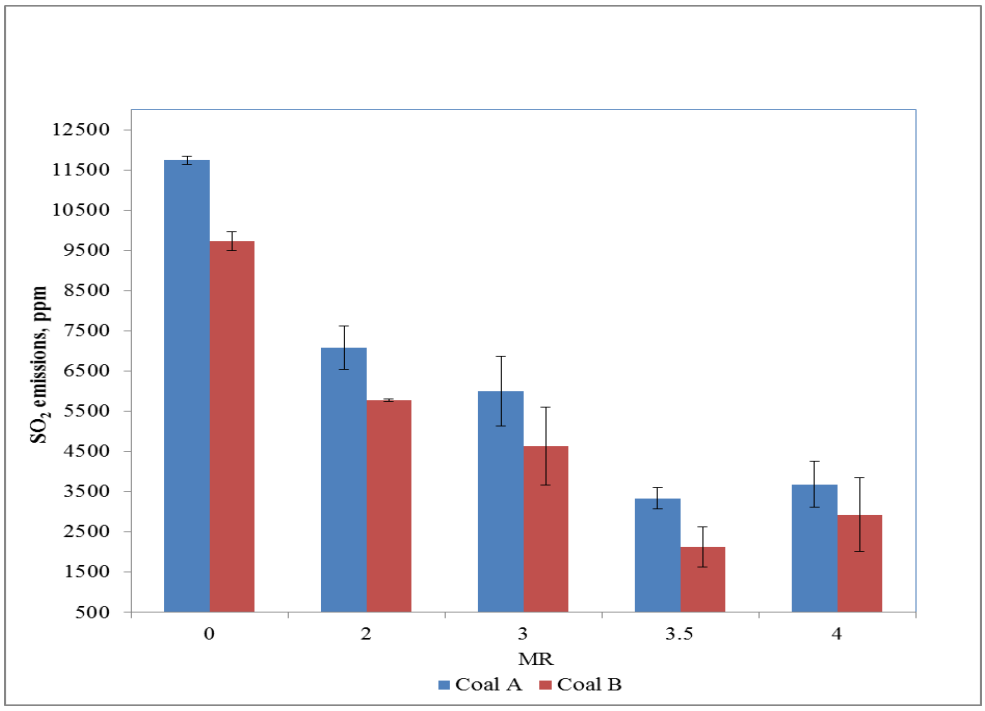

Fig. 6.17 Comparison of different MRs and sulfur dioxide (SO_2) emissions for coal A and coal B

It can also be observed from Fig. 6.17 that at MR = 2, a significant reduction in SO_2 emission occurred (40% for coal A and 41% for coal B). With further addition of 50% in limestone quantity (at MR = 3), only 9% and 11% were added to initial SO_2

reduction for coal A and coal B respectively. Although overall SO_2 emissions are decreased with the increase in MR values but desulfurization efficiency decreased at higher MR values. Therefore, it is evident from the results that desulfurization efficiency strongly depends on the initial concentration of SO_2 in the bed.

Above results are in accordance with the investigation of Braganca and Castellan [40] which reveals that SO_2 retention efficiencies are 48%, 60%, 68% and 77% at MR values of 1, 2, 3 and 4 respectively during coal combustion in FBC. Their results also show that the amount of limestone utilization lies in the MR range from 1 to 4 to meet the environmental norms and further rise in MR value will not be economically feasible. According to the study of Tarelho et al. [41], the range of MR is from 1 to 5 for various developed/ developing countries to meet the SO_2 emission norms and high SO_2 removal efficiencies can be attained at MR = 3.5.

Limestone reacts with SO_2 in presence of O_2 to form calcium sulfate ($CaSO_4$).

A number of reactions are possible including the following:

$$CaCO_3 + SO_2 + \frac{1}{2}O_2 \rightarrow CaSO_4 + CO_2 \quad \Delta H = -303 \frac{kJ}{mole} \tag{6.1}$$

$$CaO + SO_2 + \frac{1}{2}O_2 \rightarrow CaSO_4 \quad \Delta H = -481 \frac{kJ}{mole} \tag{6.2}$$

Stoichiometric calculations show that one mole of limestone feed can reduce one mole of sulphur [42]. Molar volume of $CaSO_4$ is greater than that of either CaO or $CaCO_3$ which leads to the plugging of pores and therefore, complete conversion of the adsorbent particle is impossible. Also sulfation only proceeds at the outer surface of the CaO particle. The sulfation process continues until external pores are blocked significantly and an impenetrable $CaSO_4$ shell is formed leaving a considerable amount of unreacted CaO core. The increase in SO_2 emissions for both coals beyond MR of 3.5 value may be due to the equilibrium of sulfation and reduction of $CaSO_4$ [43]. According to Cheng et al. [44], operational parameters including MRs, furnace temperature, residence time and SO_2 partial pressure affect the sulfation reaction.

Furthermore, the lower SO_2 emissions at all MR values in case of coal B relative to its counterpart coal A is attributed to its lower inherited sulfur [46] as shown in table 5.3.

6.2.4.2 Effect of Limestone on NO_x

Figure 6.18 displays the effect of different MRs on NO_x emissions for coal A and coal B. It is clear from the graph that there is an increase in NO_x emission with increase in MR from 2 to 3.5 for coal A and Coal B and maximum increase occurs at MR = 3.5. Further increase in the MR beyond the value of 3.5 results in decrease of NO_x emission. The results are in line with the study of Liu and Gibbs [47] explaining that the NO_x emission increases with addition of limestone during coal combustion.

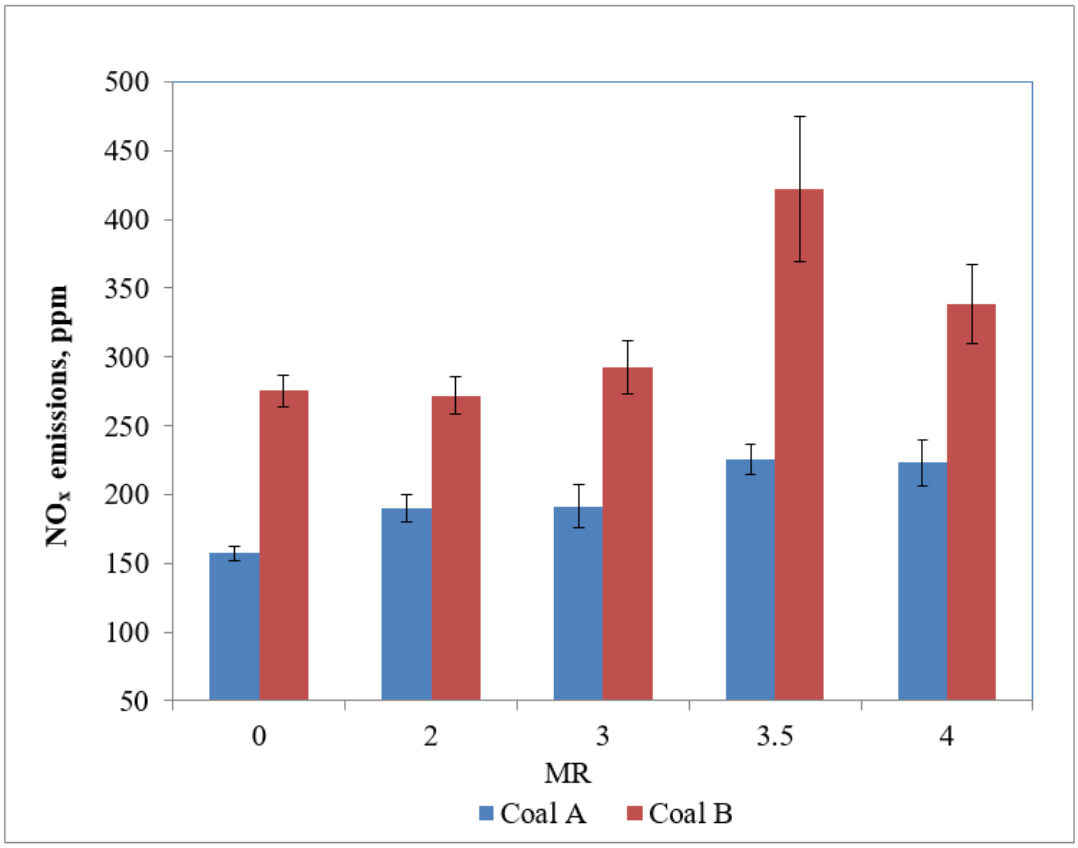

Fig. 6.18 Comparison of nitrogen oxides (NO_x) emissions at different MR_s

Some previous studies also show that taking the coal combustion without limestone as a reference, the addition of limestone results in increase of NO_x emission. Increase in MR to control SO_2 emissions has prominent impact on NO_x emissions. There are three major mechanisms which explain the reason of this increase in NO_x emission during limestone addition: the catalytic oxidation of NH_3 to NO by CaO surfaces, the catalytic oxidation of CO to CO_2 over CaO, and the catalytic oxidation of HCN to NO over CaO [120]. The reaction scheme summarizing the selectivity of CaO towards NH_3, HCN and CO is given below.

$$NH_3 + O_2 \xrightarrow{CaO} NO + N_2 \quad (6.3)$$

$$HCN + O_2 \xrightarrow{CaO} NO + N_2 \quad (6.4)$$

$$NO + CO \xrightarrow{CaO} \frac{1}{2}N_2 + CO_2 \quad (6.5)$$

Addition of limestone may result the shift from the homogeneous HCN oxidation mechanism to the catalytic one, which results in a higher selectivity for NO formation and a lower one for N_2O.

Decrease in NO_x emission beyond the MR = 3.5 at which maximum desulfurization occurred, is supported by the fact that catalytic conversion of NH_3 to NO is affected by the desulfurization. Limestone (CaO based sorbent) is an active catalysts for the oxidation of NH_3 to NO but pore plugging of limestone occurs at higher MRs when the maximum conversion of CaO to $CaSO_4$ is reached, which reduces NO formation from NH_3 [121].

6.2.4.3 Effect of Limestone on CO

Figure 6.19 shows the influence of MR on CO emissions. It is clear from the Fig. 6.19 that CO emissions decrease with increase in the value of MR up to 3, for both of the coals. As the MR is further increased to 3.5, CO emissions increase but decrease again as the MR is increased to 4. The maximum decrease in CO emissions is observed at MR = 3

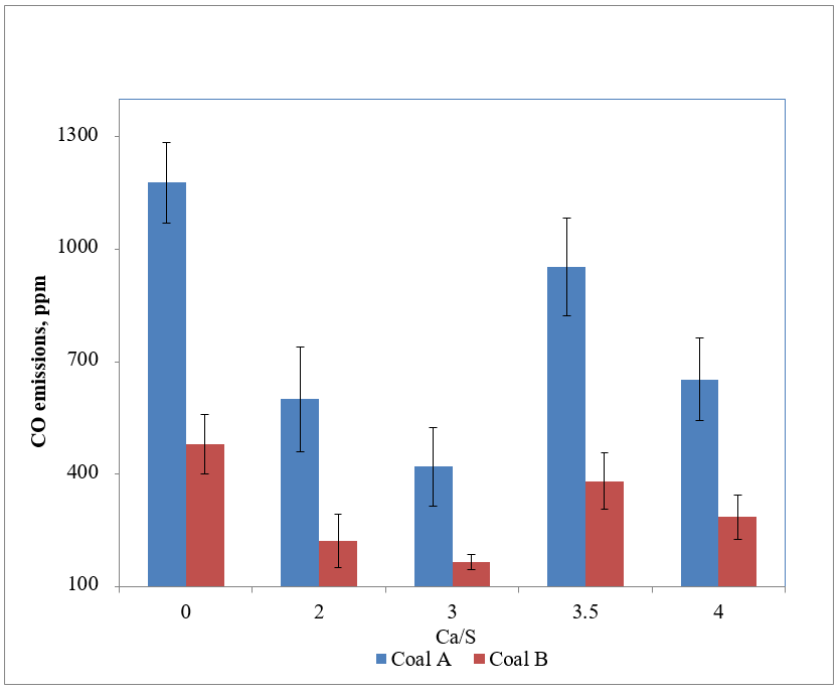

Fig. 6.19 Comparison of carbon monoxide (CO) emissions at different MR_s

Decrease in CO emissions up to MR = 3, is in accordance with the study of Liu and Gibbs [73] who investigated the effect of limestone addition on gaseous emissions in a CFB combustor and concluded that with increase of MR, concentration of CO decreases during coal combustion in CFB. Tarelho et al. [41] also found that CO and N_2O emissions decrease and NO emissions increase with addition of limestone during coal combustion in FBC. But for higher MRs, CO emissions increase and maximum concentration of CO is observed at MR = 3.5 at which maximum desulfurization occurred. There is significant decrease in CO emissions with further increase in MR beyond 3.5 for both coal A and coal B. Armesto et al. [67] reported that CO emissions are related with concentration of O_2, temperature, reaction time/phase and mixing of fuel with air. Lyngfelt et al. [46] studied the effect of lime used for desulfurization in 12 MW CFB research plant. Their results reveal that the influence of SO_2 on NO/N_2O chemistry is not dependent on the catalytic effect of the lime surface and CO acts as an important intermediary species in these reactions. They also concluded that increase in SO_2 results in decrease of NO_x accompanied by increase in CO emissions. The relation between SO_2 and NO_x has already been discussed and reasoned in the previous section 3.2 of this article. However, the increase of CO with rise in SO_2 has not been fully understood and needs further investigation. Authors are of the view that the rise in CO emission at and beyond MR = 3.5, might be due to the fact that as NO formation from NH_3 reduces at higher MRs and the rate of catalytic reduction of NO by CO also decreases thereby reducing the consumption of CO. This may result in increase of CO emissions at higher MRs, however this phenomenon needs further investigation.

6.2.4.4 Effect of Limestone on CO_2

Figure 6.20 shows the influence of limestone in terms of MR on CO_2 emissions. It is evident from the Fig. 6.20 that the CO_2 emissions increased at MRs 2, 3 and decreased for higher MRs for coal A. Similarly CO_2 increased at MRs 2, 3 & 3.5 and decreased for higher MRs for coal B. At high temperatures CO_2 can be separated by the calcium oxide (sorbent) and high–temperature CO_2 capture systems are based on carbonation reaction when coupled with a calcination step. Grasa and Abanades [122] experimentally investigated the evolution with cycling of the capture capacity of CaO. Stanmore and Gilot [42] examined some aspects of using lime from limestone to sequester CO_2 from combustion systems.

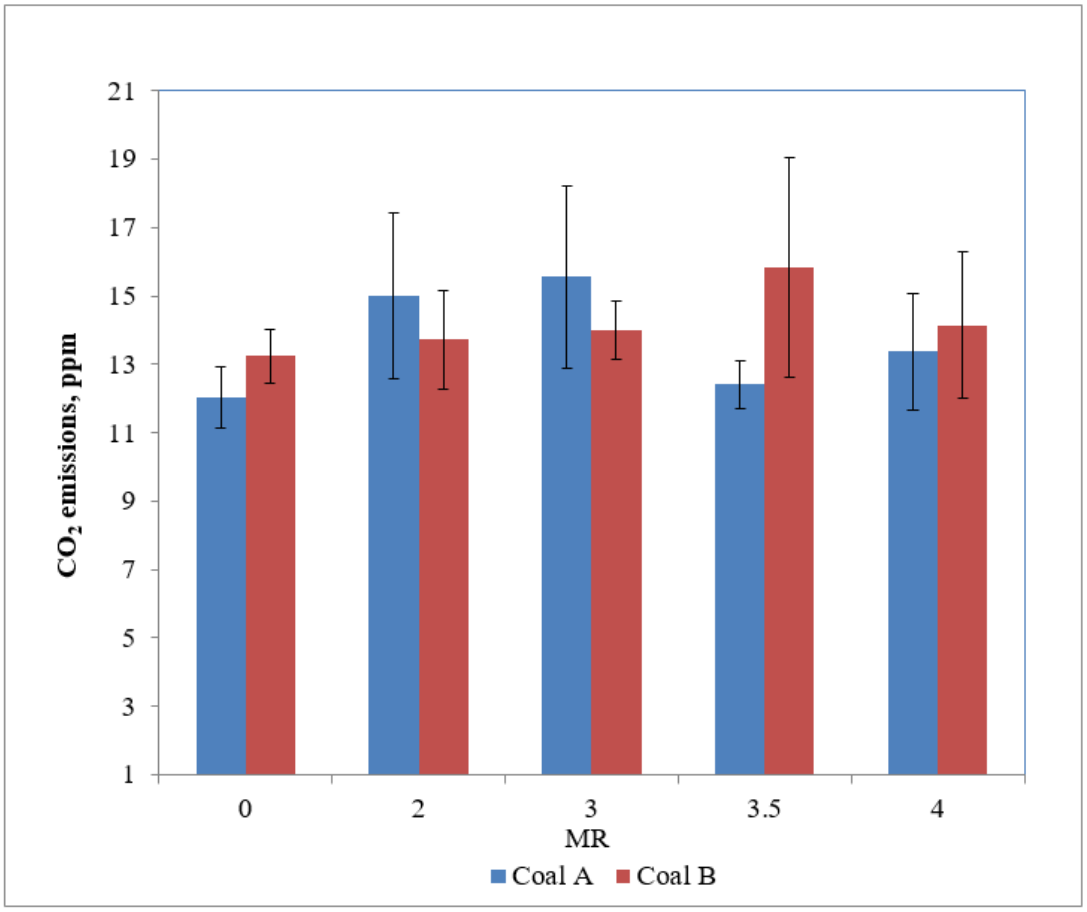

Fig. 6.20 Comparison of carbon dioxide (CO_2) emissions at different MR_s

6.2.4.5 Effect of Bed Temperature on SO_2

Figure 6.21 displays the effect of bed temperature on SO_2 emissions for coal B. This coal has been selected here owing to its better reduction of SO_2 emissions as demonstrated in previous case. In this case, MR of 3.5 is kept which has proved to be optimum value for maximum desulfurization of both coals from Salt Range and Trans Indus Range. It is clear from the Fig. 6.21 that there is slight increase in SO_2 emission against the bed temperature range from 700–750 °C in the beginning of the combustion but there is decrease in SO_2 emission for bed temperature window of 750–800°C. For bed temperature beyond 800 °C, SO_2 emissions increase significantly revealing that further increase in temperature is not prone to control of SO_2 emissions. Therefore, the value of bed temperature of 800 °C is optimum temperature for maximum desulfurization of the coal under study at MR = 3.5. This behavior is also in accordance with previous research findings that the efficiency of SO_2 removal by limestone appears to decrease with an increase in the bed temperature [41].

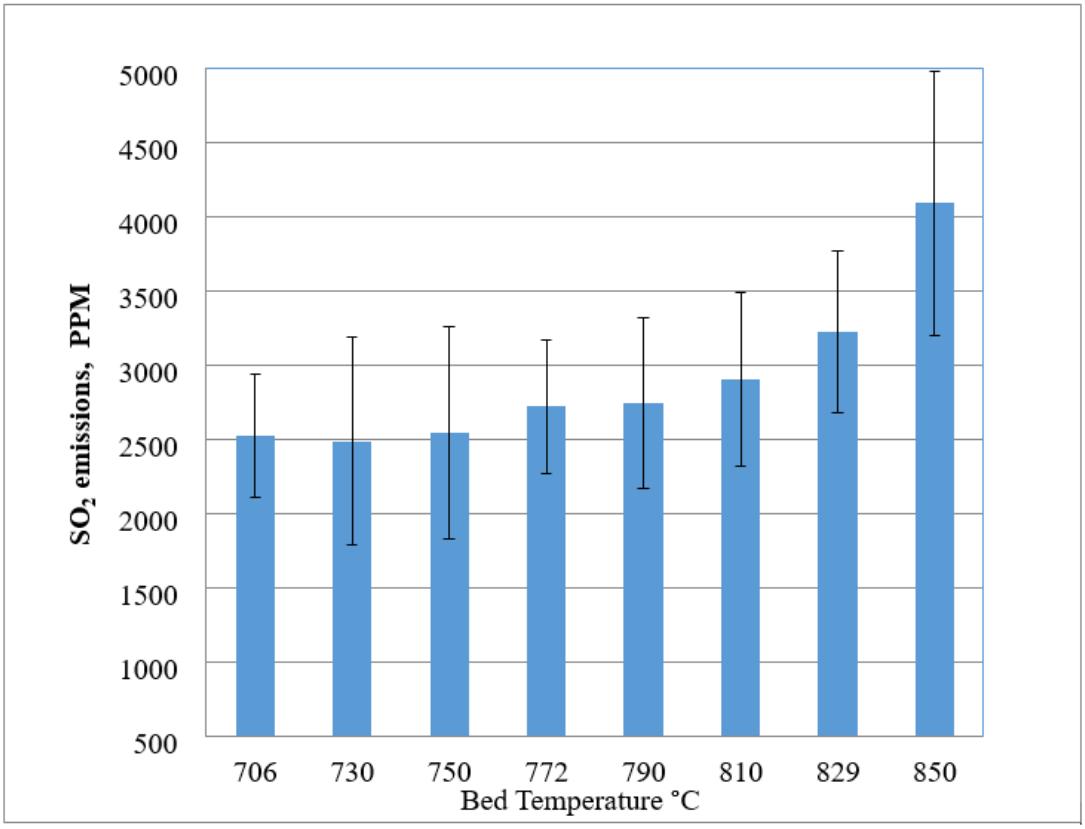

Fig. 6.21 Bed temperature Vs SO_2 emissions for coal B

According to Braganca and Castellan [40], the optimum bed temperature is 850 ºC for maximum desulfurization, while Tarelho et al. [41] conducted their tests in FBC pilot plant facility and investigated that SO_2 removal efficiency decreases with the increase in bed temperature ranging from 825–900 °C, and there by maximum rise in SO_2 removal efficiency occurred around 825 °C which has been reported as optimum temperature.

Anthony and Granatestein [43] are of the view that there is still not consensus over the explanation of maximum temperature in FBC boiler for optimum sulfur retention, and its value depends on the operational parameters, adsorbent used for desulfurization and types of coal etc.

The seize in SO_2 reduction beyond 800 °C in current study may be attributed either to one or more possible reasons including physical properties of limestone such as solid sintering and choking of porous structure, reductive decomposition of $CaSO_4$, or a net balance between limestone sulfation and $CaSO_4$ decomposition, at high bed temperatures [40].

6.2.4.6 Effect of Limestone Particle Size on SO_2

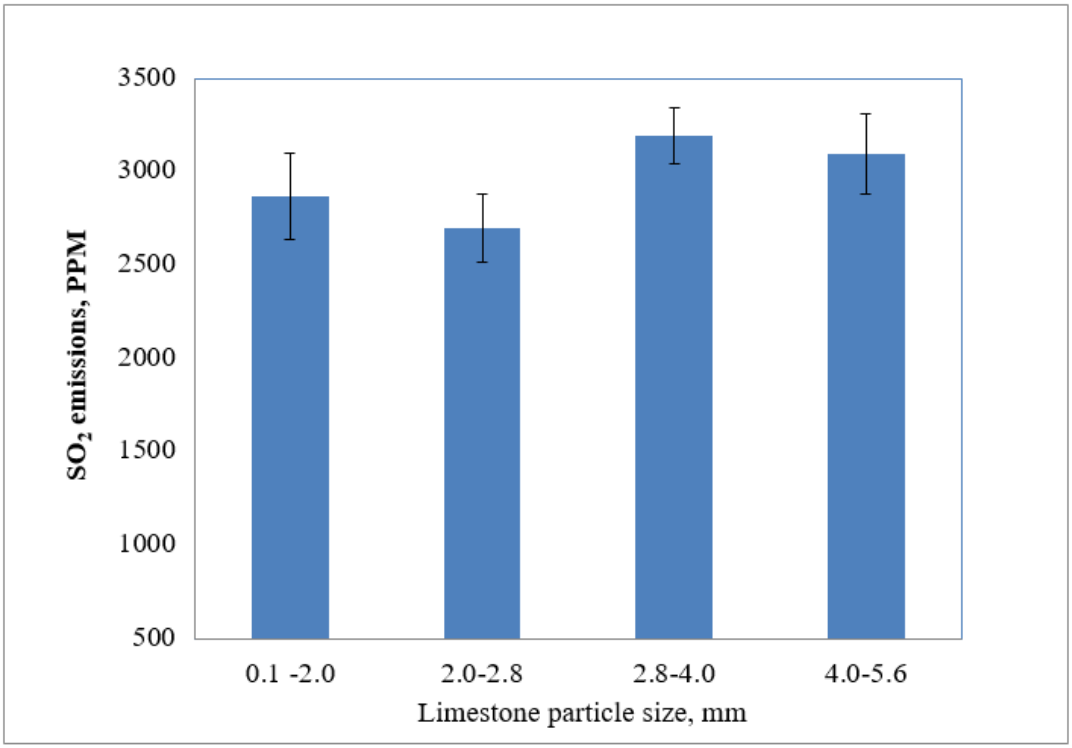

Fig. 6.22 Limestone particle size Vs SO_2 emissions for coal B

Figure 6.22 shows the influence of particle size of limestone on sulfur reduction efficiency. It is evident from the Fig. that the reduction efficiency is higher for fine particle size ranging 0.1–2.0 mm and 2.0–2.8 mm relative to coarse particle size ranging 2.8–4.0 mm and 4.0–5.6 mm, at same MR of 3.5. Fine particle–size ranges have the higher surface area for reaction than coarse particle–size ranges, as surface area is the most important factor for better performance of finer particle sizes for SO_2 retention. Maximum sulfur retention efficiency of 72% is achieved at limestone particle–size range of 2.0–2.8 mm instead of finer particle–size range of 0.1–2.0 mm. Excessive elutriation of finer limestone particle size reduces the lower retention efficiency which is potential limitation for the investigation of finer sorbents [41].

Braganca and Castell [40] investigated two different dolomite particle sizes of 0.47 mm and 0.32 mm during desulfurization of coal with high oxidizing conditions in FBC pilot scale facility at bed temperature = 850 °C. According to their results, finer particle size achieved 60% while the coarser gained only 30% SO_2 retention efficiency at same MR.

6.2.4.7 Effect of Co–Firing on SO_2

Figure 6.23 shows the influence of different quantities of biomass (added in to the bed) on SO_2 emissions during combustion of the coal A and coal B. It is clear from the graph that with increase in biomass percentage from 30% to 60%, SO_2 emissions decrease from 47.5% to 68.3%, for coal A and 36.3% to 67.8% for coal B. There is no considerable difference in SO_2 emissions at 40% and 50% biomass for coal. A but for coal B, SO_2 emissions are 58% and 53% respectively at 40% and 50% biomass. A decrease in SO_2 emissions at 50% biomass in comparison to 40% for coal B could be due to error in measurement during experimental work. Maximum decrease of 68.3% in SO_2 emissions for coal A and 67.8% for coal B achieved at 60% biomass fractions. This is in accordance with the study of Narayanan et al. [61], they got 50% reduction in SO_2 with addition of 60% biomass. During their study, it was also found that the decrease in SO_2 emissions remained up to 16% and 36% with co–firing of 20% and 40% biomass, respectively. Study of Demirbas [56] also showed reduction in SO_2 with increase in the biomass proportion.

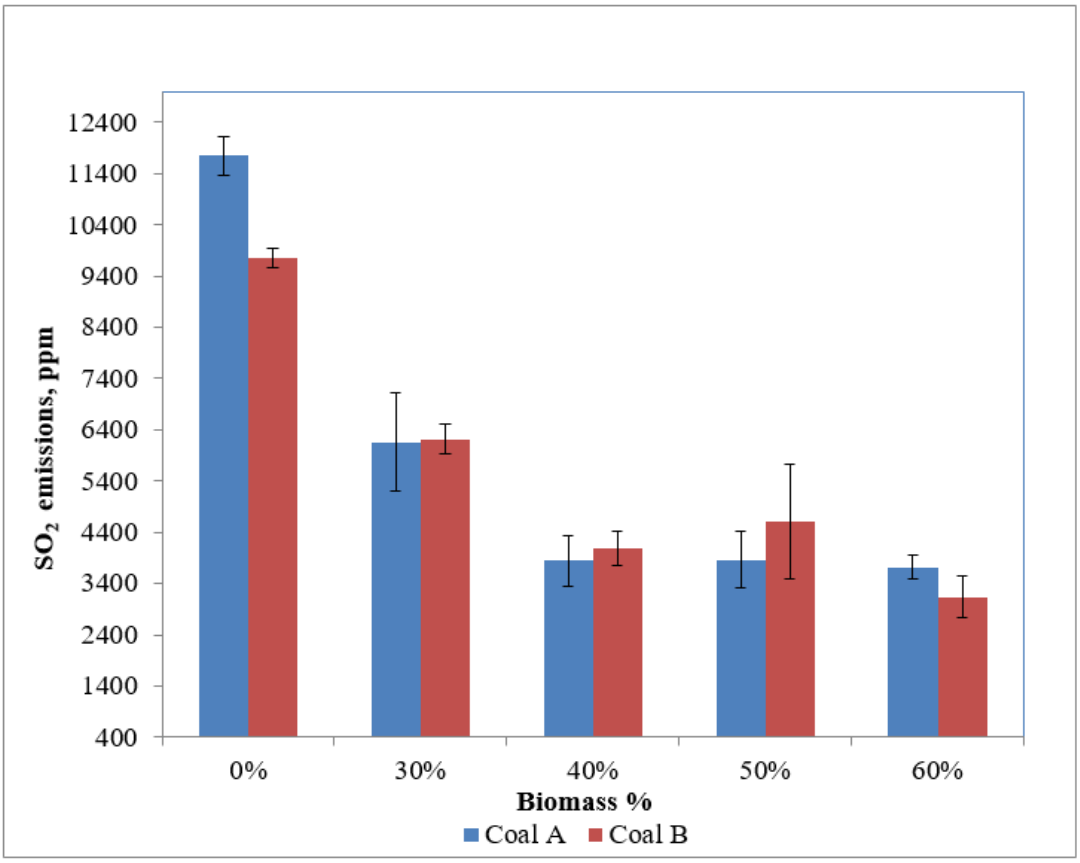

Fig. 6.23 Comparison of biomass (%) and SO_2 emissions for coal A and Coal B

Hein and Bemtgen [62] explained the results of 2–years research project launched by the European Commission in which the co–combustion, in laboratory, pilot and full–scale units was studied with the objective to investigate the effect of biomass addition on the gaseous emissions. They confirmed that co–combustion of biomass with coal has a significant effect on SO_2 reductions reaching up to 75%. The reduction in SO_2 with increase in biomass is ascribed to the dilution effect, as the biomass contains negligible amount of sulfur. CaO and K_2O present in the biomass, have ability to capture SO_2 by forming $CaSO_4$ and K_2SO_4 in the presence of O_2 just like SO_2 capture using limestone [65].

6.2.4.8 Effect of Biomass on NO_x Emissions

Figure 6.24 shows that the reduction in NO_x varies from 1 to 16% with the corresponding increase in biomass from 20 to 60%. Comparing with coal, wood used as a biomass has small amount of fuel–N. Therefore, co–firing with the biomass is deemed to decrease NO_x emissions.

In FBC systems, the temperature is usually below 900 °C. No chance of Thermal NO_x. This decrease in NO_x with biomass is ascribed to decrease in bed temperature with the increase in biomass. The fuel–N in biomass most probably is responsible to produce more ammonia (NH_3) content relative to HCN, with the consequent decrease in NO_x.

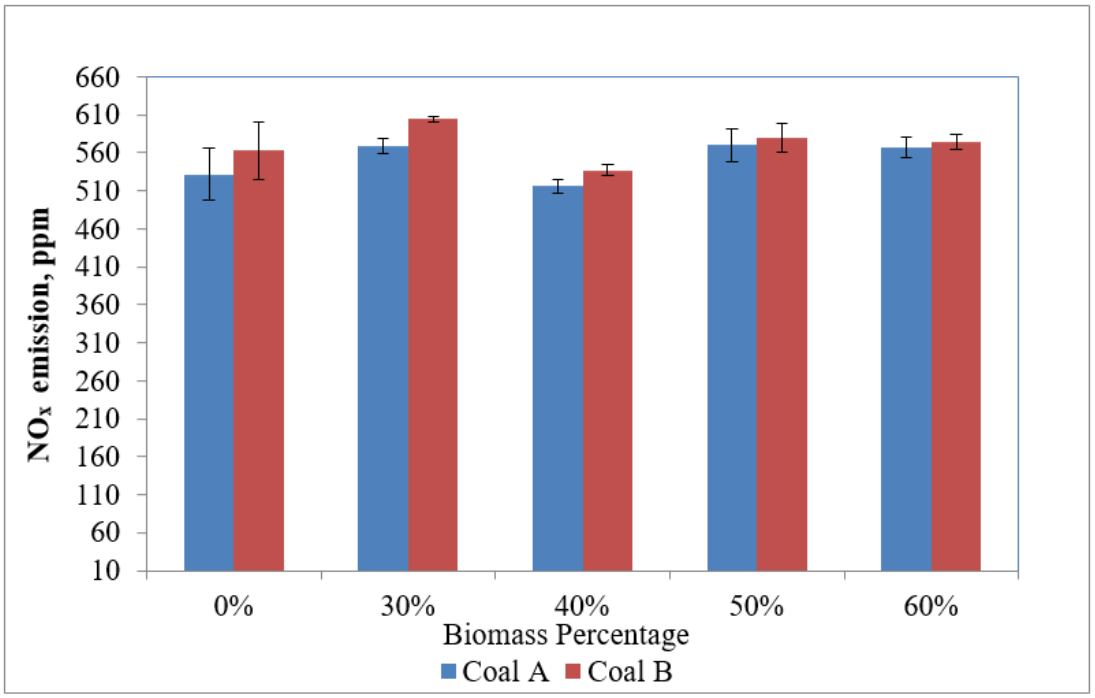

Fig. 6.24 Comparison of biomass (%) and NO_x emissions for coal A and Coal B

CHAPTER NO. 7

CONCLUSIONS AND RECOMMENDATIONS

Following are the conclusions of the study:

The results of coal quality characteristics confirmed that the coals of Salt Range and Trans–Indus Range of Punjab, Pakistan have high sulfur (3.3–11.1%), high ash (14.2–50.3%) and low GCV (10.2–25.7 MJ/kg) and belong to the category of sub–bituminous coals as per ASTM standards. Ash fusion temperatures (>1350 °C) and ash composition indicate that the examined coals have non slagging behavior and no fouling problem.

The analyses of combustion characteristics reveal that ignition temperatures of all the coals are (355–392 °C) which are <400 °C indicating that the coal is easy to ignite. Value of F_z is 1.5–2.0 for the coal samples 1, 2 and 6, and >2.0 for all the remaining coals. Value of C of all the discussed coals is (2.6–3.1) which is >2.3, indicating that these coals have better flammability characteristics. The value of M is (3.5–4.1) which is >3.3 and thus leading to the fact that these coals have better characteristics inheriting the stable firing.

During Emission characteristics study, the potential of limestone and biomass for reduction in gaseous emissions such as SO_2, NO_x, CO and CO_2 has been demonstrated on two different coal samples (coal A and coal B) using a pilot scale FBC facility.

The optimization based on process parameters show that the SO_2 reduction was influenced by fuel properties, firing methodology (pure coal/co–firing with biomass), different values of MR, fine/coarse particle sizes of limestone and the bed temperature. It was observed that maximum desulfurization of coal A and coal B remained 72% and 78% respectively at the optimum MR value of 3.5. There was a predominant impact of bed temperature in the window of 750–800 °C on SO_2 reduction, revealing the maximum reduction of 70% at 800 °C with the same MR of 3.5.The effect of limestone particle size was studied on SO_2 emission which exhibited that maximum desulfurization of 72% occurred at fine particle size range of 2.0–2.8 mm, relative to finer and coarse mode particles owing to the excessive elutriation and small surface area respectively.

There was a significant decrease in SO_2 emissions with the increase in percentage of biomass (30–60%) during co–firing with coal. Consequently, a remarkable decrease of 68% in SO_2 was observed with 60% biomass relative to other proportions. Meanwhile, NO_x were reduced up to 16% and CO were abated up to 78%.

7.1 Novice Contribution

i) Investigation of quality and combustion characteristics of high sulfur coal was carried out.
ii) Key emission characteristics of high sulfur coal were studied during coal combustion with limestone addition and co–firing with biomass in FBC Pilot facility.
iii) Experimental optimization of process parameters such as Ca/S ratio, bed temperature, limestone particle size and biomass proportion was made to minimize the major gaseous emissions particularly SO_2 emissions during combustion in FBC pilot facility.

7.2 Future Recommendation

i) The current study is based on the combustion of high sulfur coal in FBC pilot facility and has great potential for new coal based power projects especially under China Pakistan Economic Corridor (CPEC) program for the control of regulated as well as unregulated emissions.
ii) The study would also provide useful knowledge to the international scientific and engineering community for optimization, design and development of the thermal power plants based on high sulfur coal.

REFERENCES

[1] S. Shafiee and E. Topal, "When will fossil fuel reserves be diminished?," *Energy policy*, vol. 37, pp. 181-189, 2009.

[2] Q. Zhu, "Developments in circulating fluidised bed combustion," *CCC/219 ISBN*, pp. 978-92, 2013.

[3] A. Wolela, "Fossil fuel energy resources of Ethiopia: Coal deposits," *International journal of coal geology*, vol. 72, pp. 293-314, 2007.

[4] A. I. Taub, P. E. Krajewski, A. A. Luo, and J. N. Owens, "The evolution of technology for materials processing over the last 50 years: The automotive example," *Journal of the Minerals, Metals and Materials Society*, vol. 59, pp. 48-57, 2007.

[5] R. Chandra, H. Takeuchi, and T. Hasegawa, "Methane production from lignocellulosic agricultural crop wastes: A review in context to second generation of biofuel production," *Renewable and Sustainable Energy Reviews*, vol. 16, pp. 1462-1476, 2012.

[6] J. R. Fanchi and C. J. Fanchi, *Energy in the 21st Century*: World Scientific Publishing Co Inc, 2016.

[7] Pakistan Energy Yearbook, "Hydrocarbon development institute of Pakistan," Ministry of Petroleum and Natural Resources, Government of Pakistan (2011).

[8] "World Coal Association IEA Coal Information," BP Statistical Review of World Energy 2014. ⟨http://www.worldcoal.org/resources/coal-statistics⟩.

[9] K. Burnard and S. Bhattacharya, "Power generation from coal," 2011.

[10] National Power Policy, "Ministry of Water and Power," Government of Pakistan, pp. 1–22, 2013.

[11] "Power Generation Projects in Punjab, Energy Department," Government of Punjab, Pakistan, pp. 1–30, 2012.

[12] "Punjab's Initiative for development of Coal Fired Power Projects, Energy Department," Government of Punjab, Pakistan, pp. 1–19, 2014.

[13] S. Rehman, A. N. Shah, H. U. Mughal, M. T. Javed, M. Akram, S. Chilton, *et al.*, "Geology and combustion perspectives of Pakistani coals from Salt Range and Trans Indus Range," *International Journal of Coal Geology*, vol. 168, pp. 202-213, 2016.

[14] S. N. Oka, "Fundamental processes during coal combustion in Fluidized Beds," *n: E.J. Anthony, Fluidized Bed Combustion, BASEL, Marcel Dekker Inc; New York, 2004, pp. 211–355.*, 2004.

[15] J. Koornneef, M. Junginger, and A. Faaij, "Development of fluidized bed combustion—An overview of trends, performance and cost," *Progress in energy and combustion science,* vol. 33, pp. 19-55, 2007.

[16] M. Valk, *Atmospheric fluidized bed coal combustion: research, development and application*, vol. 22: Elsevier, 2013.

[17] M. A. Cuenca and E. J. Anthony, *Pressurized fluidized bed combustion*: Springer Science & Business Media, 2012.

[18] P. Haider, "A new concept for operation of a pulverized coal fired boiler using circulating fluidized bed firing," *Journal of engineering for gas turbines and power,* vol. 111, p. 627, 1989.

[19] H. R. Cloots, "Method and apparatus for fluidized bed combustion." U.S. Patent 4,646,637, issued March 3, 1987.

[20] S. Gupta, V. Agarwal, S. Singh, V. Seshadri, D. Mills, J. Singh, *et al.*, "Prediction of minimum fluidization velocity for fine tailings materials," *Powder Technology*, vol. 196, pp. 263-271, 2009.

[21] J. Van Caneghem, A. Brems, P. Lievens, C. Block, P. Billen, I. Vermeulen, *et al.*, "Fluidized bed waste incinerators: Design, operational and environmental issues," *Progress in Energy and Combustion Science,* vol. 38, pp. 551-582, 2012.

[22] R. Abe, H. Sasatsu, T. Harada, N. Misawa, and I. Saitou, "Prediction of emission gas concentration from pressurized fluidized bed combustion (PFBC) of coal under dynamic operation conditions," *Fuel,* vol. 80, pp. 135-144, 2001.

[23] B. Leckner and A. Lyngfelt, "Optimization of emissions from fluidized bed combustion of coal, biofuel and waste," *International journal of energy research,* vol. 26, pp. 1191-1202, 2002.

[24] J. A. Logan, "Nitrogen oxides in the troposphere: Global and regional budgets," *Journal of Geophysical Research: Oceans,* vol. 88, pp. 10785-10807, 1983.

[25] P. Basu, *Circulating fluidized bed boilers: design, operation and maintenance*: Springer, 2015.

[26] M. L. Souza-Santos, *Solid Fuels Combustion and Gasification: Modeling, Simulation*: CRC Press, 2010.

[27] J. J. Zhang and K. R. Smith, "Household air pollution from coal and biomass fuels in China: measurements, health impacts, and interventions," *Environmental health perspectives,* vol. 115, p. 848, 2007.

[28] J. Zhang, S. Sun, X. Hu, R. Sun, and Y. Qin, "Modeling NO−char reaction at high temperature," *Energy & Fuels,* vol. 23, pp. 2376-2382, 2009.

[29] R. I. Singh, A. Brink, and M. Hupa, "CFD modeling to study fluidized bed combustion and gasification," *Applied Thermal Engineering,* vol. 52, pp. 585-614, 2013.

[30] J. Smolik, J. Schwarz, V. Vesely, I. SIKOROVA, J. Kucera, and V. Havranek, "Influence of calcareous sorbents on particulate emissions from fluidized bed combustion of lignite," *Aerosol science and technology,* vol. 33, pp. 544-556, 2000.

[31] M. Widera, Z. Kasztelewicz, and M. Ptak, "Lignite mining and electricity generation in Poland: The current state and future prospects," *Energy Policy,* vol. 92, pp. 151-157, 2016.

[32] K. Findlay and S. Probert, "Limiting NO_x and SO_2 emissions from an industrial-size fluidised-bed combustor," *Applied energy,* vol. 45, pp. 1-99, 1993.

[33] P. D. Warwick and B. R. Wardlaw, *Regional studies of the Potwar plateau area, northern Pakistan*: Geological Survey (US), 2007.

[34] Coal Resource Report, Snowden, "Mines and Minerals Department," Government of Punjab, Project No 00778, Coal Resources of Salt Range and Trans Indus Range Punjab. Brisbane. pp. 23-35, 2012.

[35] Pakistan Energy Yearbook, "Hydrocarbon development institute of Pakistan," Ministry of Petroleum and Natural Resources, Government of Pakistan, 2015.

[36] S. Daood, M. Javed, A. Rizvi, and W. Nimmo, "Combustion of Pakistani lignite (Thar coal) in a pilot-scale pulverized fuel down-fired combustion test facility," *Energy & Fuels,* vol. 28, pp. 1541-1547, 2014.

[37] S. A. H. Zaidi, "Coal reactivity: correlations with fuel and NMR data," *Fuel processing technology,* vol. 41, pp. 253-259, 1995.

[38] M. Iqbal, T. Akhtar, A. Karim, and F. Khan, "An Investigation into the Thermal Behavior of Tharparker Coal," *Journal-Chemical Society of Pakistan,* vol. 28, p. 519, 2006.

[39] S. Naveed, A. Malik, M. Akram, M. Deary, and A. Roskilly, "Gasification perspective of Pakistani coal," *Journal of the Energy Institute,* vol. 86, pp. 1-7, 2013.

[40] S. R. Braganca and J. L. Castellan, "FBC desulfurization process using coal with low sulfur content, high oxidizing conditions and metamorphic limestones," *Brazilian Journal of Chemical Engineering,* vol. 26, pp. 375-383, 2009.

[41] L. A. C. Tarelho, M. A. A. Matos, and F. J. M. A. Pereira, "The influence of operational parameters on SO_2 removal by limestone during fluidised bed coal combustion," *Fuel Processing Technology,* vol. 86, pp. 1385-1401, 2005.

[42] B. Stanmore and P. Gilot, "calcination and carbonation of limestone during thermal cycling for CO_2 sequestration," *Fuel Processing Technology,* vol. 86, pp. 1707-1743, 2005.

[43] E. Anthony and D. Granatstein, "Sulfation phenomena in fluidized bed combustion systems," *Progress in energy and Combustion Science,* vol. 27, pp. 215-236, 2001.

[44] J. Cheng, J. Zhou, J. Liu, Z. Zhou, Z. Huang, X. Cao, *et al.*, "Sulfur removal at high temperature during coal combustion in furnaces: a review," *Progress in Energy and Combustion Science,* vol. 29, pp. 381-405, 2003.

[45] K. Svoboda and M. Pohořelý, "Influence of operating conditions and coal properties on NO_x and N_2O emissions in pressurized fluidized bed combustion of subbituminous coals," *Fuel,* vol. 83, pp. 1095-1103, 2004.

[46] A. Lyngfelt and B. Leckner, "Sulphur capture in circulating fluidized-bed boilers: can the efficiency be predicted?," *Chemical Engineering Science,* vol. 54, pp. 5573-5584, 1999.

[47] H. Liu and B. M. Gibbs, "The influence of limestone addition at different positions on gaseous emissions from a coal-fired circulating fluidized bed combustor," *Fuel,* vol. 77, pp. 1569-1577, 1998.

[48] H. Altindag, Y. Gogebakan, and N. Selçuk, "Sulfur capture for fluidized-bed combustion of high-sulfur content lignites," *Applied energy,* vol. 79, pp. 403-424, 2004.

[49] T. Shimizu, M. Peglow, K. Yamagiwa, M. Tanaka, S. Sakuno, N. Misawa, *et al.*, "A simplified model of SO_2 capture by limestone in 71 MW_e pressurized fluidized bed combustor," *Chemical Engineering Science,* vol. 57, pp. 4117-4128, 2002.

[50] A. Gungor and N. Eskin, "Hydrodynamic modeling of a circulating fluidized bed," *Powder Technology,* vol. 172, pp. 1-13, 2007.

[51] Y. Huang, J. McMullan, and B. Williams, "Influences of coal type on the performance of a pressurised fluidised bed combustion power plant," *Fuel,* vol. 79, pp. 1595-1601, 2000.

[52] A. Khan, W. Jong, P. Jansens, and H. Spliethoff, "Biomass combustion in fluidized bed boilers: potential problems and remedies," *Fuel processing technology,* vol. 90, pp. 21-50, 2009.

[53] L. Baxter, "Biomass-coal co-combustion: opportunity for affordable renewable energy," *Fuel,* vol. 84, pp. 1295-1302, 2005.

[54] M. Sami, K. Annamalai, and M. Wooldridge, "Co-firing of coal and biomass fuel blends," *Progress in energy and combustion science,* vol. 27, pp. 171-214, 2001.

[55] M. Hupa, "Interaction of fuels in co-firing in FBC," *Fuel,* vol. 84, pp. 1312-1319, 2005.

[56] A. Demirbas, "Combustion characteristics of different biomass fuels," *Progress in energy and combustion science,* vol. 30, pp. 219-230, 2004.

[57] B. J. Cardinale, J. P. Wright, M. W. Cadotte, I. T. Carroll, A. Hector, D. S. Srivastava, *et al.*, "Impacts of plant diversity on biomass production increase through time because of species complementarity," *Proceedings of the National Academy of Sciences,* vol. 104, pp. 18123-18128, 2007.

[58] K. Savolainen, "Co-firing of biomass in coal-fired utility boilers," *Applied Energy,* vol. 74, pp. 369-381, 2003.

[59] W. Jong and J. V. Ommen, "Scale-up in fluidized bed biomass combustion," *Scale-up in Combustion (ed. M. Lackner), Verlag ProcessEng GmbH,* pp. 33-60, 2009.

[60] H. Maier, H. Spliethoff, A. Kicherer, A. Fingerle, and K. Hein, "Effect of coal blending and particle size on NO_x emission and burnout," *Fuel,* vol. 73, pp. 1447-1452, 1994.

[61] K. Narayanan and E. Natarajan, "Experimental studies on cofiring of coal and biomass blends in India," *Renewable Energy*, vol. 32, pp. 2548-2558, 2007.

[62] K. Hein and J. Bemtgen, "EU clean coal technology—co-combustion of coal and biomass," *Fuel processing technology*, vol. 54, pp. 159-169, 1998.

[63] P. Sun, J. Grace, C. Lim, and E. Anthony, "The effect of CaO sintering on cyclic CO_2 capture in energy systems," *AIChE Journal*, vol. 53, pp. 2432-2442, 2007.

[64] D. Mao, J. R. Edwards, A. V. Kuznetsov, and R. K. Srivastava, "Three-dimensional numerical simulation of a circulating fluidized bed reactor for multi-pollutant control," *Chemical engineering science*, vol. 59, pp. 4279-4289, 2004.

[65] P. Gayan, J. Adanez, F. Luis, F. García-Labiano, A. Cabanillas, A. Bahillo, *et al.*, "Circulating fluidised bed co-combustion of coal and biomass," *Fuel*, vol. 83, pp. 277-286, 2004.

[66] M. Öhman, A. Nordin, B.-J. Skrifvars, R. Backman, and M. Hupa, "Bed agglomeration characteristics during fluidized bed combustion of biomass fuels," *Energy & Fuels*, vol. 14, pp. 169-178, 2000.

[67] L. Armesto, A. Bahillo, A. Cabanillas, K. Veijonen, J. Otero, A. Plumed, *et al.*, "Co-combustion of coal and olive oil industry residues in fluidised bed," *Fuel*, vol. 82, pp. 993-1000, 2003.

[68] M. Montgomery, A. Karlsson, and O. H. Larsen, "Field test corrosion experiments in Denmark with biomass fuels. Part 1: Straw- firing," *Materials and Corrosion*, vol. 53, pp. 121-131, 2002.

[69] J. XIE, X. YANG, L. ZHANG, T. DING, W. SONG, and W. LIN, "Emissions of SO_2, NO and N_2O in a circulating fluidized bed combustor during co-firing coal and biomass," *Journal of Environmental Sciences*, vol. 19, pp. 109-116, 2007.

[70] W. Permchart and V. I. Kouprianov, "Emission performance and combustion efficiency of a conical fluidized-bed combustor firing various biomass fuels," *Bioresource technology*, vol. 92, pp. 83-91, 2004.

[71] M. J. F. Gutierrez, D. Baxter, C. Hunter, and K. Svoboda, "Nitrous oxide (N_2O) emissions from waste and biomass to energy plants," *Waste management & research*, vol. 23, pp. 133-147, 2005.

[72] L. Armesto, A. Bahillo, K. Veijonen, A. Cabanillas, and J. Otero, "Combustion behaviour of rice husk in a bubbling fluidised bed," *Biomass and Bioenergy*, vol. 23, pp. 171-179, 2002.

[73] H. Liu and B. M. Gibbs, "Modelling of NO and N_2O emissions from biomass-fired circulating fluidized bed combustors," *Fuel*, vol. 81, pp. 271-280, 2002.

[74] A. Kicherer, H. Spliethoff, H. Maier, and K. Hein, "The effect of different reburning fuels on NO_x-reduction," *Fuel*, vol. 73, pp. 1443-1446, 1994.

[75] A. Rainio, V. Sharma, M. Bolhàr-Nordenkampf, C. Brunner, J. Lind, and J. Crosher, "Fluidized Bed Technologies for Biomass Combustion," in *ASME Power Conference*, 2009, pp. 21-23.

[76] A. A. Khan, "Combustion and co-combustion of biomass in a bubbling fluidized bed boiler," 2007.

[77] Y. Tan, E. Croiset, M. A. Douglas, and K. V. Thambimuthu, "Combustion characteristics of coal in a mixture of oxygen and recycled flue gas," *Fuel*, vol. 85, pp. 507-512, 2006.

[78] L. Jia, Y. Tan, C. Wang, and E. Anthony, "Experimental study of oxy-fuel combustion and sulfur capture in a mini-CFBC," *Energy & Fuels*, vol. 21, pp. 3160-3164, 2007.

[79] L. Jia, Y. Tan, and E. Anthony, "Emissions of SO2 and NO x during Oxy− Fuel CFB Combustion Tests in a Mini-Circulating Fluidized Bed Combustion Reactor," *Energy & Fuels*, vol. 24, pp. 910-915, 2009.

[80] H. Liu, Y. Chao, S. Dong, X. Yuan, Z. Zeng, T. Ando, *et al.*, "Efficient Desulfurization in a new scheme of oxyfuel combined with partial CO_2 removal from recycled gas and MILD combustion," *Energy & Fuels*, vol. 27, pp. 1513-1521, 2013.

[81] H. Liu, H. Yao, X. Yuan, X. Xu, Y. Fan, T. Ando, *et al.*, "Efficient desulfurization in O_2/CO_2 combustion: dependence on combustion conditions and sorbent properties," *Chemical engineering communications*, vol. 199, pp. 991-1011, 2012.

[82] L. Jia, Y. Tan, D. McCalden, Y. Wu, I. He, R. Symonds, *et al.*, "Commissioning of a 0.8 MW_{th} CFBC for oxy-fuel combustion," *International Journal of Greenhouse Gas Control*, vol. 7, pp. 240-243, 2012.

[83] B. Roy, L. Chen, and S. Bhattacharya, "Nitrogen oxides, sulfur trioxide, and mercury emissions during oxy-fuel fluidized bed combustion of Victorian

brown coal," *Environmental Science & Technology*, vol. 48, pp. 14844-14850, 2014.

[84] J. Yoo, Y. Seo, and T. Shinagawa, "Particle-size distributions and heavy metal partitioning in emission gas from different coal-fired power plants," *Environmental Engineering Science*, vol. 22, pp. 272-279, 2005.

[85] D. Pudasainee, J. Kim, and Y. Seo, "Mercury emission trend influenced by stringent air pollutants regulation for coal-fired power plants in Korea," *Atmospheric Environment*, vol. 43, pp. 6254-6259, 2009.

[86] E. Furimsky, "Characterization of trace element emissions from coal combustion by equilibrium calculations," *Fuel Processing Technology*, vol. 63, pp. 29-44, 2000.

[87] L. Li, "Circulating Fludized Bed Boiler," *Changsha University of Science and Technology (CUST) Changsha, Hunan, China.*, Jan, 19, 2009.

[88] C. J. Wandrey, B. Law, and H. A. Shah, *Patala-Nammal composite total petroleum system, Kohat-Potwar geologic province, Pakistan*: US Department of the Interior, US Geological Survey, 2004.

[89] T. M. Jaswal, "Structure and evolution of the Dhurnal oil field, northern Potwar deformed zone, Pakistan," 1990.

[90] S. J. Sameeni, "PaleoParks-The Protection and Conservation of Fossil Sites Worldwide: Chapter 6; The Salt Range: Pakistan's unique field museum of geology and paleontology," 2009.

[91] S. M. I. Shah, *Stratigraphy and economic geology of Central Salt Range* vol. 52: Geological Survey of Pakistan, 1980.

[92] P. J. McCabe, *Depositional environments of coal and coal- bearing strata*: Wiley Online Library, 1984.

[93] S. Vessey and R. Bustin, "Sedimentology of the coal-bearing Mist Mountain Formation, Line Creek, Southern Canadian Cordillera: relationships to coal quality," *International journal of coal geology*, vol. 42, pp. 129-158, 2000.

[94] E. J. Anthony, S. N. Oka, "Fluidized Bed Combustion," *Laboratory for Thermal Engineering and Energy Institute VIN A Belgrade, Serbia and Montenegro, CANMET Energy Technology Centre (CETC) Natural Resources Canada Ottawa, Ontario, Canada*, 2004.

[95] K. W. Ragland and K. M. Bryden, *Combustion engineering*: CRC press, 2011.

[96] J. Randolph and G. M. Masters, *Energy for sustainability: technology, planning, policy*: Island Press, 2008.

[97] D. S. Belić, "Global warming and greenhouse gases," *Facta universitatis-series: Physics, Chemistry and Technology*, vol. 4, pp. 45-55, 2006.

[98] P. Sun, J. R. Grace, C. J. Lim, and E. J. Anthony, "Removal of CO_2 by calcium-based sorbents in the presence of SO_2," *Energy & Fuels*, vol. 21, pp. 163-170, 2007.

[99] P. Hansen, K. Dam-Johansen, and K. Østergaard, "High-temperature reaction between sulphur dioxide and limestone—V. The effect of periodically changing oxidizing and reducing conditions," *Chemical Engineering Science*, vol. 48, pp. 1325-1341, 1993.

[100] P. Abelha, I. Gulyurtlu, and I. Cabrita, "Release of nitrogen precursors from coal and biomass residues in a bubbling fluidized bed," *Energy & Fuels*, vol. 22, pp. 363-371, 2007.

[101] A. Williams, M. Pourkashanian, and J. Jones, "The combustion of coal and some other solid fuels," *Proceedings of the Combustion Institute*, vol. 28, pp. 2141-2162, 2000.

[102] A. Hayhurst and A. Lawrence, "The effect of solid CaO on the production of NO_x and N_2O in fluidized bed combustors: Studies using pyridine as a prototypical nitrogenous fuel," *Combustion and flame*, vol. 105, pp. 511-527, 1996.

[103] N. MacDowell, N. Florin, A. Buchard, J. Hallett, A. Galindo, G. Jackson, *et al.*, "An overview of CO_2 capture technologies," *Energy & Environmental Science*, vol. 3, pp. 1645-1669, 2010.

[104] W. Liu, H. An, C. Qin, J. Yin, G. Wang, B. Feng, *et al.*, "Performance enhancement of calcium oxide sorbents for cyclic CO_2 capture A review," *Energy & Fuels*, vol. 26, pp. 2751-2767, 2012.

[105] C. Lupiáñez, I. Guedea, I. Bolea, L. I. Díez, and L. M. Romeo, "Experimental study of SO_2 and NO_x emissions in fluidized bed oxy-fuel combustion," *Fuel processing technology*, vol. 106, pp. 587-594, 2013.

[106] H. Li, J. Zhang, Y. Zhao, C.-Y. Wu, and C. Zheng, "Wettability of fly ashes from four coal-fired power plants in China," *Industrial & Engineering Chemistry Research*, vol. 50, pp. 7763-7771, 2011.

[107] N. P. Cheremisinoff, *Clean Electricity Through Advanced Coal Technologies: Handbook of Pollution Prevention and Cleaner Production* vol. 4: William Andrew, 2012.

[108] R. Kuusik, M. Uibu, and K. Kirsimae, "Characterization of oil shale ashes formed at industrial-scale CFBC boilers," *Oil Shale,* vol. 22, pp. 407-420, 2005.

[109] G. Özbayoğlu and M. E. Özbayoğlu, "A new approach for the prediction of ash fusion temperatures: a case study using Turkish lignites," *Fuel,* vol. 85, pp. 545-552, 2006.

[110] A. B. Khadilkar, *Development of a fluidized bed agglomeration modeling methodology to include particle-level heterogeneities in ash chemistry and granular physics*: The Pennsylvania State University, 2016.

[111] M. Aho and E. Ferrer, "Importance of coal ash composition in protecting the boiler against chlorine deposition during combustion of chlorine-rich biomass," *Fuel,* vol. 84, pp. 201-212, 2005.

[112] C. G. Veras, J. Saastamoinen, J. Carvalho, and M. Aho, "Overlapping of the devolatilization and char combustion stages in the burning of coal particles," *Combustion and Flame,* vol. 116, pp. 567-579, 1999.

[113] H. Thunman, K. Davidsson, and B. Leckner, "Separation of drying and devolatilization during conversion of solid fuels," *Combustion and flame,* vol. 137, pp. 242-250, 2004.

[114] D. CHE, "Boilers-Theory, Design and Operation," *X'ian Jiao tong University Press,* 2008.

[115] S. Krishnaswamy, S. Bhat, R. D. Gunn, and P. K. Agarwal, "Low-temperature oxidation of coal. 1. A single-particle reaction-diffusion model," *Fuel,* vol. 75, pp. 333-343, 1996.

[116] J. C. Hower, U. M. Graham, A. S. Wong, J. D. Robertson, B. O. Haeberlin, G. A. Thomas, and W. H. Schram. "Influence of flue-gas desulfurization systems on coal combustion by-product quality at Kentucky power stations burning high-sulfur coal." *Waste Management,*vol. 17, pp. 523-533, 1998.

[117] A. H. Clemens and T. W. Matheson, "The role of moisture in the self-heating of low-rank coals," *Fuel,* vol. 75, pp. 891-895, 1996.

[118] M. Wojtowicz, J. Pels, and J. Moulijn, "Combustion of coal as a source of N_2O emission," *Fuel Processing Technology,* vol. 34, pp. 1-71, 1993.

[119] T. Wu, M. Gong, E. Lester, and P. Hall, "Characteristics and synergistic effects of co-firing of coal and carbonaceous wastes," *Fuel*, vol. 104, pp. 194-200, 2013.

[120] G. J. Zijlma, A. Jensen, J. E. Johnsson, and C. Van den Bleek, "NH_3 oxidation catalysed by calcined limestone—a kinetic study," *Fuel*, vol. 81, pp. 1871-1881, 2002.

[121] W. Lin, J. E. Johnsson, K. Dam-Johansen, and C. M. Bleek, "Interaction between emissions of sulfur dioxide and nitrogen oxides in fluidized bed combustion," *Fuel*, vol. 73, pp. 1202-1208, 1994.

[122] G. S. Grasa and J. C. Abanades, "CO_2 capture capacity of CaO in long series of carbonation/calcination cycles," *Industrial & Engineering Chemistry Research*, vol. 45, pp. 8846-8851, 2006.